AD-A042 319 VOUGHT CORP ADVANCED TECHNOLOGY CENTER INC DALLAS TEX F/G 1/3
V-STOL EJECTOR SHORT DIFFUSER STUDY.(U)
JUN 76 R M O'DONNELL, R A SQUYERS N62269-75-C-0317
UNCLASSIFIED ATC-B-94300/6CR-26 NADC-77165-30 NL

1 OF 1
ADA042319

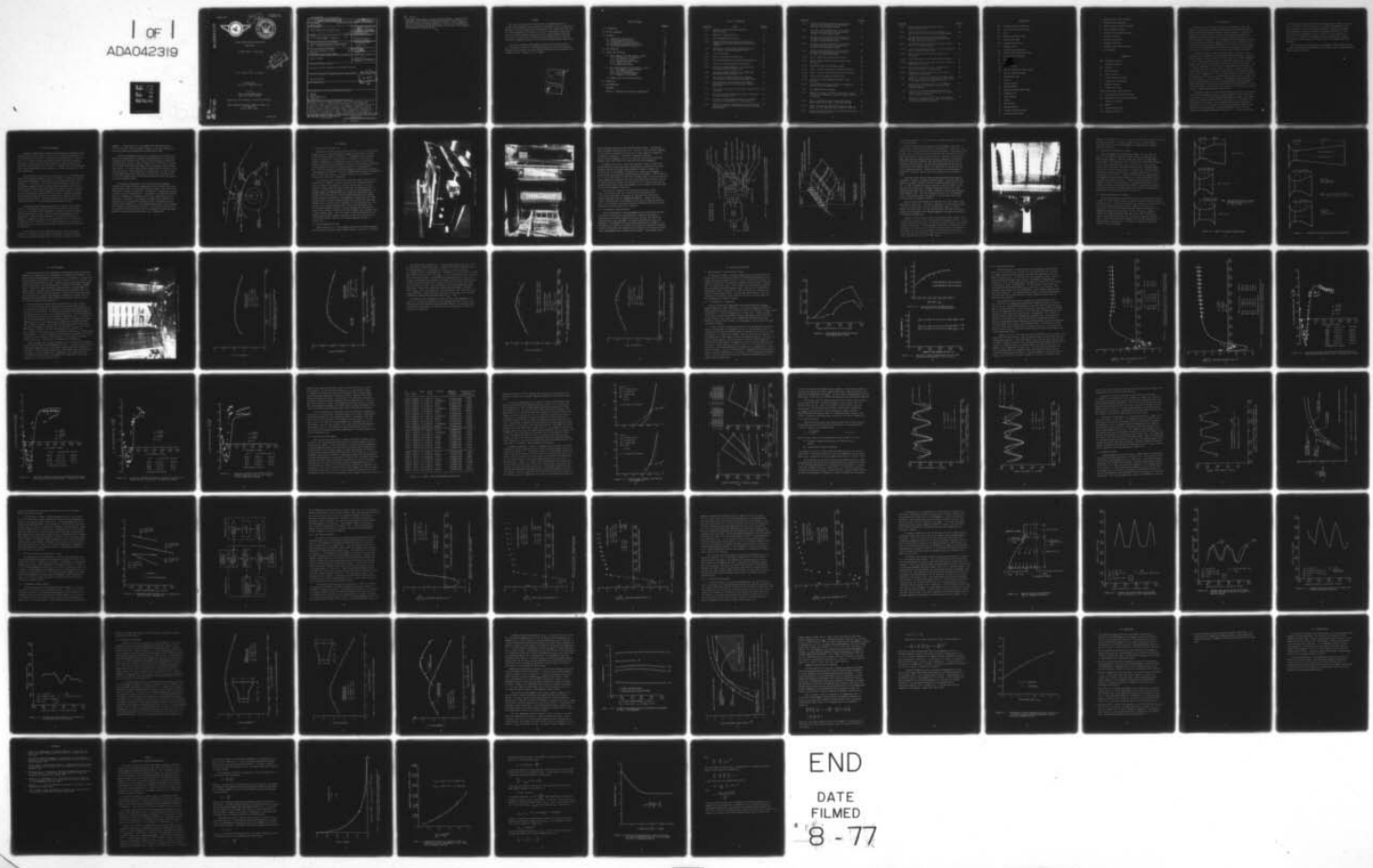

END

DATE FILMED
8-77

UNCLASSIFIED

ATC Report No.
B-94300/6CR-26

AD A042319

V/STOL EJECTOR SHORT DIFFUSER STUDY

FINAL REPORT

(17 MARCH 1975 - 16 JUNE 1976)

DDC
JUL 26 1977
C

by
R. M. O'Donnell and R. A. Squyers

Prepared under
Contract No. N62269-75-C-0317

For the
NAVAL AIR DEVELOPMENT CENTER
NAVAL AIR SYSTEMS COMMAND

Approved for Public Release: Distribution Unlimited

VOUGHT CORPORATION ADVANCED TECHNOLOGY CENTER, INC.
P. O. BOX 6144
DALLAS, TEXAS 75222

AD No.
DDC FILE COPY

UNCLASSIFIED

UNCLASSIFIED

SECURITY CLASSIFICATION OF THIS PAGE *(When Data Entered)*

REPORT DOCUMENTATION PAGE

READ INSTRUCTIONS BEFORE COMPLETING FORM

1. REPORT NUMBER: NADC-77165-30	2. GOVT ACCESSION NO.
3. RECIPIENT'S CATALOG NUMBER	
4. TITLE *(and Subtitle)*: V-STOL Ejector Short Diffuser Study,	5. TYPE OF REPORT & PERIOD COVERED: FINAL rept. March 1975 - June 1976
6. PERFORMING ORG. REPORT NUMBER: B-94300/6CR-26	
7. AUTHOR(s): R. M. O'Donnell and R. A. Squyers	8. CONTRACT OR GRANT NUMBER(s): N62269-75-C-0317
9. PERFORMING ORGANIZATION NAME AND ADDRESS: Vought Corporation Advanced Technology Center, Inc., P.O. Box 6144, Dallas, Texas 75222	10. PROGRAM ELEMENT, PROJECT, TASK AREA & WORK UNIT NUMBERS: 62 P
11. CONTROLLING OFFICE NAME AND ADDRESS: Naval Air Development Center, Code 3014, Warminster, Pennsylvania 18974	12. REPORT DATE: 16 June 1976
	13. NUMBER OF PAGES: 80
14. MONITORING AGENCY NAME & ADDRESS *(if different from Controlling Office)*: Same as Block 11	15. SECURITY CLASS. *(of this report)*: Unclassified
	15a. DECLASSIFICATION/DOWNGRADING SCHEDULE

16. DISTRIBUTION STATEMENT *(of this Report)*

Approved for Public Release and Distribution Unlimited

17. DISTRIBUTION STATEMENT *(of the abstract entered in Block 20, if different from Report)*

Same as Block 16

DDC RECEIVED JUL 26 1977 C

18. SUPPLEMENTARY NOTES

19. KEY WORDS *(Continue on reverse side if necessary and identify by block number)*

Ejector
Diffuser
Thrust Augmentation
Propulsion

20. ABSTRACT *(Continue on reverse side if necessary and identify by block number)*

Development of thrust augmenting ejectors has produced ejector/diffuser configurations capable of achieving the high levels of thrust augmentation necessary for VTOL aircraft propulsion requirements. Experimental testing has shown that thrust augmenting ejectors can be made more compact by reducing diffuser length with active diffusion boundary layer control employing the Antiseparation Tailored Contour (ATC). Thrust augmentation and internal flow measurements were determined in compact high performance thrust augmentors with various length diffusers. The short ATC/diffusers tested showed significant

DD FORM 1 JAN 73 1473 EDITION OF 1 NOV 65 IS OBSOLETE S/N 0102-014-6601 |

UNCLASSIFIED

SECURITY CLASSIFICATION OF THIS PAGE *(When Data Entered)*

389 797

Enclosure 2

20. Abstract

improvements when compared to previous ejector diffusers. Measured thrust augmentation ratios with an optimum short ATC/diffuser were 10% greater than those with an equivalent straight wall diffuser. Length reductions of 36% were indicated for nominal augmentation ratios of 1.7. The important factors which influence the design and operation of compact thrust augmentor ejector/diffusers have been defined.

PREFACE

This report describes work done under Contract N62269-75-C-0317 with the Naval Air Development Center, Warminster, Pennsylvania under the auspices of the Naval Air Systems Command during the period of March 1975 through June 1976. This effort represents an extension of an earlier investigation during which the short diffuser boundary layer control work of Vought Advanced Technology Center was first successfully combined with the high performance, large area ratio thrust augmentor research of the Air Force Aerospace Research Laboratories.

The authors gratefully acknowledge the interest and advice provided by Mr. John Cyrus of the Naval Air Development Center who monitored the contract. The work was conducted by the Vought Advanced Technology Center Aerodynamics and Propulsion Group headed by Dr. C. H. Haight.

TABLE OF CONTENTS

LIST OF ILLUSTRATIONS

NOMENCLATURE

ARL	Aerospace Research Laboratories
ATC	Antiseparation Tailored Contour
A	Area
AR	Diffuser Area Ratio, A_3/A_2
α	Diffuser Half Angle
BLC	Boundary Layer Control
β	Skewness Factor
C_p	Local Pressure Coefficient
$\overline{C}_p$	Diffuser Pressure Recovery Factor
C	Local Spanwise Coordinate
$\mathbb{C}$	Centerline
Hg	Mercury
L_D	Diffuser Length
L_M	Constant Area Mixing Region Length
L'	Specific Downstream Length
$\dot{m}$	Weighted Mass Flow
P	Pressure
q	Dynamic Pressure
R_e	Reynolds Number,
S	Downstream Diffuser Wall Length
TV	Trapped Vortex
u	Local Velocity
V	Velocity
V'	Mean Velocity
$\overline{V}$	Average Velocity
W	Constant Area Mixing Width
W'	Mixing Width Coordinate

y	Boundary Layer Height Coordinate
Z	Spanwise Height Coordinate
Z'	Relative Spanwise Height Coordinate
ϕ	Thrust Augmentation Ratio
$\overline{\phi}$	Average Thrust Augmentation Ratio
γ	Correlation Factor
δ	Boundary Layer Height
η	Component Efficiency
θ	Boundary Layer Momentum Thickness
ξ	Loss Parameter

SUBSCRIPTS

ATM	Atmospheric Condition
∞	Freestream Condition
EFF	Effective
D	Diffuser Region
ew	Endwall Location
0	Primary Ejector Exit Plane
1	Induced Flow Inlet Region
2	Blowing Lip Plane
3	Diffuser Exit Plane
01,02	Primary Plenum Total Condition
0_j	ATC Blowing Plenum Total Condition
0ew	Endwall Blowing Plenum Total Condition
L	Blowing Lip Location
max	Maximum
N	Ejector Nozzle Region
ref	Reference Condition

Data was then recorded at a rate of 1 scan per second while each data sample was

1.0 INTRODUCTION

The concept of thrust augmenting ejectors for advanced aircraft V/STOL capabilities was greatly enhanced by the development of hypermixing ejector nozzles at Aerospace Research Laboratories (ARL), Reference 1. Research and development of ejector/diffusers produced thrust augmentor configurations capable of achieving the high levels of thrust augmentation necessary for VTOL requirements, Reference 2. As a prerequisite to good performance, however, a penalty was paid by the above augmentor/diffusers by the requirement of an extremely long diffuser length. Compatibility with V/STOL aircraft configurations such as the Navy/Rockwell XFV-12A requires a truncation of the ejector's overall length while maintaining or improving thrust augmentor performance.

At Vought Corporation Advanced Technology Center, feasibility tests showed that thrust augmenting ejectors could be made more compact by reducing diffuser length with active diffusion boundary layer control (BLC), Reference 3. The two basic proprietary devices for active diffusion control are the Trapped Vortex (TV) cavity and the Antiseparation Tailored Contour (ATC). The TV results in Reference 3 provided for the same augmentation performance with a 21 percent reduction in overall length, relative to the best original ARL configuration, and up to a 71 percent length reduction for acceptable degradations in thrust augmentation. Further in-house feasibility testing showed the less complex ATC diffusion control technique to perform as well or better than the TV BLC device in a thrust augmentor. Performance/sizing improvements, as predicted for configurations utilizing advanced ARL/H-8 hypermixing ejector nozzles (Reference 4) and optimized ATC diffusion control, motivated the initiation of the present contract effort for detailed design, testing, and evaluation studies of compact ejector/diffuser combinations.

The primary objective of the present program was to identify the important factors which influence the design of compact augmentors using ATC BLC technology (Section 2.0) and to use the developed design techniques to configure and test an optimized augmentor/diffuser configuration. This objective was accomplished in two phases. Using the experimental apparatus described in Section 3.0, the initial (Phase I) testing was performed on three basic augmentor/diffuser configurations to obtain fundamental internal flow and augmentation performance measurements (Section 5.1). The results of Phase I,

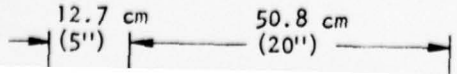

including the definition of an efficient testing procedure, (Section 4.0), were used in the Phase II design and testing of a compact ATC augmentor/diffuser optimized subject to a specified sizing constraint. Predicted performance, and consequently the design techniques for configured ATC/diffusers, were verified with the experimental results of Phase II testing (Section 5.2). Section 5.3 is a summation of an augmentor design and prediction technique based on empiricisms and analytical formulations for the augmentor/diffuser parameters.

Following the conclusions related to achievement of the program objective, the report concludes with recommendations for further studies of high performance compact augmentor/diffusers.

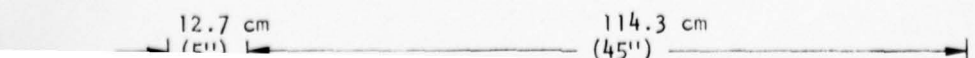

2.0 ATC BLC TECHNOLOGY

Augmentors basically are propulsive devices whereby an exhausting primary propulsive jet suitably located in the inlet of the device causes ambient air to be entrained into the inlet. The expulsion of this additional air then results in an increase in thrust over that provided by the primary propulsion jets alone. Properly designed thrust augmentors can generate thrust levels over double that provided by the primary jets. The desirability for the possible use of such high performance thrust augmentors in V/STOL type aircraft is thus easily appreciated.

With the advent of a new type of primary nozzle, a so called hypermixing nozzle, which generated numerous vortice's to increase mixing, and a very low loss augmentor (Reference 1),high levels of thrust augmentation were finally achieved. It is important to note that although the diffuser attached was a conventional straight wall type, the high thrust augmentation could not be achieved unless boundary layer control (BLC) was utilized to control separation in the diffuser. Also of great importance was the proper length of constant area mixing immediately following the primary nozzles. Numerous experiments were performed to determine the optimum combination of constant area mixing length and diffuser length. The optimum configuration finally attained was termed Configuration 'F' by Aerospace Research Laboratories (ARL).

Although the latter augmentor generated high levels of thrust augmentation, it's adaptation to practical aircraft was made very difficult because of its very long diffuser requirement. Shorter straight wall diffusers could have been used, of course, but this would undoubtably have required more blowing to control diffuser separation. Since the performance of an augmentor is measured principally by its augmentation ratio (ϕ = total thrust produced/sum total of thrusts of all individual blowing jets), lower levels of augmentation ratio would have been achieved through the use of conventional BLC techniques.

To circumvent this loss in augmentation rates, while significantly shortening the diffuser and thus the overall augmentor, Advanced Technology Center, Inc. successfully applied their in-house BLC techniques to the ARL

augmentor. As noted previously, the trapped vortex BLC technique was initially utilized. This was replaced, however, by the more advanced and more easily fabricated Antiseparation Tailored Contour (ATC).

Briefly, ATC boundary layer control is based on the utilization of a device that combines efficient boundary layer energization with a specially configured severe diffusion step. The principal advantage of using an ATC diffusion device, such as is shown in Figure 2.0-1, in a diffuser is that an air stream can be diffused quite rapidly with no separation, due to boundary layer control, in a significantly shorter distance than can be done in a conventional diffuser. The Antiseparation Tailored Contour is closely related to the Trapped Vortex Cavity, also shown in Figure 2.0-1, but uses control of a new thin boundary layer building along the ATC wall rather than control of the vortex boundary layer.

The dominant consideration in the use of ATC BLC for augmentor diffusion is the highly efficient energization of the relatively thick mainstream boundary layer, thus minimizing the primary ejector flow diverted from the primary fin nozzle mixing process. Energization is accomplished by means of the jet issuing from the ATC slot. The design of the proper ATC diffusion contour in conjunction with augmentor diffuser wall length and area ratio constraints is performed in the rheoelectric analog facility (Section 3.1). Calculations for the required BLC blowing are made in accordance with the iteration loop of Section 5.2.1 using the predicted values of initial boundary layer losses at the ATC blowing lip location. The ability of the ATC device to successfully diffuse flow rapidly with no separation has been shown experimentally in previous Navy contract efforts (e.g., Reference 5).

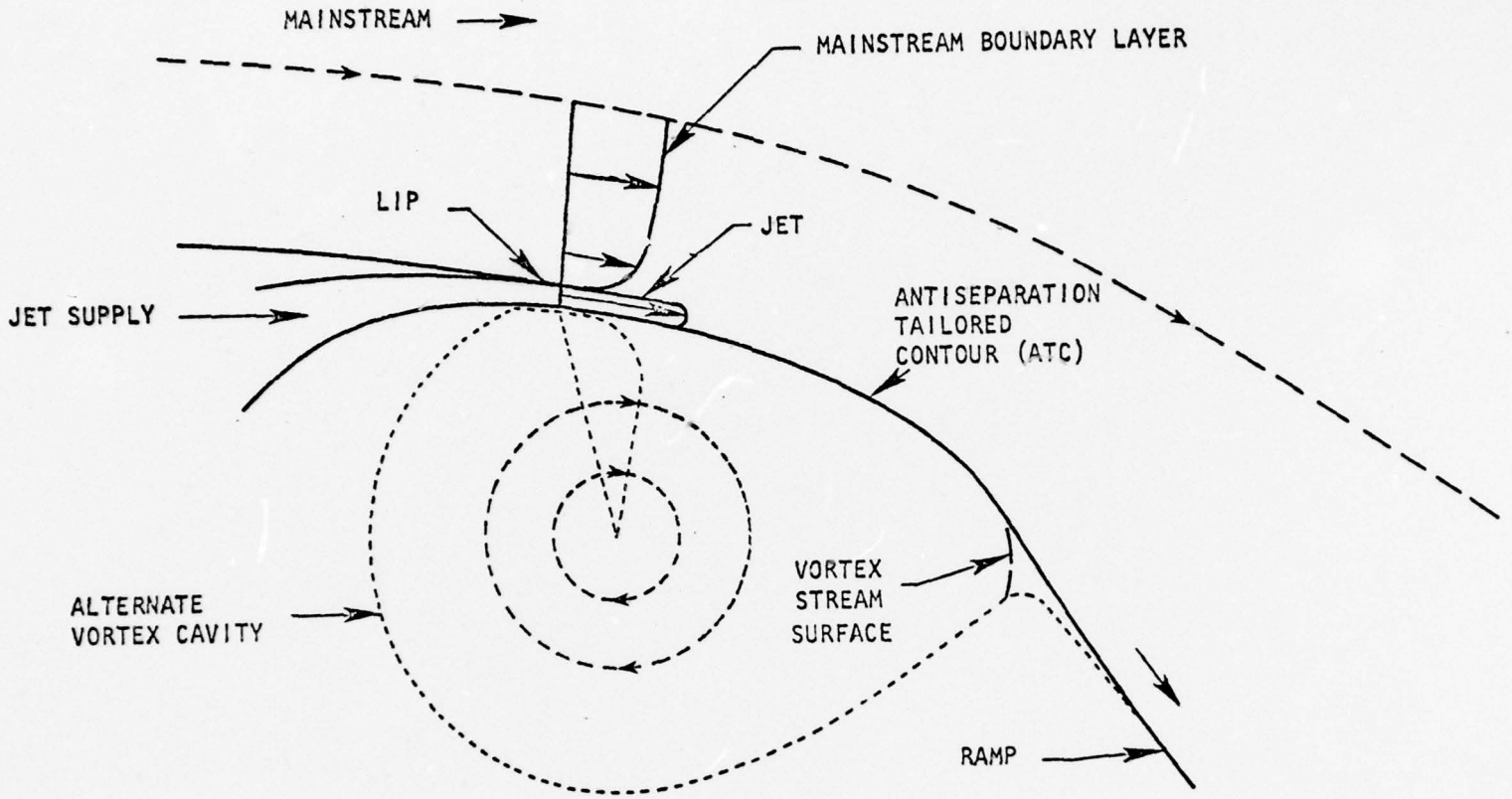

FIGURE 2.0-1. SCHEMATIC OF ATC AND TV ACTIVE DIFFUSION CONTROL DEVICES

3.0 APPARATUS

3.1 Rheoelectric Analog Facility

The rheoelectric analog facility shown in Figure 3.1-1 is the preliminary design tool used in the establishment of augmentor antiseparation tailored contours (ATC) and diffuser wall contours. A deformable conducting copper surface is inserted into the analog facility to model full scale ejector/augmentor configurations. The mapping of inviscid flows for ATC/diffuser contours is achieved in the rheoelectric facility by investigating the generated voltage gradients between the conducting contours in a two-dimensional mode. The field produced in the conducting medium is mathematically analogous to the potential for the fluid flow of an incompressible, inviscid fluid about the desired ATC/diffuser contours. The basic principles of the rheoelectric analog facility are given in Reference 6.

The designing of short ATC/diffuser contours for ejector testing is completed when the rheoelectric analog results are used in conjunction with a turbulent boundary layer analysis to verify that the flow will be either completely attached along the entire diffuser wall or attached as far as possible. Given the required geometry of the desired ejector/augmentor, the diffuser length, L_D, diffuser area ratio, A_3/A_2, and the boundary layer thickness at the blowing lip, inviscid pressure distributions on the ATC/diffuser contours are obtained in the rheoelectric analog facility and then analyzed with an in-house turbulent boundary layer routine that calculates boundary layer characteristics and separation criteria along the ATC. With the aid of the turbulent boundary layer routine, the ATC/diffuser walls are optionally designed through an iteration procedure to allow rapid diffusion of the internal turbulent flow, control boundary layer thickness, and minimize diffuser losses. The final shaping of the contour produces a predicted stable turbulent boundary layer and a uniform exit velocity profile at the end of the ATC. Results of this design technique are shown in Section 5.2.2.

3.2 Ejector/Augmentor Test Bed

Shown in Figure 3.2-1 is the suspended test bed of the ejector/augmentor facility used in the ejector short diffuser studies. The facility is located

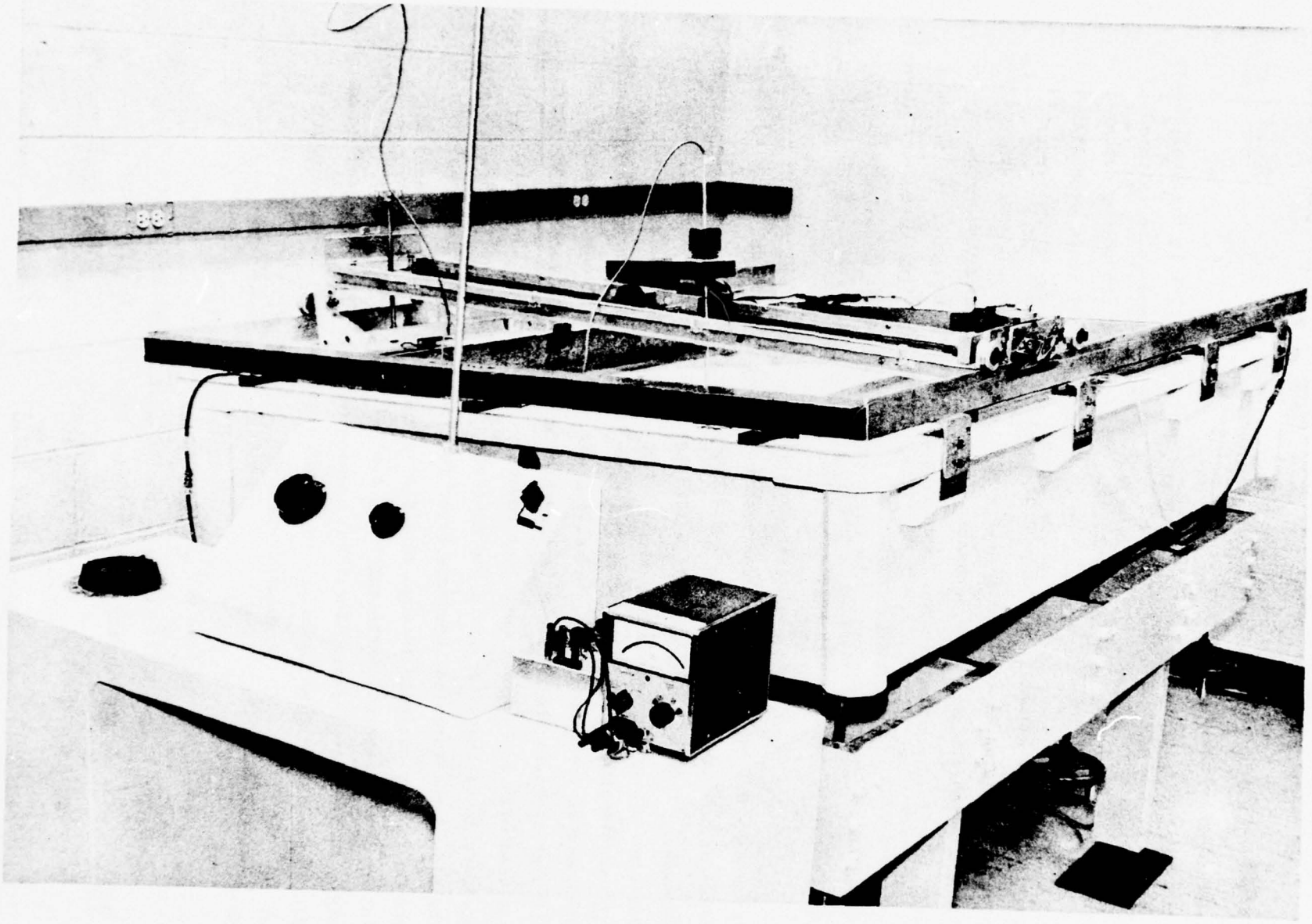

FIGURE 3.1-1. RHEOELECTRIC ANALOG FACILITY

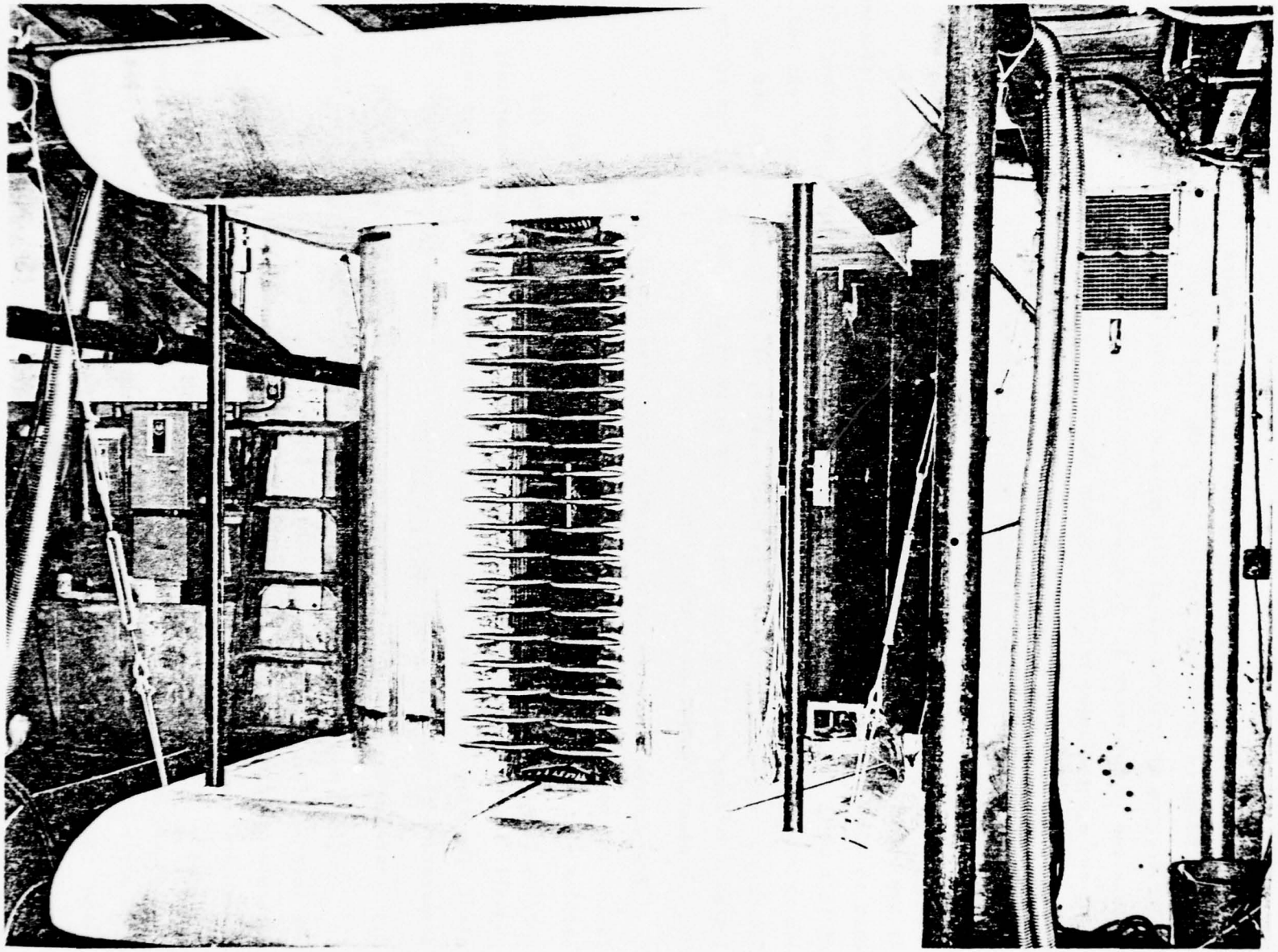

FIGURE 1. EJECTOR/AUGMENTOR TEST FACILITY

within the Vought Corporation High Speed Wind Tunnel complex. Designed and built at Advanced Technology Center, Inc., the facility was previously employed in the testing of trapped vortex diffusers with large area ratio augmentors as reported in Reference 3. Subsequent investigative research using the ejector/augmentor facility has shown the feasibility of mating ATC boundary layer control (BLC) with large area ratio thrust augmentors.

A schematic of the basic ejector test bed used is shown in Figure 3.2-2. The ATC diffusion control device was incorporated into the facility by simply modifying the existing trapped vortex plenums, as shown in Figure 3.2-3. As may be seen in the schematic of Figure 3.2-2, a jack-screw arrangement is used to adjust and control the flexible diffuser wall contours. Shorter diffusers of 12.7 cm (5 Inch) and 20.32 cm (8 Inch) in length (Phase 1) were pre-formed, following rheoelectric analog criteria, and simply bolted into the ejector test bed. The modular design of constant area mixing walls, ATC diffusion device, and adjustable diffuser walls allows interchangeability on the ejector test bed to any desired ejector/augmentor combination.

Pressurized air supplied by the High Speed Wind Tunnel storage tanks to the ejector test bed is measured using calibrated A.S.M.E. orifice plate flow meters. The ejector test bed total mass flow and ATC blowing plenum mass flow are independently measured. Endwall nozzle and endwall lip blowing jets use a common flow meter and are measured separately also. The flow meters record total pressure, differential pressure, and total temperature of the high pressure air supplied.

3.3 Instrumentation and Data Systems

Detailed measurements of ejector/augmentor pressurized blowing parameters and internal flow quantities were obtained for evaluation and analysis. Hypermixing nozzle primary plenum pressures, P_{01} and P_{02}, ATC blowing slot plenum pressures, P_{0j}, and endwall jet nozzle plenum pressures, P_{0ew}, were measured by $\pm$ 17.24 N/cm^2 ($\pm$ 25 psig) Statham gage pressure transducers. All transducers were carefully calibrated with a reference U-tube mercury manometer. Flow meter and plenum total temperatures were measured with calibrated Chromel-Alumel thermocouples and a reference junction heater. The resultant thrust

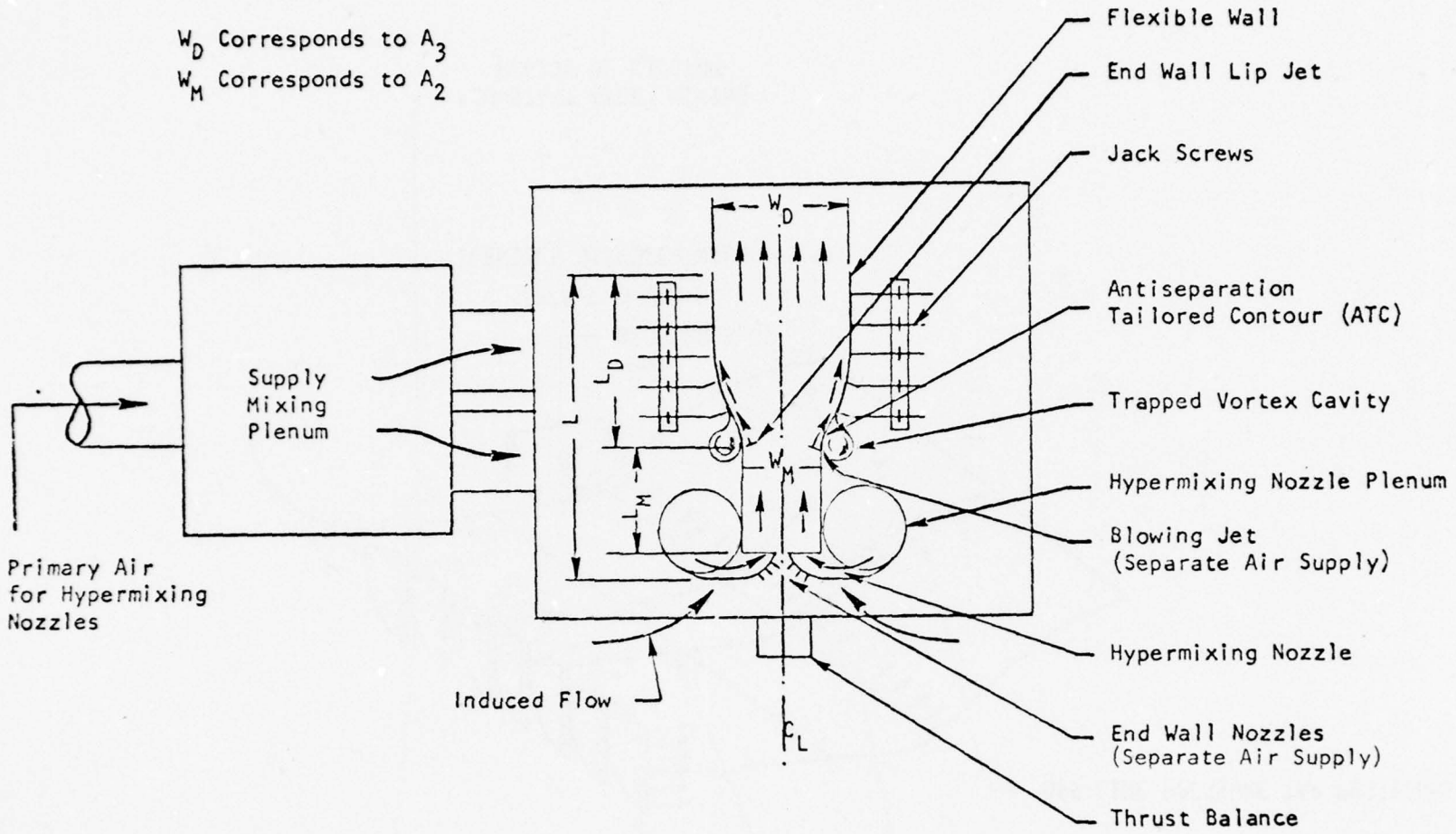

FIGURE 3.2-2. SCHEMATIC OF ARL EJECTOR COMBINED WITH THE ATC TRAPPED VORTEX AND ANTISEPARATION TAILORED CONTOUR DIFFUSERS.

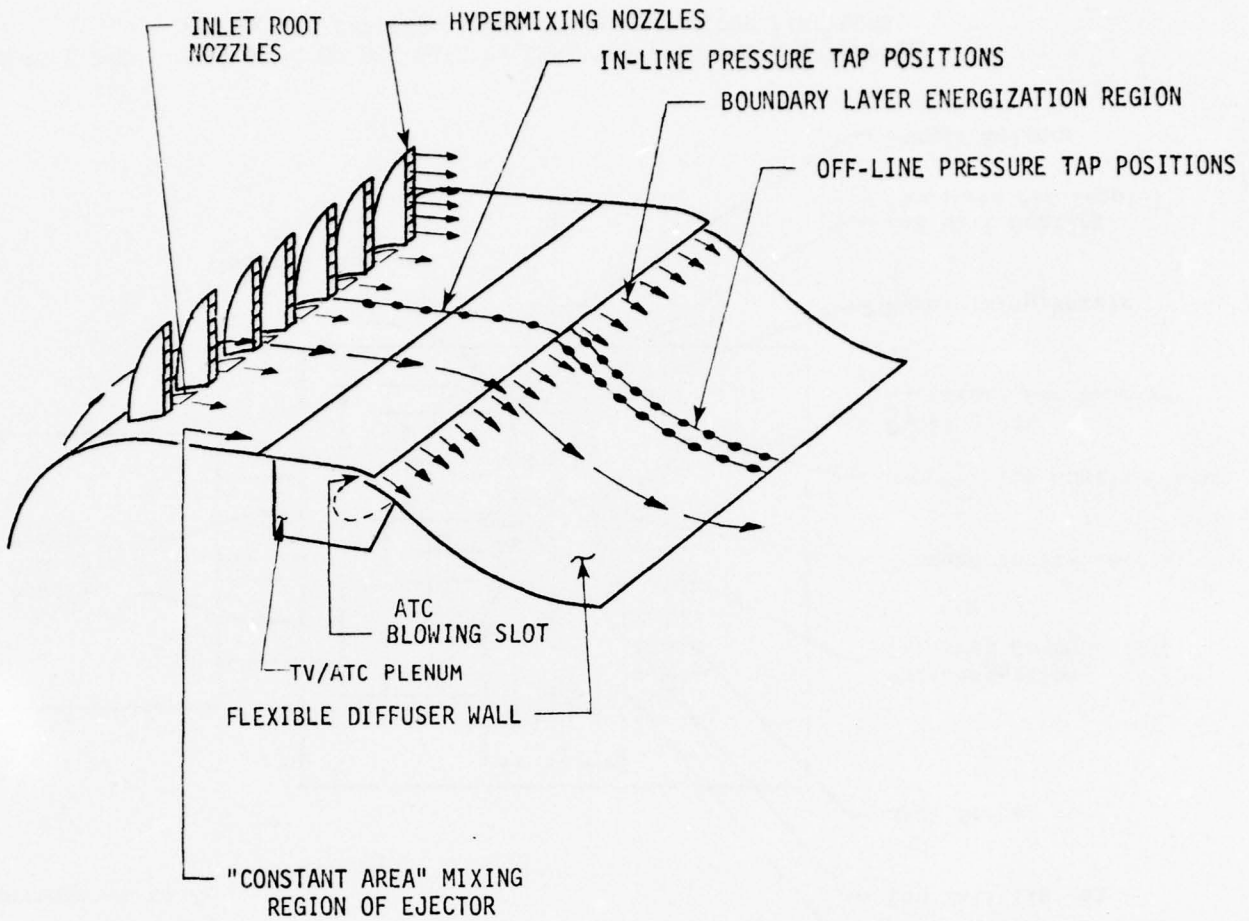

FIGURE 3.2-3. MODIFICATION OF EXISTING BLC PLENUM FOR ATC WALL AND LOCATION OF SURFACE PRESSURE ORIFICES

of the ejector/augmentor was monitored from a permanently mounted six component strain gauge balance.

Internal flow data from the operating ejector/augmentor consisted of measurements from fixed and adjustable instrumentation. Mixing, ATC, and diffuser wall surface pressure distributions were sensed by flush mounted static pressure taps. Individual ports were monitored using a 50 channel scanivalve. General orientation of surface pressure taps is illustrated in Figure 3.2-3. Static taps along the constant area mixing walls, spaced at 1.27 cm (1/2") intervals in the axial direction, were positioned in-line and off-line of primary hypermixing nozzles. Surface pressure measurements along the ATC diffusion wall were spaced 0.635 cm (1/4") apart both in-line and off-line, in the streamwise direction. Diffuser wall pressure taps were placed at 2.54 cm (1") intervals, from the ATC diffusion region to the diffuser exit plane.

A total and static pressure probe was manufactured and calibrated for measurement of blowing lip augmentor boundary layers. The total probe telescoped to a 0.0445 cm (0.0175") OD with a flattened 0.0305 cm (0.012") oval tip. A 0.070 cm (0.0275") OD static probe with a cone tip 0.635 cm (1/4") long had three surface taps 16 diameters downstream from the tip. Both probes were positioned with a micrometer mechanism which was mounted external to the augmentor flow. With the micrometer mechanism, the interchangeable probes could traverse normal and parallel to the flow and be positioned with an accuracy of 0.00254 cm (0.001").

Velocity profiles and skewness were measured with a fast response flow rake shown in Figure 3.3-1. The rake is composed of 17 total pressure probes 1.27 cm (1/2") apart, and a centrally mounted static probe of 0.070 cm (0.0275") OD brass tubing. For fast positioning,the flow rake was mated to a traversing sting mechanism that allowed placement of the rake at any position in the ejector internal flow.

Because of the low pressure levels involved,wall static, boundary layer, and internal flow rake pressures were monitored through an MKS Baritron digital voltmeter measuring pressures on a 0-100 mm Hg heated transducer to an accuracy of $\pm$0.01 mm of mercury. Ejector/augmentor blowing system measurements were monitored at all times by an on-site data reduction system. For purposes of data acquisition and reduction, however, all transducer and thermocouple electrical signals were balanced, amplified, and transferred on-line to the remote High Speed Wind Tunnel IBM 1800 computer.

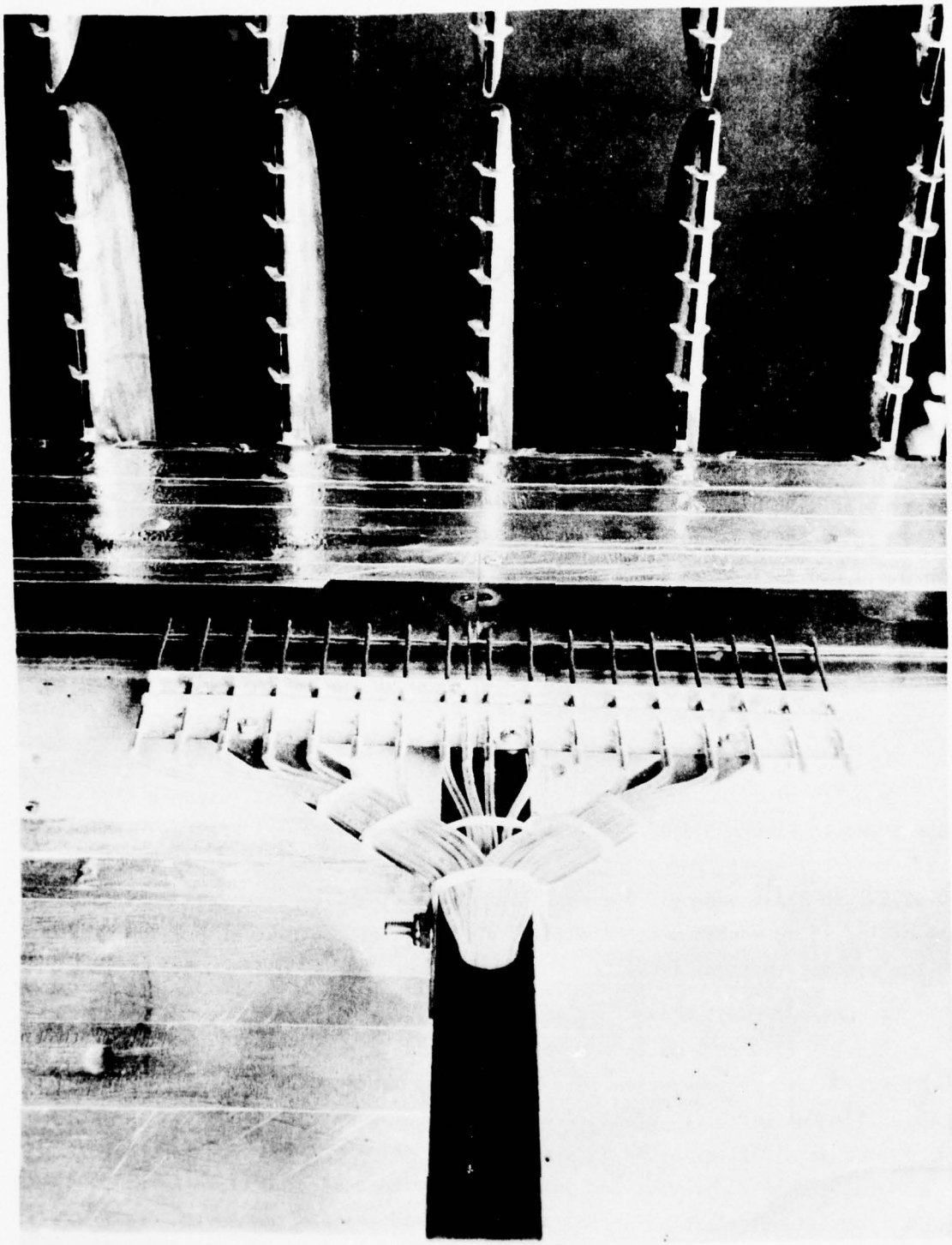

FIGURE 3.3-1. INTERNAL FLOW RAKE

Data was then recorded at a rate of 1 scan per second, while each data sample was 10 seconds in duration. A digital program on file in the IBM computer, especially written for the ejector/augmentor, reduced data for immediate output and evaluation.

3.4 ATC/Diffuser Configuration of Phase I

The ejector/augmentor configurations for Phase I testing, utilizing ARL's 2-D inlet and H-8 hypermixing ejector nozzles, were designed and fabricated for augmentor trade-off studies and internal flow measurements. Initial Phase I configurations, shown in Figure 3.4-1, had diffuser lengths of 50.8 cm (20") and 20.32 cm (8") with L_M = 12.7 cm (5"). Both ejector/diffusers were optimized as described in Section 4.0, for maximum augmentation ratios at diffuser area ratios of 1.50 and 2.00. The final Phase I ATC/diffuser was also tested at A_3/A_2 = 1.50 and 2.00 but with L_M = 25.4 cm (10") and L_D = 12.7 cm (5"). Contoured ATC/diffuser walls were designed corresponding to total diffuser lengths of 12.7, 20.32, and 50.8 cm, using the rheoelectric analog facility. A single ATC diffusion control contour, compatible with all six configurations was designed, fabricated, and installed into the existing trapped vortex plenums. Provisions were made for wall pressure, blowing lip boundary layer, and internal flow measurements according to the techniques outlined in Section 3.3.

3.5 Optimized ATC/Diffuser of Phase II

The optimized ATC/diffuser configuration, with the constraints finalized through the Contract Technical Monitor, adhered to specific dimensions and was extensively tested. The optimized configuration employed the two-dimensional ARL inlet and H-8 hypermixing ejector nozzles. Shown in Figure 3.5-1 at an area ratio of 2.0, the optimum ATC/diffuser contour was designed in the rheoelectric analog facility with L_M = 12.7 cm (5") and L_D = 29.85 cm (11.75") for a range of diffuser area ratios up to 2.50. Previous and Phase I empirical results were used in the design of the optimum ATC/diffuser. A base line straight wall diffuser as well as ARL configuration 'F' are also shown in Figure 3.5-1. As in Phase I the constant area mixing width, W, is 25.4 centimeters.

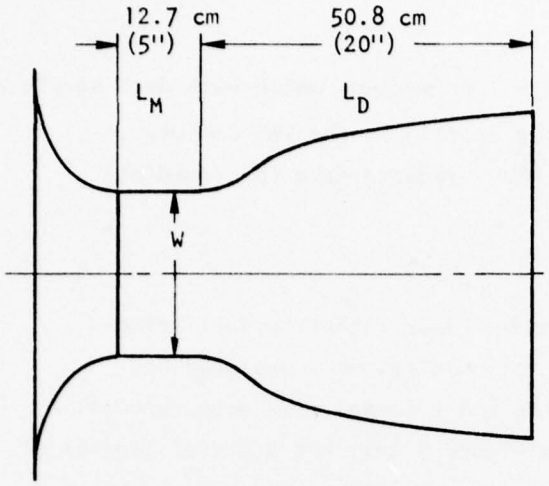

AR = 1.5, 2.0

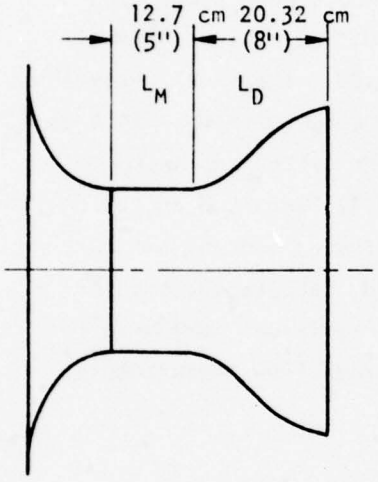

AR = 1.5, 2.0

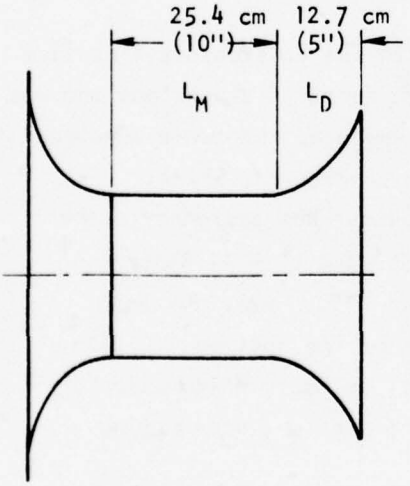

AR = 1.5, 2.0

NOTE: Configurations shown are H-8/ATC Diffusers at A_3/A_2 = 2.0 with W = 25.4 cm (10")

FIGURE 3.4-1. PHASE I ATC DIFFUSER CONFIGURATIONS

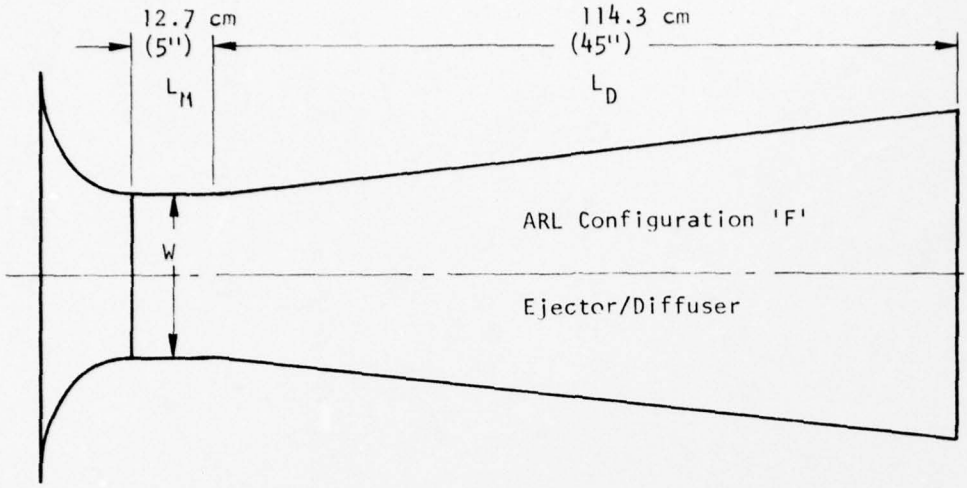

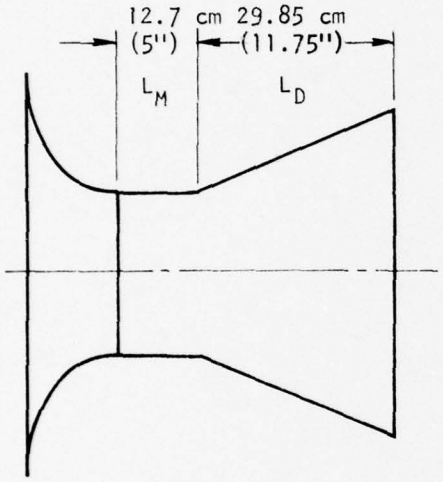

Base Line
H-8/Straight Wall
Ejector/Diffuser

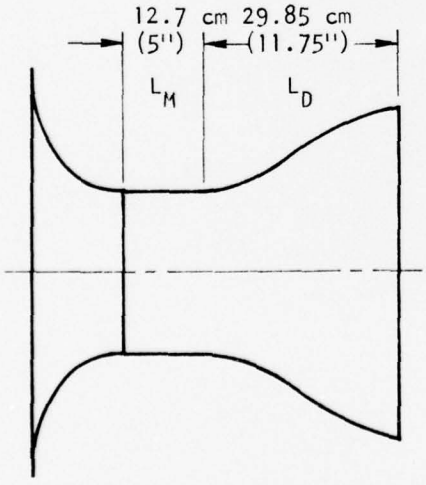

Optimized
H-8/ATC
Ejector/Diffuser

NOTE: All Configurations Shown at A_3/A_2 = 2.0 and W = 25.4 cm (10")

FIGURE 3.5-1. OPTIMIZED ATC/DIFFUSER WITH BASELINE CONFIGURATIONS

4.0 TEST PROCEDURE

To achieve optimum levels of augmentation performance with short ATC ejector/augmentors, an experimental testing procedure was developed and implemented. For each particular ejector/augmentor configuration, prior knowledge of flow quantities such as blowing lip and endwall boundary layer characteristics, wall pressures, and internal flow skewness does not exist. Balanced values of ATC/diffuser and endwall nozzle blowing rates in the configuration are required for high levels of augmentation. Figure 4.0-1 shows the location and orientation of the BLC endwall jet nozzles, endwall lip blowing jets, and ATC blowing slot and diffusion wall in a short diffuser, high area ratio configuration. A matrix of ATC and endwall blowing rates must be run, and the data analyzed, to determine the proper levels of blowing for efficient boundary layer energization and endwall diffusion control for each thrust augmentor configuration.

With the hypermixing nozzle plenums pressurized to P_{01} = 2.54 - 25.4cm (1 - 10") Hg, the ATC and endwall blowing rates are varied systematically in the blowing matrix procedure. An example of an endwall blowing optimization run can be seen in Figure 4.0-2. For this baseline straight wall diffuser augmentor the only BLC control variable is the endwall blowing rate. With the configuration installed in the ejector test bed, the endwall blowing rate, $\dot{m}_{ew}$, is increased until the endwall boundary layer is completely overblown. Data scans of ejector augmentation ratio, ϕ, are taken as $\dot{m}_{ew}$ is reduced until the endwall boundary layer completely separates. The data is then analyzed to determine the proper $\dot{m}_{ew}$ that will energize the boundary layer for attainment of ϕ_{max}. The straight wall diffuser in Figure 4.0-2 with a low diffuser area ratio of 1.25 at P_{01} = 2.54cm (1.0") Hg, shows a ϕ_{max} of approximately 1.59 with $\dot{m}_{ew}$ = 0.0612 kg/sec (0.135 lbm/sec). A similar straight wall configuration, Figure 4.0-3, at a higher area ratio of 1.50, exhibits the same trends in ϕ with variation in endwall blowing, where ϕ_{max} = 1.69 with $\dot{m}_{ew}$ = 0.0658 kg/sec (0.145 lbm/sec).

Below the proper level of $\dot{m}_{ew}$ the boundary layer is under blown and momentum and skin friction losses degrade augmentation ratio. In high area ratio diffusers, insufficient endwall blowing allows endwall separation and rapid degradation of performance. Above the optimum level of $\dot{m}_{ew}$, the boundary layer is attached and over-blown with a more gradual loss in augmentation ratio stemming from the utilization of the air supply in the endwall jets rather than in the primary nozzle where it will entrain additional air.

FIGURE 4.0-1. ORIENTATION OF ATC AND ENDWALL BLOWING JETS

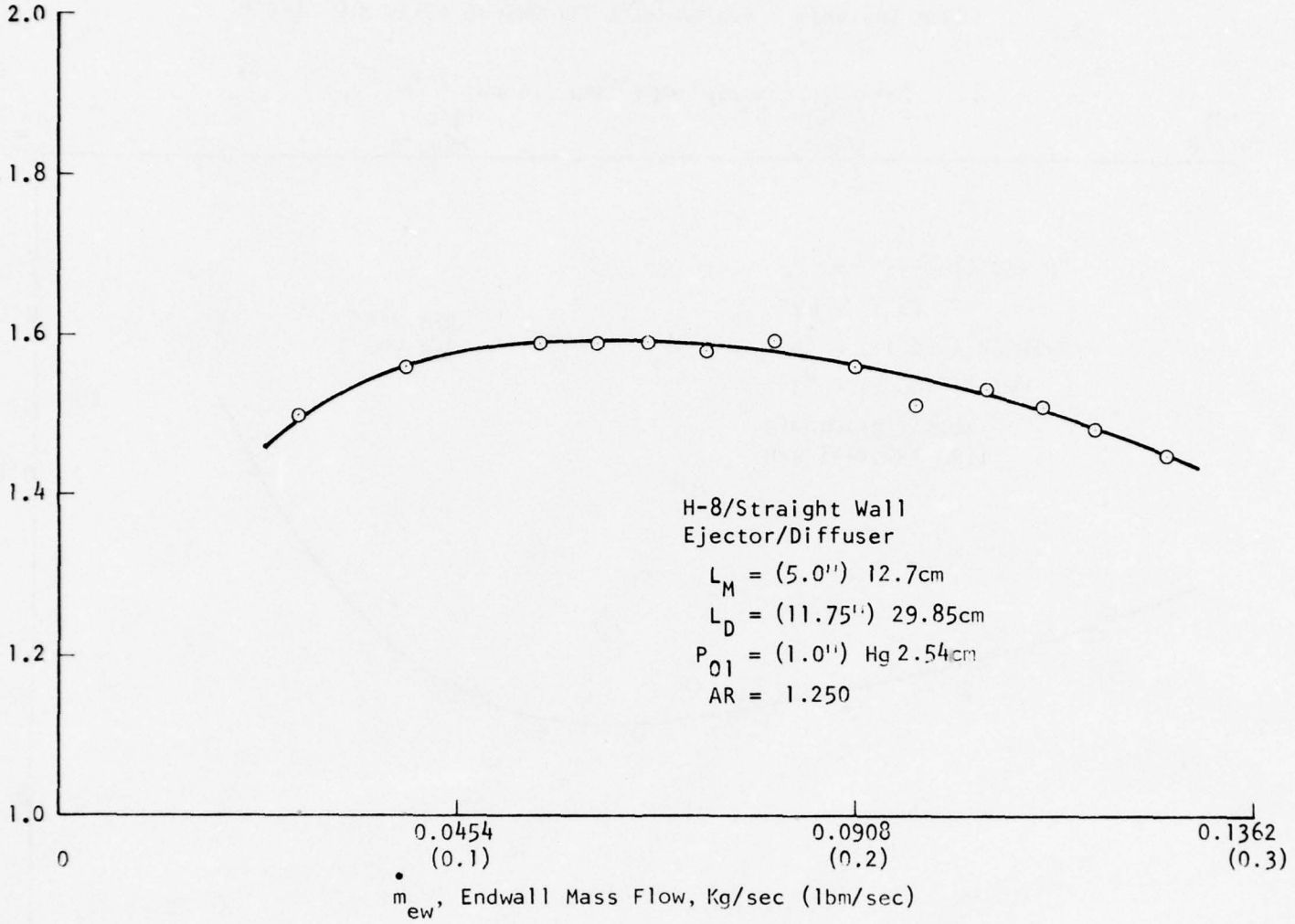

FIGURE 4.0-2. VARIATION OF ENDWALL BLOWING FOR A STRAIGHT WALL EJECTOR/DIFFUSER WITH A_3/A_2 = 1.25

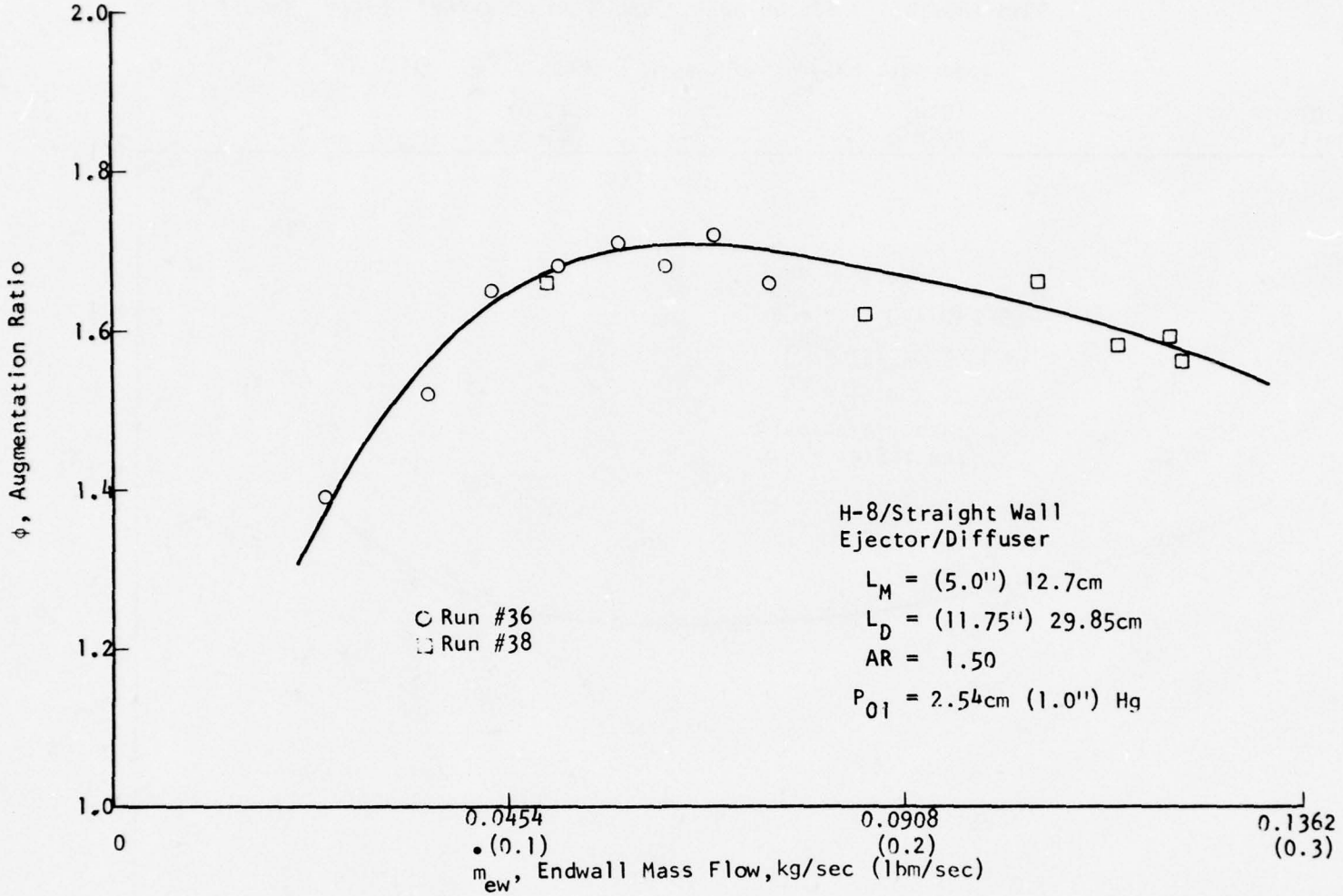

4.0-3. VARIATION OF ENDWALL BLOWING FOR A STRAIGHT WALL EJECTOR/DIFFUSER WITH A_3/A_2 = 1.50

With ATC/diffuser configurations, a similar blowing matrix technique is used for optimization of BLC blowing levels. Figures 4.0-4 and 4.0-5 show the results of a blowing matrix for a large area ratio, A_3/A_2 = 2.10, short diffuser, L_D = 29.85cm (11.75"), ejector/augmentor. The trend of ϕ in Figure 4.0-4, for fixed rates of ATC blowing slot mass flow, $\dot{m}_{ATC}$, is clearly defined and similar to that of the straight wall diffuser. For ATC/diffuser configurations, an initial value of $\dot{m}_{ATC}$ is determined from the observed attachment of the diffuser wall flow using a flow visualization technique of internal tufts and also by sensing diffuser exit plane pressure values. With the diffuser walls then attached and/or over-blown, $\dot{m}_{ew}$ is varied until the optimum value has been determined. The proper level of $\dot{m}_{ATC}$ is then investigated in a similar procedure, with the correct value of $\dot{m}_{ew}$ held fixed. Figure 4.0-5 shows the optimization of $\dot{m}_{ATC}$ and an improved configuration augmentation performance peak of ϕ_{max} = 1.84.

To summarize, the ϕ performance of each particular ejector/augmentor configration is continuously scanned during the blowing optimization by the on-site data system and then recorded by remote IBM 1800 computer. At the proper levels of blowing for peak performance, computer scans are taken and all internal flow quanitities are measured.

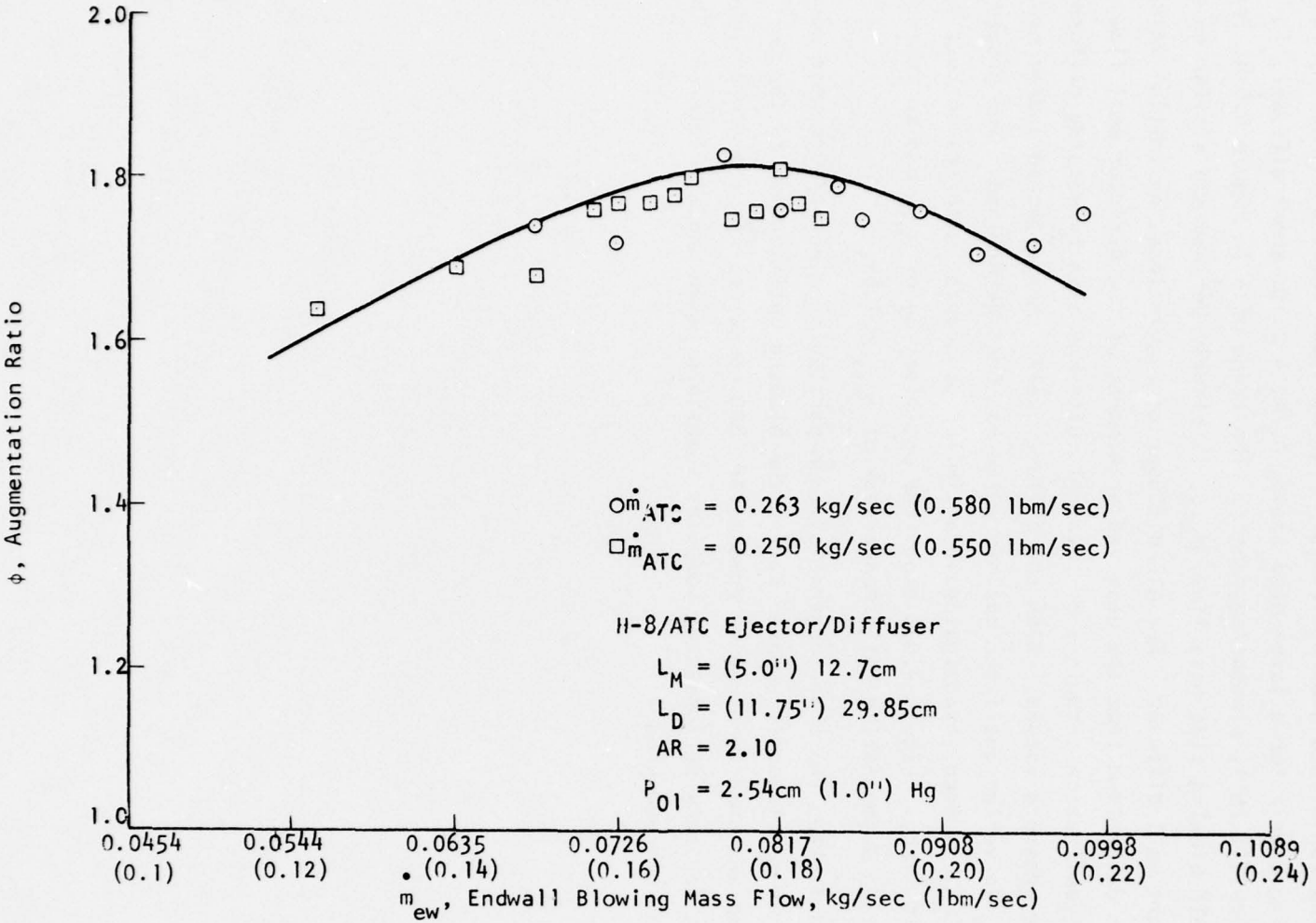

FIGURE 4.0-4. OPTIMIZATION OF ENDWALL BLOWING FOR A H-8/ATC EJECTOR/ DIFFUSER WITH ATC SLOT BLOWING RATE FIXED

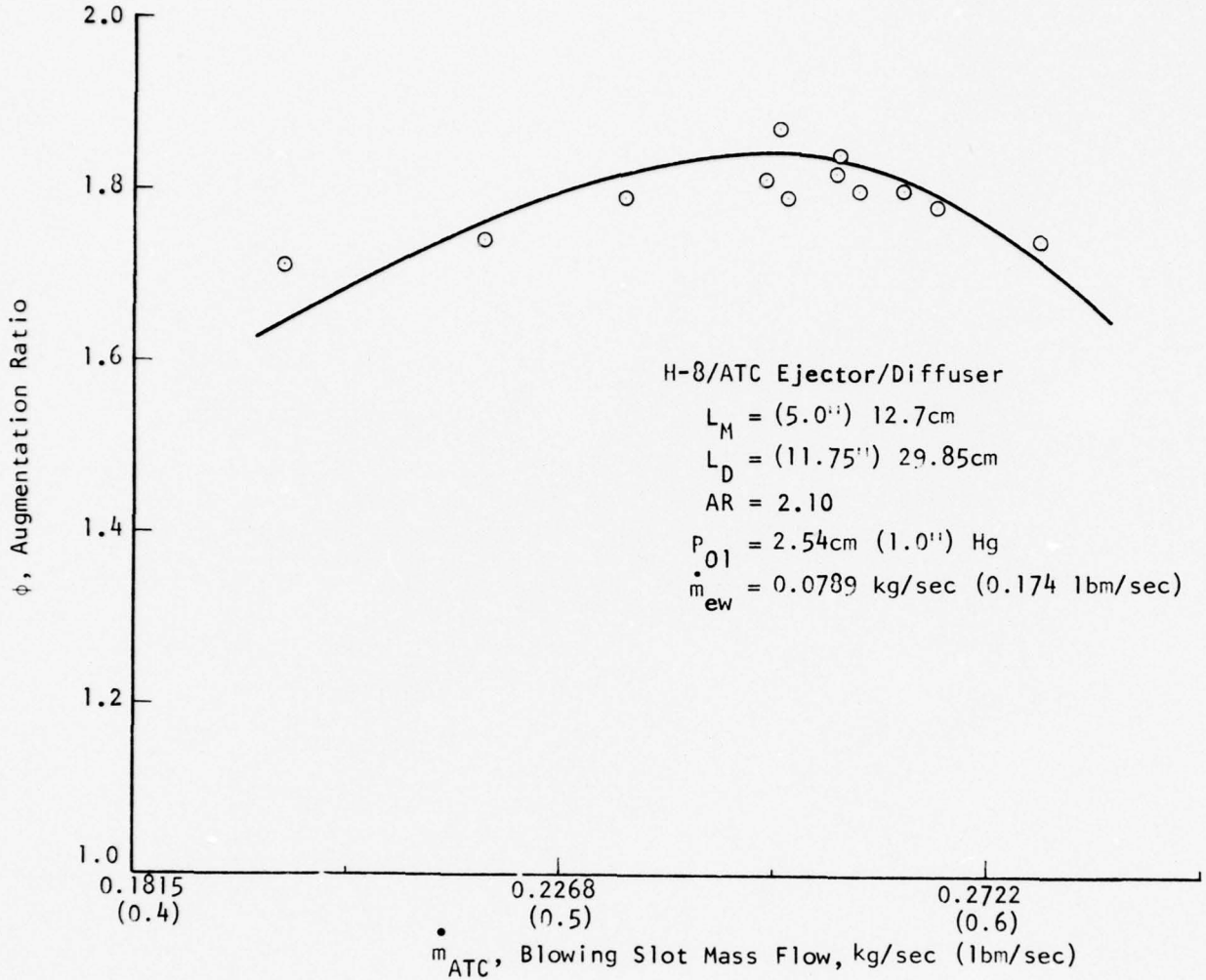

FIGURE 4.0-5. OPTIMIZATION OF ATC SLOT BLOWING FOR A H-8/ATC EJECTOR/ DIFFUSER WITH THE PROPER ENDWALL BLOWING RATE FIXED

5.0 RESULTS AND DISCUSSION

5.1 Basic Augmentor Flow Measurements- Phase I

The objective of Phase I testing was modification and calibration of the ejector test facility and identification of the important parameters which influence the design of compact ejectors. Prior to installation of ejector configurations,the ejector test bed was instrumented and pressurized for measurement of induced thrust loads. Proper alignment of the suspension system minimized the levels of test bed induced thrusts. The results of adjustment of the suspension system in Figure 5.1-1 shows the variation of induced thrust loads with plenum pressurization. The test bed induced loads are less than 0.5 percent of the ejector thrust levels for the entire pressure range up to 25.4 centimeters (10 inches) of mercury

5.1.1 Configuration 'F' Comparison

Originally high thrust augmentation ratios were obtained by Aerospace Research Laboratories (ARL), Reference 2, for an ejector equipped with ARL/H-4 primary hypermixing nozzles and a long 114.3 cm (45 ") straight wall diffuser termed configuration 'F', and shown schematically in Figure 3.5-1. However, because of the need for superior performance by hypermixing nozzles at the much shorter diffuser lengths of the present study, advanced ARL/H-8 hypermixing nozzles, Reference 4, were utilized in Phase I as replacements for the original low aspect ratio ARL/H-4 nozzles.

In order to further establish the validity of the new ARL/H-8 short diffuser results to be obtained in the augmentor facility, it was decided to perform an investigation utilizing the ARL/H-8 nozzles in conjunction with the 114.3 cm (45") Configuration 'F' straight wall diffuser. Based on the results of Reference 4, it was expected that if the augmentor facility was operating properly, the higher skin friction losses imposed in the long diffuser by the more rapidly expanding H-8 nozzles would slightly reduce the augmentation levels previously developed by the H-4 nozzles. As was expected, as shown in Figure 5.1-2, the long 114.3 cm (45") diffuser with H-8 nozzles generated a 2-5 percent loss in augmentation as compared to the H-4 nozzles. Since this difference was in agreement with the experimental results presented in Reference 4, the validity of the high performance augmentation results to be obtained with the very short diffusers and ARL/H-8 nozzles of the present study was established.

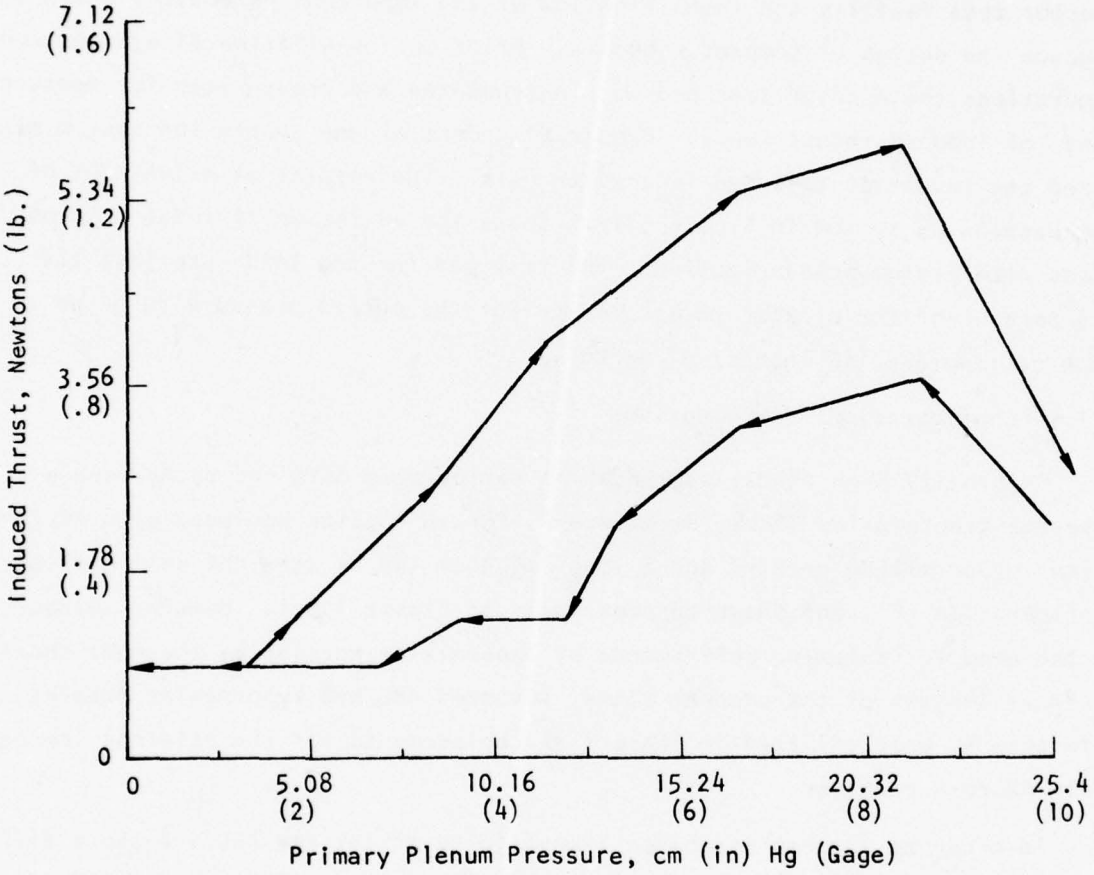

FIGURE 5.1-1. FORCE INDUCED ON EJECTOR TEST BED DUE TO PRESSURIZATION OF SYSTEM

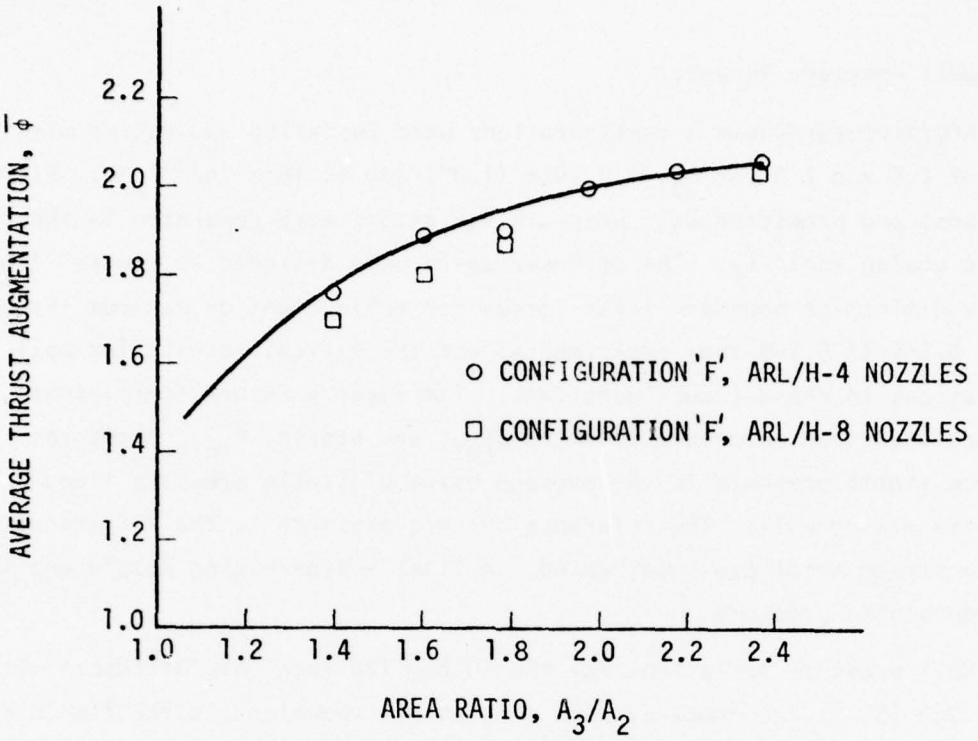

FIGURE 5.1-2. VARIATION OF THRUST AUGMENTATION WITH EXIT AREA RATIO FOR ARL CONFIGURATION 'F'

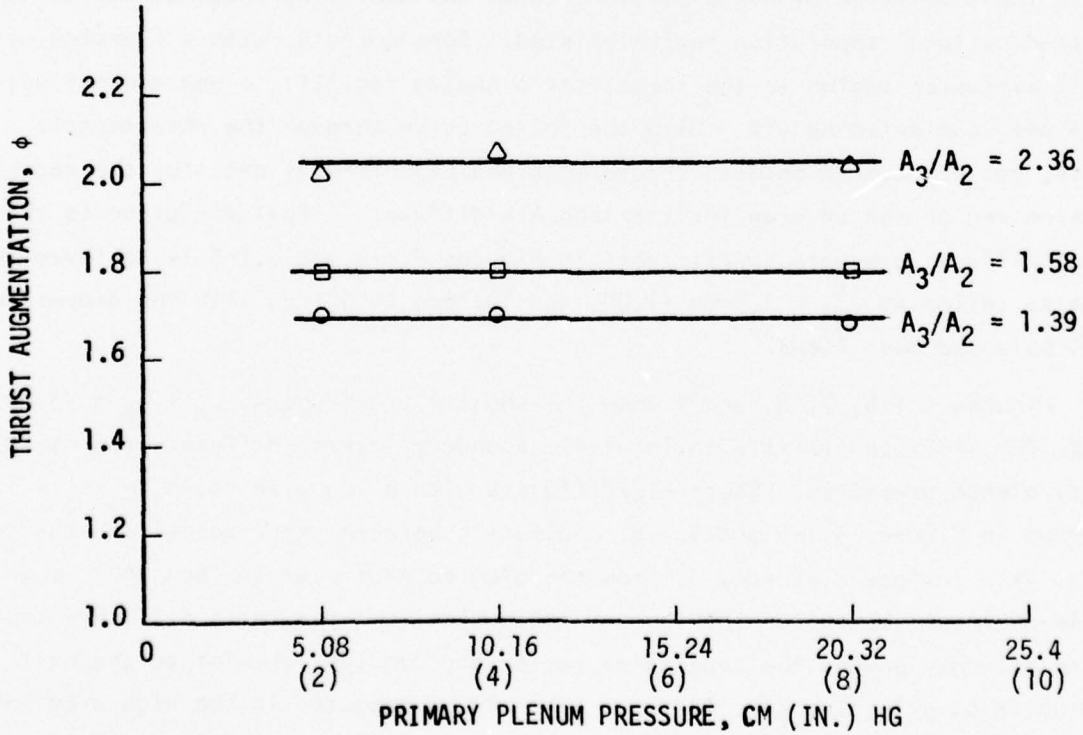

FIGURE 5.1-3. VARIATION OF THRUST AUGMENTATION RATIO WITH PLENUM PRESSURE FOR CONFIGURATION 'F' WITH H-8 NOZZLES

5.1.2 Wall Pressure Surveys

ATC/diffuser Phase I configurations were installed and tested with area ratios of 1.5 and 2.0 for P_{01} = 2.54cm (1.0") and 10.16cm (4.0") Hg. Diffuser wall shapes and predicted wall pressure variations were generated in the rheoelectric analog facility. The diffuser walls were designed to control flow diffusion and minimize boundary layer losses for achievement of maximum thrust. Figures 5.1-4 to 5.1-9 show experimental and theoretical results for wall pressure distributions in Phase I configurations. The local pressure coefficients, C_p, are calculated from reference dynamic, q_{ref}, and static, P_{ref}, pressures. The reference static pressure is the average value of static pressure along the constant area mixing wall. The reference dynamic pressure is the difference between the free stream total pressure behind (in-line) a hypermixing nozzle and the reference static pressure.

Wall pressure variations for the 50.8cm (20 inch) ATC/diffusers with L_M = 12.7cm (5.0") are compared with theoretical rheoelectric results in Figures 5.1-4 and 5.1-5. The predicted theoretical results were obtained from the contour used in the analog facility. Initial testing with these longer diffusers indicated that at the completion of ATC diffusion, which was occurring somewhat earlier than predicted, a local separation region existed. Consequently, with a redesign of the ATC diffusion region in the rheoelectric analog facility, a new contour was placed over the existing ATC. With the faired curve through the rheoelectric results, good agreement between theoretical and experimental data for the redesigned diffusion region can be seen for the long ATC/diffusers. Full diffusion to theoretical diffuser pressure coefficients in Figures 5.1-4 and 5.1-5 is achieved for both area ratios at P_{01} = 2.54cm (1.0") and 10.16cm (4.0") Hg with the proper levels of BLC balanced mass flows.

Figures 5.1-6, 7, 8, and 9 show the short ATC/diffusers, $L_M + L_D$ = 33.02 cm (13") and 38.10cm (15"), sensitivity to local lip boundary layers, diffuser area ratio, and primary plenum pressures. Short ATC/diffusers with a low area ratio, A_3/A_2 = 1.50, are shown in Figures 5.1-6 and 5.1-8. Deviation between experimental and theoretical results at a surface distance, S, from the blowing slot near 10.16cm (4") is an example of local separation in Figure 5.1-6. With low area ratio diffusers the flow re-attaches beyond the separation region and remains attached to the exit plane while experiencing some losses. As would be expected in the high area ratio (A_3/A_2 = 2.0), very short diffusers of Figures 5.1-7 and 5.1-9 regions of local

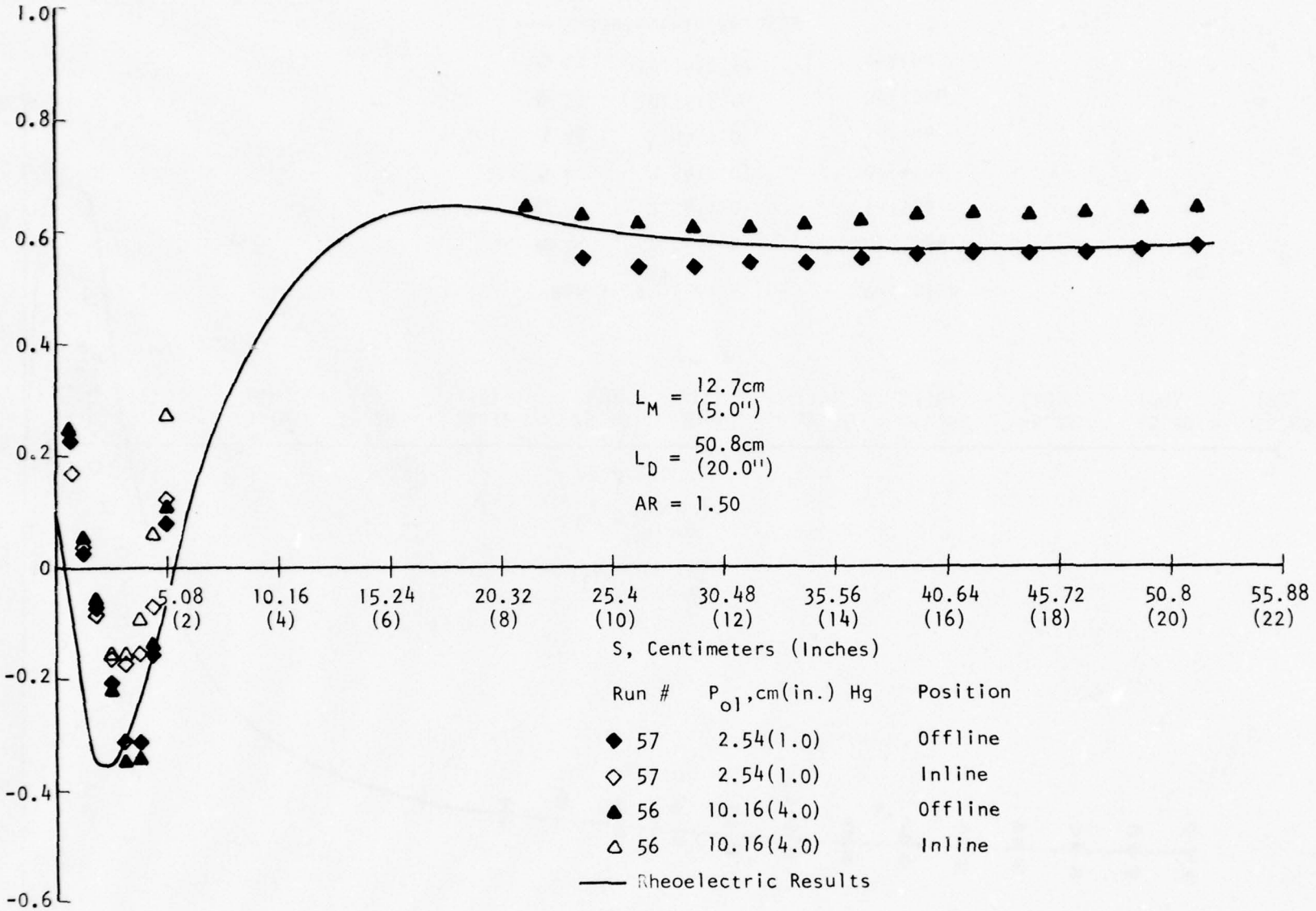

FIGURE 5.1-4. VARIATION OF PRESSURE COEFFICIENT WITH SURFACE DISTANCE ALONG THE DIFFUSER FOR THE 50.8cm (20 INCH), 1.50 AREA RATIO DIFFUSER

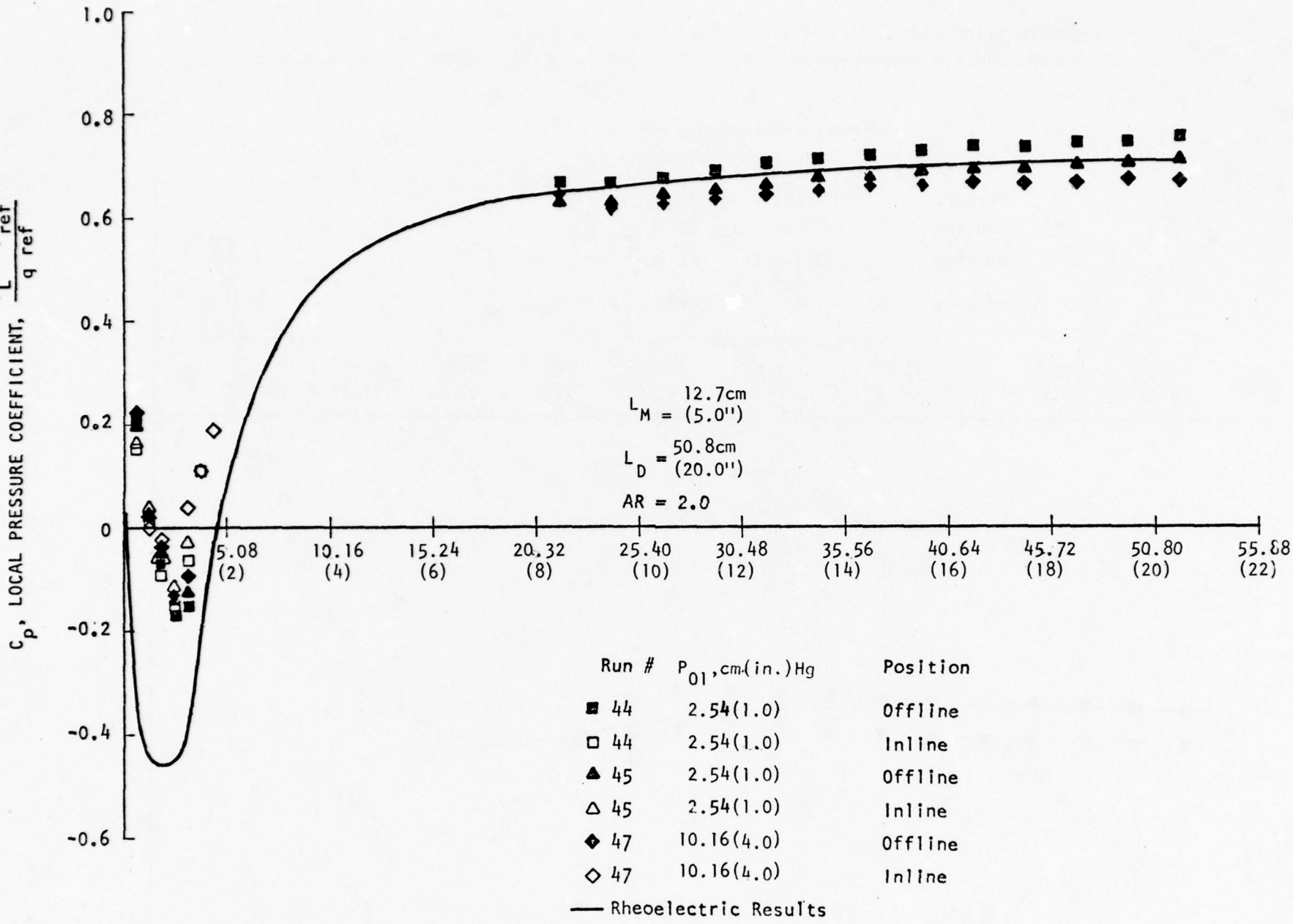

FIGURE 5.1-5. VARIATION OF PRESSURE COEFFICIENT WITH SURFACE DISTANCE ALONG THE DIFFUSER FOR THE 50.8 CM (20 INCH), 2.0 AREA RATIO DIFFUSER

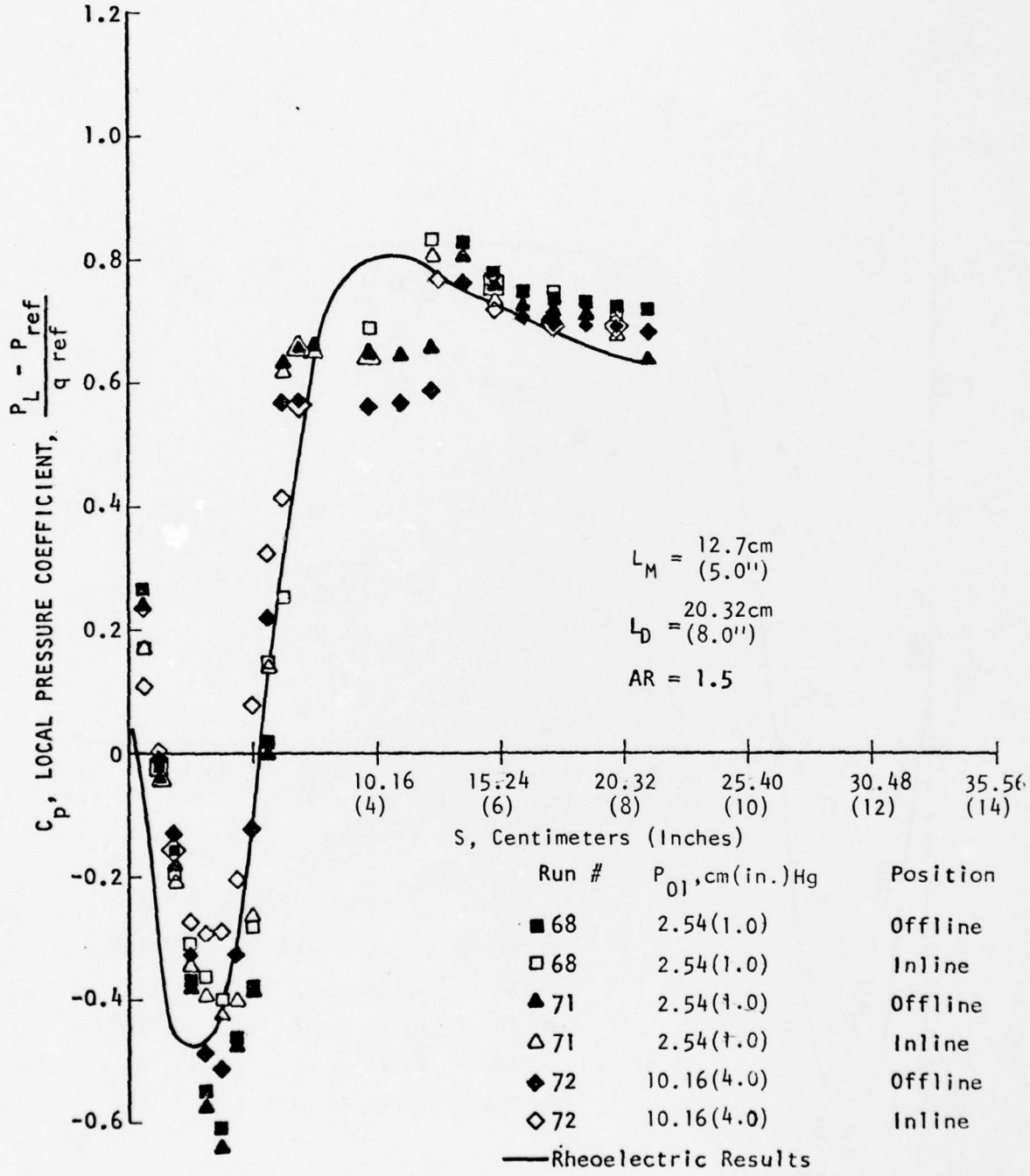

FIGURE 5.1-6. VARIATION OF PRESSURE COEFFICIENT WITH SURFACE DISTANCE ALONG THE DIFFUSER FOR THE 20.32CM (8 INCH), 1.50 AREA RATIO DIFFUSER

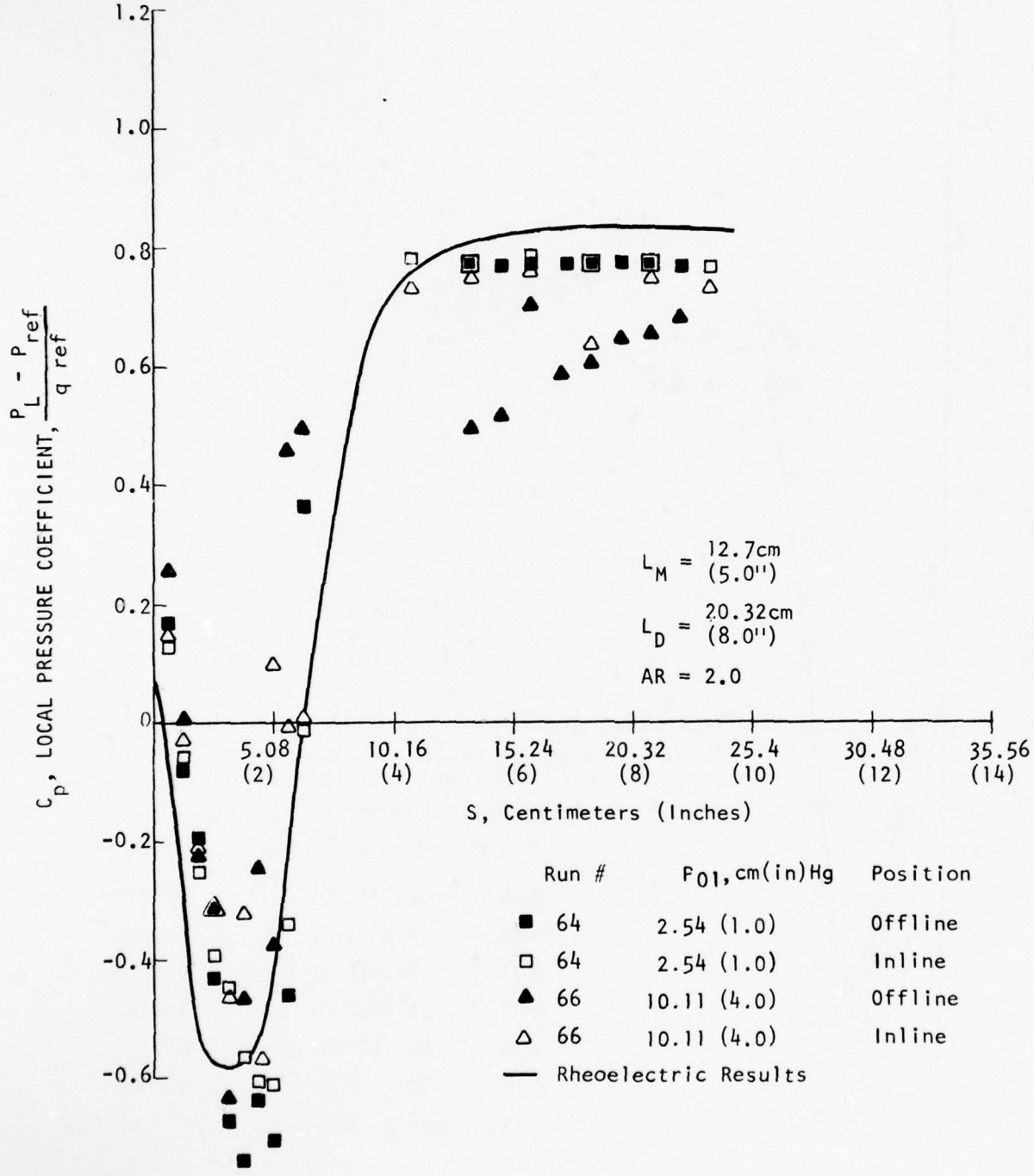

FIGURE 5.1-7. VARIATION OF PRESSURE COEFFICIENT WITH SURFACE DISTANCE ALONG THE DIFFUSER FOR THE 20.32CM (8 INCH), 2.0 AREA RATIO DIFFUSER

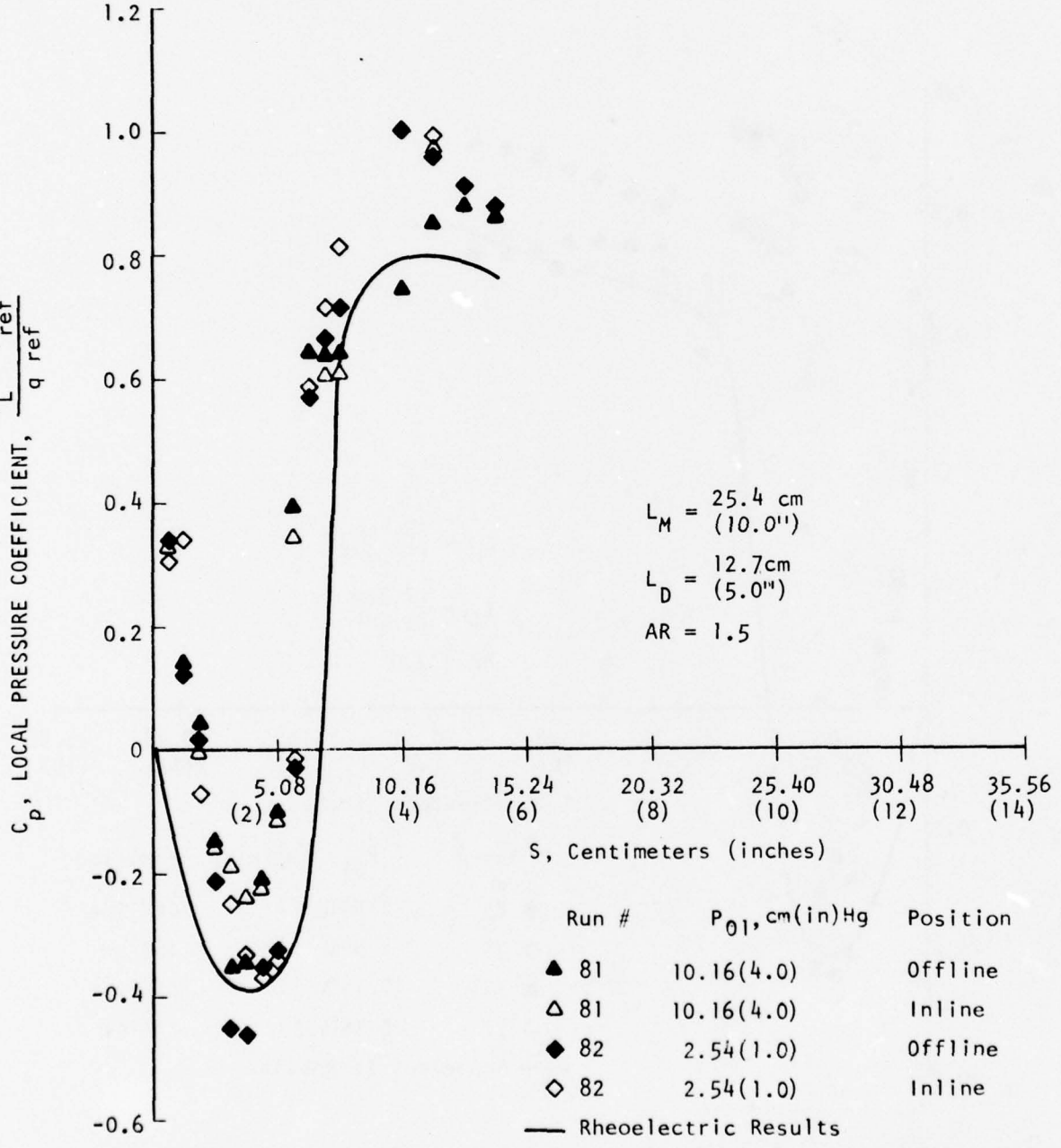

FIGURE 5.1-8. VARIATION OF PRESSURE COEFFICIENT WITH SURFACE DISTANCE ALONG THE DIFFUSER FOR THE 12.7CM (5 INCH) 1.50 AREA RATIO DIFFUSER

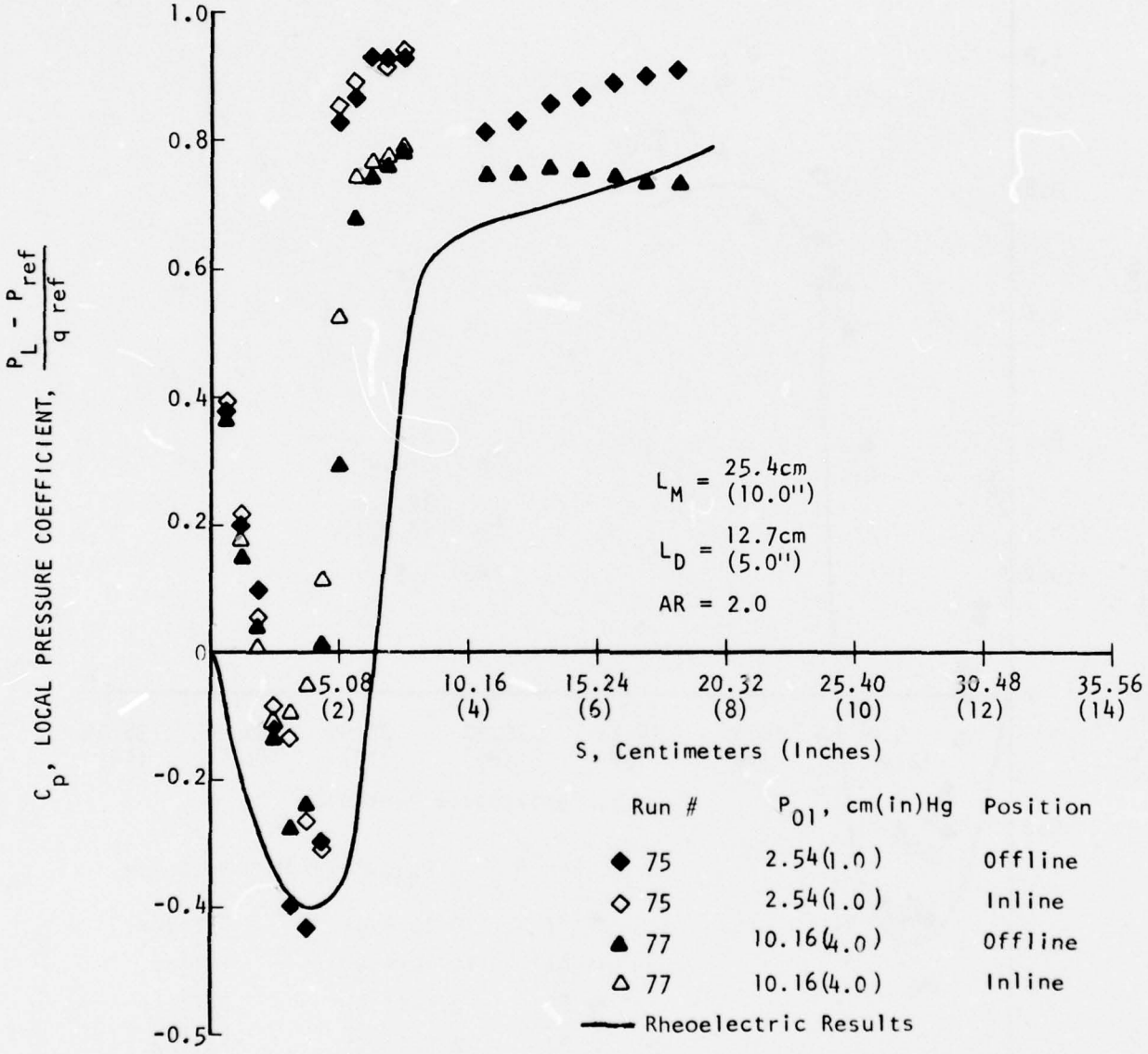

FIGURE 5.1-9. VARIATION OF PRESSURE COEFFICIENT WITH SURFACE DISTANCE ALONG THE DIFFUSER FOR THE 12.7CM (5 INCH), 2.0 AREA RATIO DIFFUSER

boundary layer separation are seen to occur for the off-line, P_{01} = 10.16cm (4") Hg results. In the very short diffusers (L_D = 12.7cm (5.0")), Figures 5.1-8 and 5.1-9 indicate that the short diffuser wall flow is actually being over diffused when compared to the predicted results. Notable for the short diffuser configurations tested is the fact that in-line and off-line pressure distributions exhibit different localized diffusion characteristics. Since the ATC mixing and diffuser regions are designed with predicted values of lip boundary layer momentum thicknesses, these data indicate a nonuniform spanwise variation of ejector/mixing wall boundary layer losses at the blowing lip location.

In the lip region where the boundary layer was sufficiently energized by the ATC active diffusion device, the wall pressures of all Phase I configurations correlated reasonably well with theoretical results. Perturbations from rheoelectric data in the lip region are attributed to ATC jet effects. As can be shown, equilibrium conditions existing between the lip boundary layer and ATC slot boundary layer can cause a slight rise in static wall pressure immediately downstream of the slot. ATC blowing slot pressure coefficients reflect this local condition by the positive pressure coefficients at a surface distance from the slot approaching zero.

5.1.3 Boundary Layer Measurements

One of the primary factors which influence the design of compact ejectors with BLC is the distribution and characteristics of internal boundary layers at the blowing lip location. Since proper design of the ATC requires a knowledge of the actual momentum thickness distribution of the boundary layer immediately proceeding the ATC, total and static pressure surveys were obtained at transverse locations approximately 0.076cm (0.030") upstream of the blowing lip. The results of boundary layer surveys for Phase I configurations operating at optimum blowing rates and peak augmentation are tabulated in Figure 5.1-10. As readily noted from the summarized data, there is definitely a nonuniform distribution of momentum thickness and local free stream velocity behind the hypermixing nozzle array at the ATC blowing lip location. The inline momentum thicknesses are apparently due principally to the initial interaction of the inlet boundary layer with the hypermixing nozzle flow itself, since it is directly behind the lower slot of a nozzle. The boundary layers of the off-line, between, position appear to be thinner due to the

L_M cm(in)	L_D cm(in)	A_3/A_2	P_{01} Hg cm(in)	Position	Momentum Thickness, Θ, cm(in)	Local Free Stream Velocity V_∞, m/sec (ft/sec)
(5)12.7	(20)50.8	1.5	2.54(1.0)	Inline	(0.0174)0.0442	(83)25
(5)12.7	(20)50.8	1.5	2.54(1.0)	Intermediate	(0.0101)0.0256	(103)31
(5)12.7	(20)50.8	1.5	2.54(1.0)	Between	(0.0062)0.0157	(119)36
(5)12.7	(20)50.8	1.5	10.16(4.0)	Inline	(0.0094)0.0239	(169)52
(5)12.7	(20)50.8	1.5	10.16(4.0)	Intermediate	(0.0095)0.0241	(203)62
(5)12.7	(20)50.8	1.5	10.16(4.0)	Between	(0.0122)0.0310	(243)74
(5)12.7	(20)50.8	2.0	2.54(1.0)	Inline	(0.0169)0.0430	(112)34
(5)12.7	(20)50.8	2.0	2.54(1.0)	Intermediate	(0.0225)0.0572	(102)31
(5)12.7	(20)50.8	2.0	2.54(1.0)	Between	(0.0109)0.0277	(140)43
(5)12.7	(20)50.8	2.0	10.16(4.0)	Inline	(0.0173)0.0439	(217)66
(5)12.7	(20)50.8	2.0	10.16(4.0)	Intermediate	(0.0197)0.0500	(220)67
(5)12.7	(20)50.8	2.0	10.16(4.0)	Between	(0.0049)0.0125	(277)84
(5)12.7	(8)20.32	1.5	2.54(1.0)	Inline	(0.0096)0.0244	(81)25
(5)12.7	(8)20.32	1.5	2.54(1.0)	Intermediate	(0.0093)0.0236	(89)27
(5)12.7	(8)20.32	1.5	10.16(4.0)	Inline	(0.0056)0.0142	(161)49
(5)12.7	(8)20.32	1.5	10.16(4.0)	Between	(0.0062)0.0157	(215)66
(5)12.7	(8)20.32	2.0	2.54(1.0)	Inline	(0.0133)0.0388	(121)37
(5)12.7	(8)20.32	2.0	2.54(1.0)	Between	(0.0082)0.0210	(151)46
(5)12.7	(8)20.32	2.0	10.16(4.0)	Inline	(0.0092)0.0234	(167)51
(5)12.7	(8)20.32	2.0	10.16(4.0)	Between	(0.0059)0.0150	(216)66
(10)25.4	(5)12.7	1.5	2.54(1.0)	Inline	(0.0236)0.0600	(78)24
(10)25.4	(5)12.7	1.5	2.54(1.0)	Between	(0.0074)0.0188	(84)26
(10)25.4	(5)12.7	1.5	10.16(4.0)	Inline	(0.0094)0.0239	(148)45
(10)25.4	(5)12.7	1.5	10.16(4.0)	Between	(0.0080)0.0203	(162)49
(10)25.4	(5)12.7	2.0	2.54(1.0)	Inline	(0.0059)0.0150	(93)28
(10)25.4	(5)12.7	2.0	2.54(1.0)	Between	(0.0044)0.0112	(101)31
(10)25.4	(5)12.7	2.0	10.16(4.0)	Inline	(0.0100)0.0254	(134)41
(10)25.4	(5)12.7	2.0	10.16(4.0)	Between	(0.0064)0.0163	(149)45

FIGURE 5.1-10. PHASE I ATC/DIFFUSER BOUNDARY LAYER RESULTS

energizing effect of the inlet boundary layer control root nozzles, shown schematically in Figure 3.2-3, located immediately upstream of this blowing lip position.

For a primary plenum pressure of 2.54cm (1") of Hg, typical boundary layer velocity profiles that were obtained are shown in Figure 5.1-11 for positions directly behind (in-line) a primary hypermixing nozzle and between (off-line) two primary nozzles. The velocity profile, when compared to a turbulent 1/7th power profile for a turbulent boundary layer, appears to indicate an addition of energy for the off-line position. This is not surprising since the off-line survey position is located directly behind the upstream root nozzles which were originally installed by ARL to prevent inlet separation between the primary nozzles. Large regions of separation had been observed to occur between the primary nozzles prior to installation of the root nozzles by ARL. The higher free stream velocity of 43 m/sec (140 ft/sec), Figure 5.1-10, 11, at the edge of the off-line boundary layer is due to the jet blowing effects provided by the root nozzles. The influence of root nozzle blowing is not seen in the in-line profile of Figure 5.1-11. The momentum thickness for the in-line profile was calculated to be 0.043cm (0.0169"), while the off-line momentum thickness was 0.0277cm (0.0109"). These values are of the same order as the design value of 0.0254cm (0.010") originally used for this Phase I ejector/augmentor configuration.

A graphical comparison of blowing lip boundary layer variations in momentum thickness for primary plenum pressures of 2.54cm (1.0") and 10.16cm (4.0") Hg is presented in Figure 5.1-12. The generally thicker in-line momentum thickness compared to the thinner energized off-line values, for a primary plenum pressure of 2.54cm (1.0") Hg, illustrate the effectiveness of the off-line root nozzles and the interference effects of the primary hypermixing nozzle on the in-line lip boundary layers. However, at a higher primary plenum pressure of 10.16cm (4.0") Hg the expansion of the primary fin nozzle jet has apparently impinged upon the constant area mixing walls and energized the in-line boundary layers such that the calculated momentum thicknesses approach the predicted values for the region investigated. The faster expansion of the hypermixing nozzle jets at higher primary plenum pressures, is apparently due primarily to the reduced static pressure

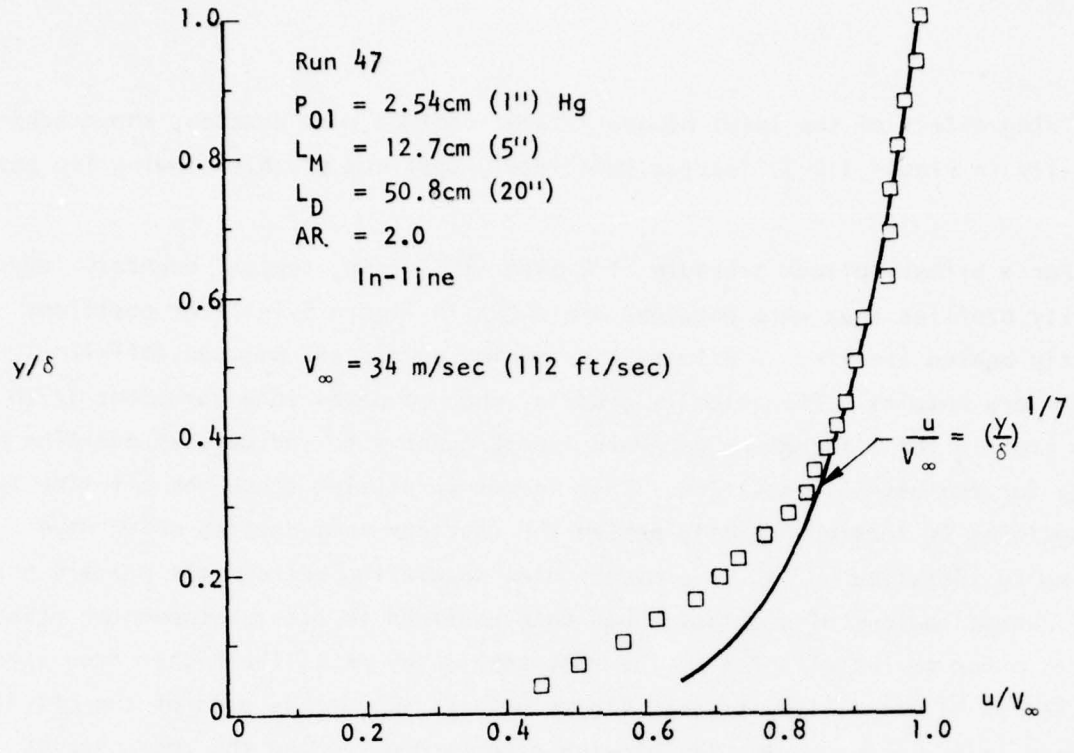

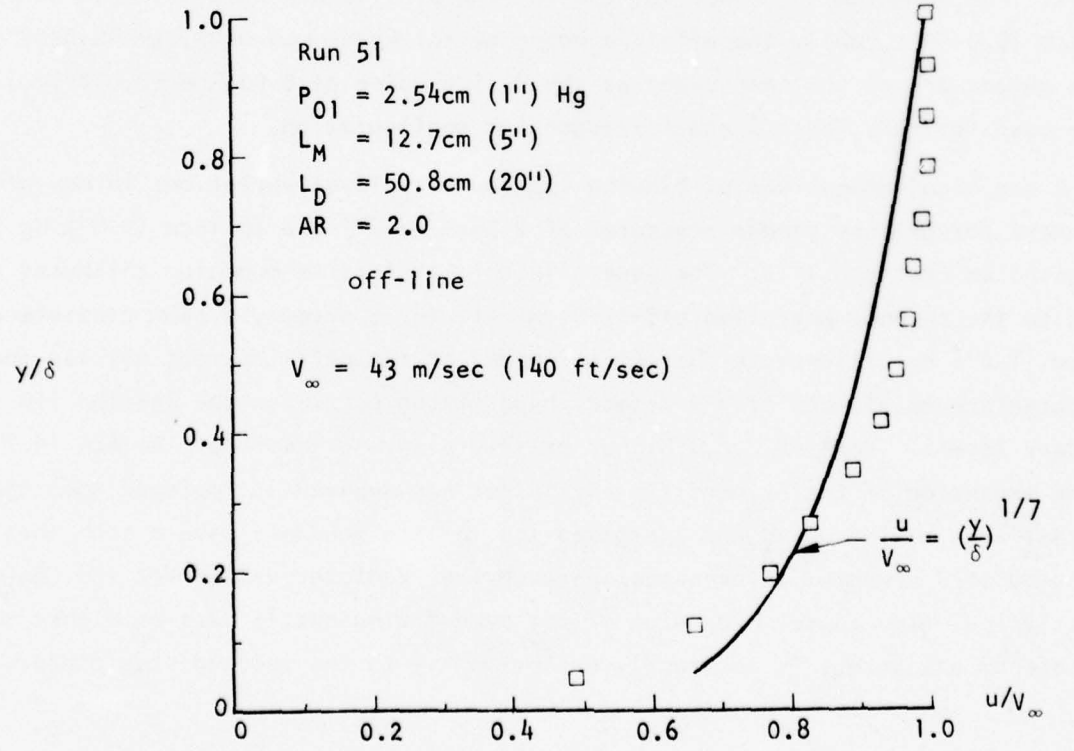

FIGURE 5.1-11. EJECTOR SIDEWALL BOUNDARY LAYER PROFILES AT ATC BLOWING LIP

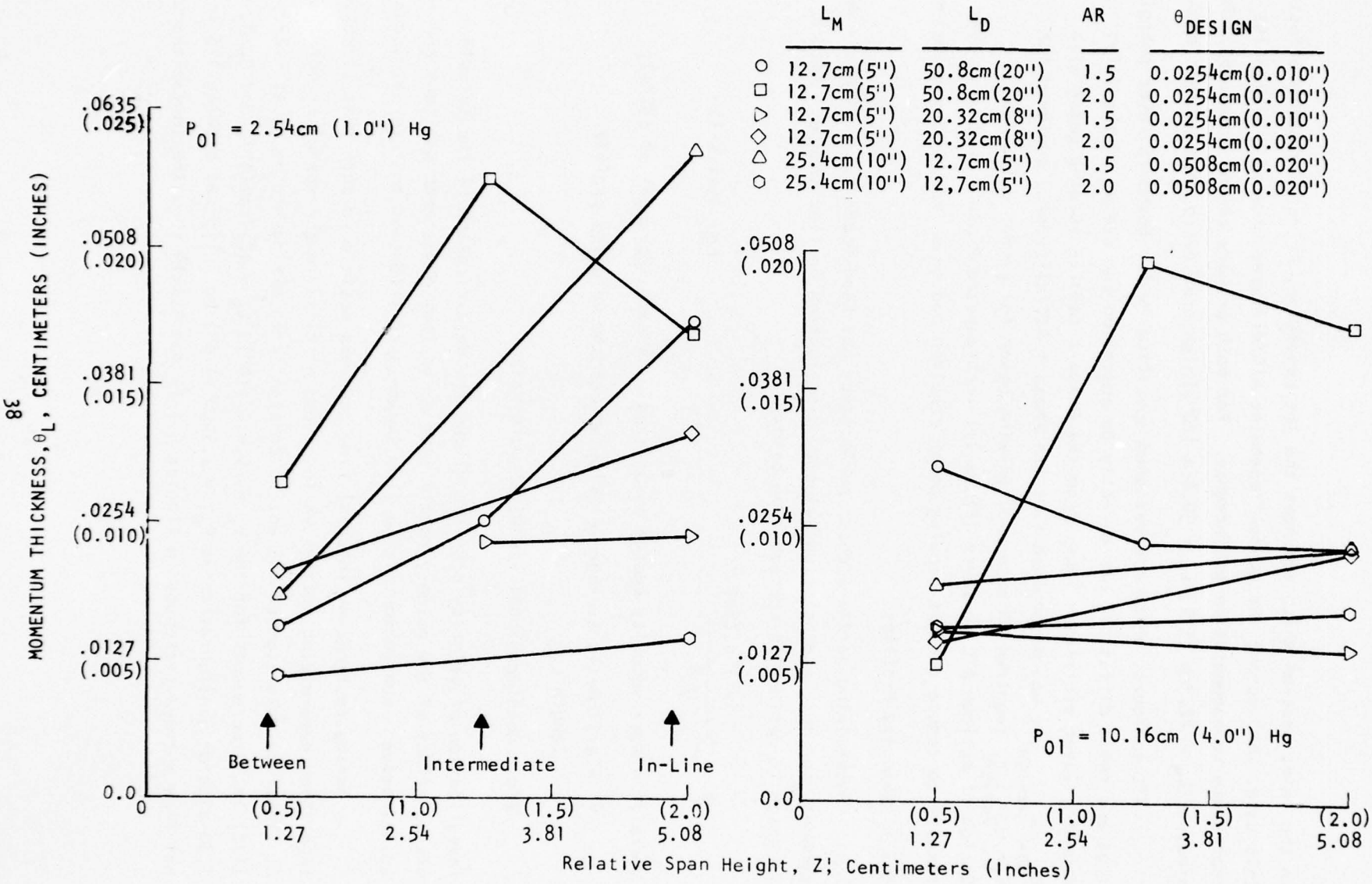

FIGURE 5.1-12. ATC/DIFFUSER BLOWING LIP BOUNDARY LAYERS

in the inlet section which enhances the jet expansion. Primary pressure effects, in this case, can improve the overall spanwise ATC/diffuser blowing efficiencies and contribute to augmentation performance. For both primary plenum pressures, the long ejector (L_M = 12.7cm (5"), L_D = 50.8cm (20")) high area ratio data exhibit anomalies.

ATC contours, which are designed specifically for boundary layer energization and rapid diffusion, are directly dependent on the status of the inlet boundary layer profiles. Thus, from the Phase I results showing cases with $\Theta_{Max} > \Theta_{Design}$, it was determined that the Phase I ATC/diffusers, designed for $\Theta_L = \Theta_{Design}$, required an excess of blowing power for proper diffusion. Design of optimum ATC contours (Phase II) incorporated Phase I boundary layer results to reduce the ATC blowing power required and thus improve augmentation.

5.1.4 Velocity Profiles

Hypermixing nozzle ejector performance has been found to be directly dependent upon the internal flow velocity distribution or flow skewness factor, β, which is defined in the equation below,

$$\beta = \frac{\int_0^1 (V')^2 d(Z/c)}{\bar{V}^2} \quad , \qquad \text{Eq. (5.1.4-1)}$$

where: V' = mean velocity vector associated with each increment of $\Delta(Z/c)$,

$\bar{V}$ = arithmetic average velocity across the velocity profile length c,

Z/c = nondimensional spanwise coordinate.

Investigation of velocity profiles allows the determination of the turbulent mixing effect of the primary nozzle jets at various downstream stations and the quantitative evaluation of the flow skewness contribution to internal losses.

During testing, an internal flow rake was positioned such that it would span three hypermixing nozzles while placed parallel to the spanwise coordinate, Z. The flow rake scanned the entire constant area mixing width, W, at 1.27cm (1/2) inch increments for the L_M = 25.4cm (10"), L_D = 12.7cm (5"), and A_3/A_2 = 1.50 ejector configuration at P_{01} = 2.54cm (1.0") Hg. Typical blowing lip internal flow surveys presented in Figures 5.1-13 and 5.1-14 show the instantaneous

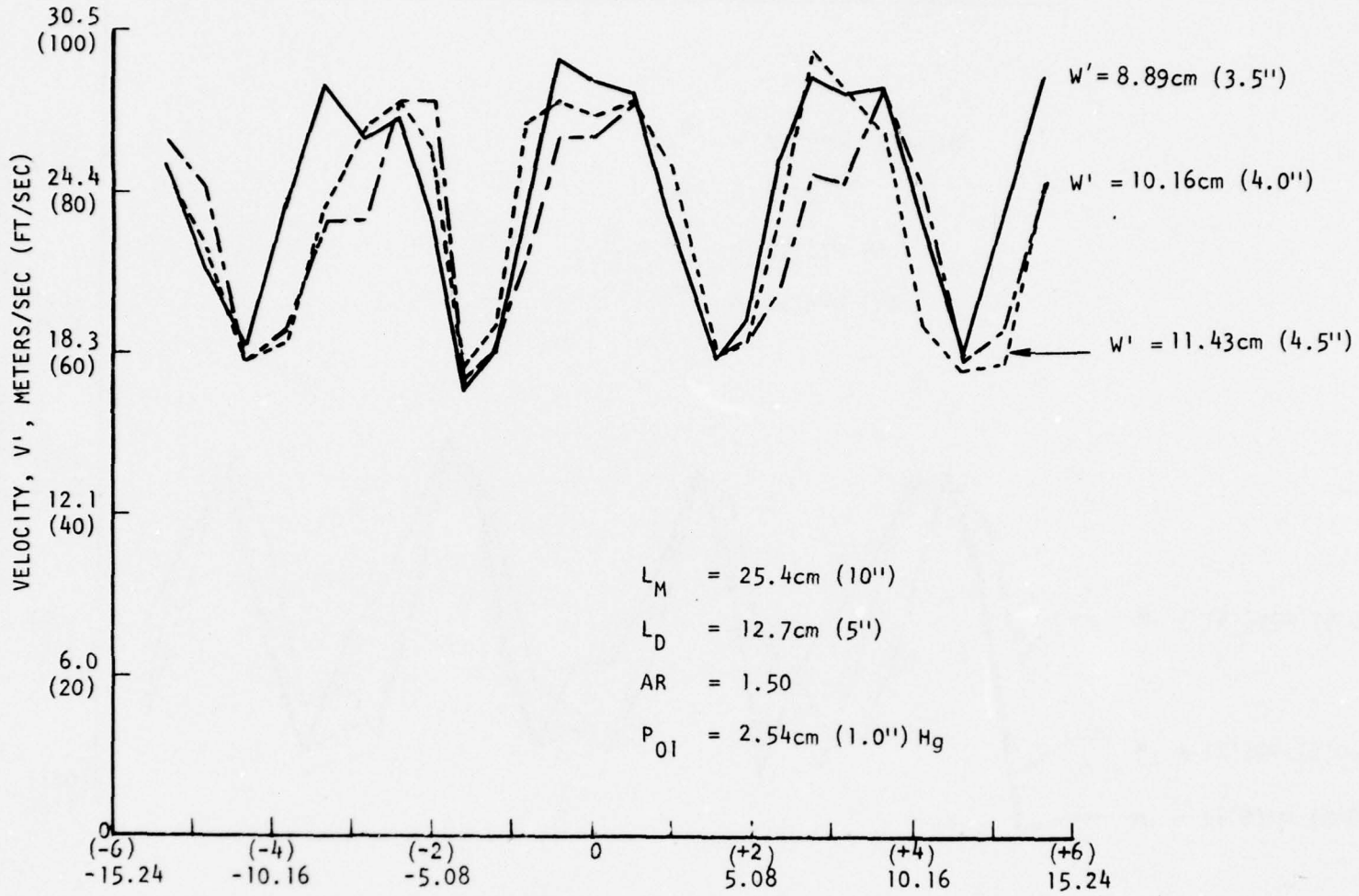

FIGURE 5.1-13. PHASE I INTERNAL FLOW BLOWING LIP VELOCITY PROFILES

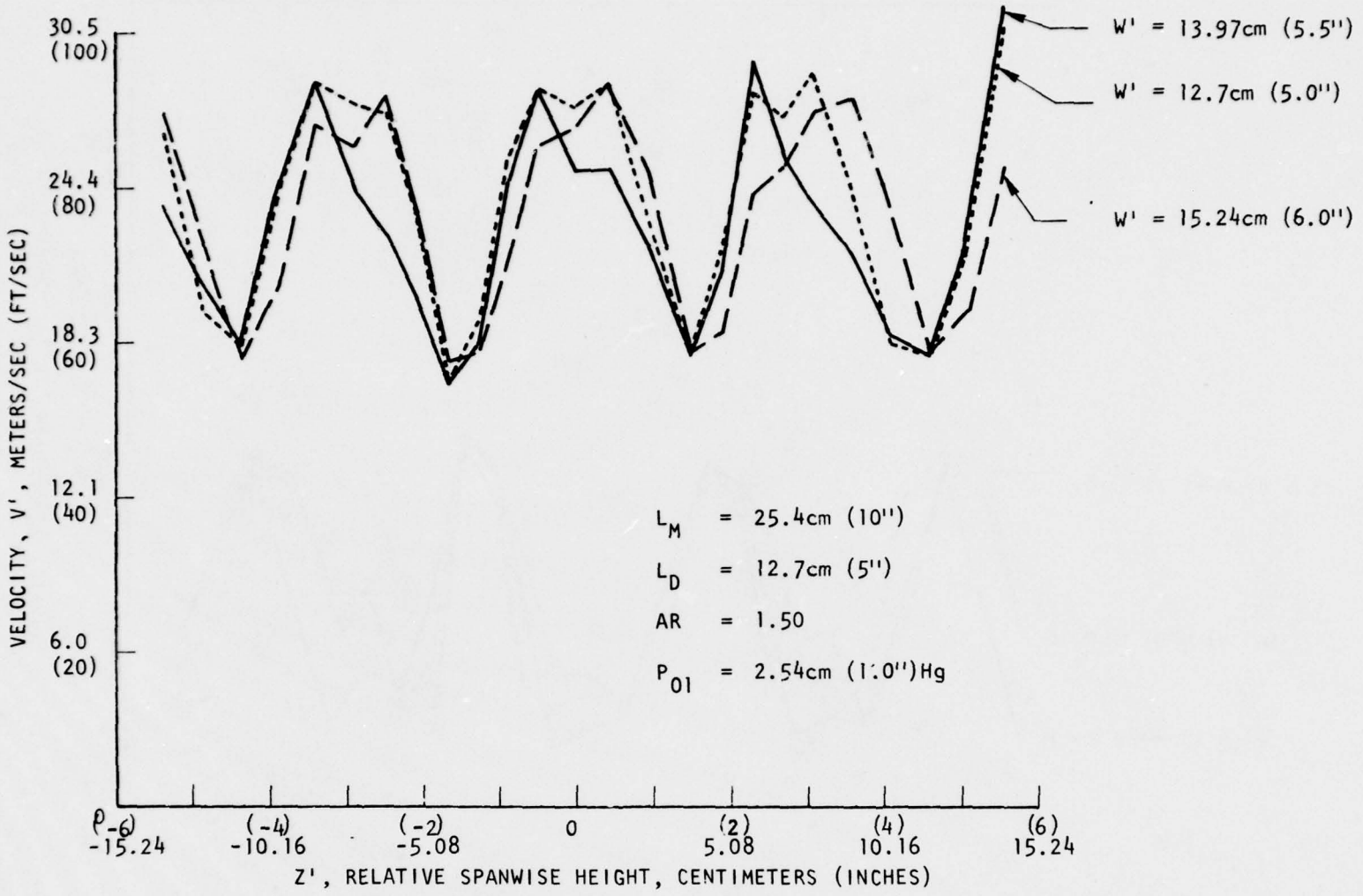

FIGURE 5.1-14. PHASE I INTERNAL FLOW BLOWING LIP VELOCITY PROFILES

velocity calculated from total probe pressures and the flow rake averaged static pressure value, for positions across the ejector.

Figures 5.1-13 and 5.1-14 present velocity profiles for distances W' = 8.89 (3.5") to 15.24cm (6.0") from a sidewall at 1.27cm (1/2") intervals, across the constant area mixing width. The centerline total probe shown to be at the relative spanwise coordinate Z' = 0cm is directly downstream from a H-8 hypermixing nozzle and 61cm (24") from the test bed floor, with each adjoining ejector nozzle at 7.62cm (3") intervals above and below the centerline probe. Most notable in the figures is the hypermixing jet effect upon the profile even at a distance of 25.4cm (10") downstream of the ejector plane.

The turbulent mixing profile of a typical velocity scan is shown in Figure 5.1-15 for W' = 12.7cm (5.0"). To indicate the level of internal mixing occurring at this position, the skewness factor of the profile is presented. Using Equation 5.1.4-1, the skewness factor was determined to be 1.0056 for this particular velocity profile. A perfectly uniform velocity profile will give an ideal skewness factor of one. The integration and evaluation of all the internal flow scans thus provides an indication of the effectiveness of the ejector mixing process to the beginning of the diffuser plane. An average skewness factor of all the velocity profile skewness factors across the mixing width for the above location was calculated to be 1.015. This average skewness factor coupled with previous ARL results and Phase II optimum configuration skewness results contribute to the data base for approximate values of internal skewness factors required in the design procedures of Section 5.3.

5.1.5 Augmentor Results

Maximum augmentation ratios for Phase I configurations with hypermixing nozzle/inlet are shown comparatively in Figure 5.1-16. The solid curve represents previous peak augmentation results, Reference 3, using ARL/H-4 hypermixing nozzles with trapped vortex diffusers. Previously measured performance of ATC diffusion in a large area ratio thrust augmentor with H-4 hypermixing nozzles is shown for a total available mixing length, $L_M + L_D$, of 63.5cm (25"). The dashed curve is an estimate of the potential performance improvement in short ejector/augmentors employing ARL/H-8 hypermixing nozzles with an optimum ATC/diffuser. The resultant augmentation ratios for ATC/augmentors, employing

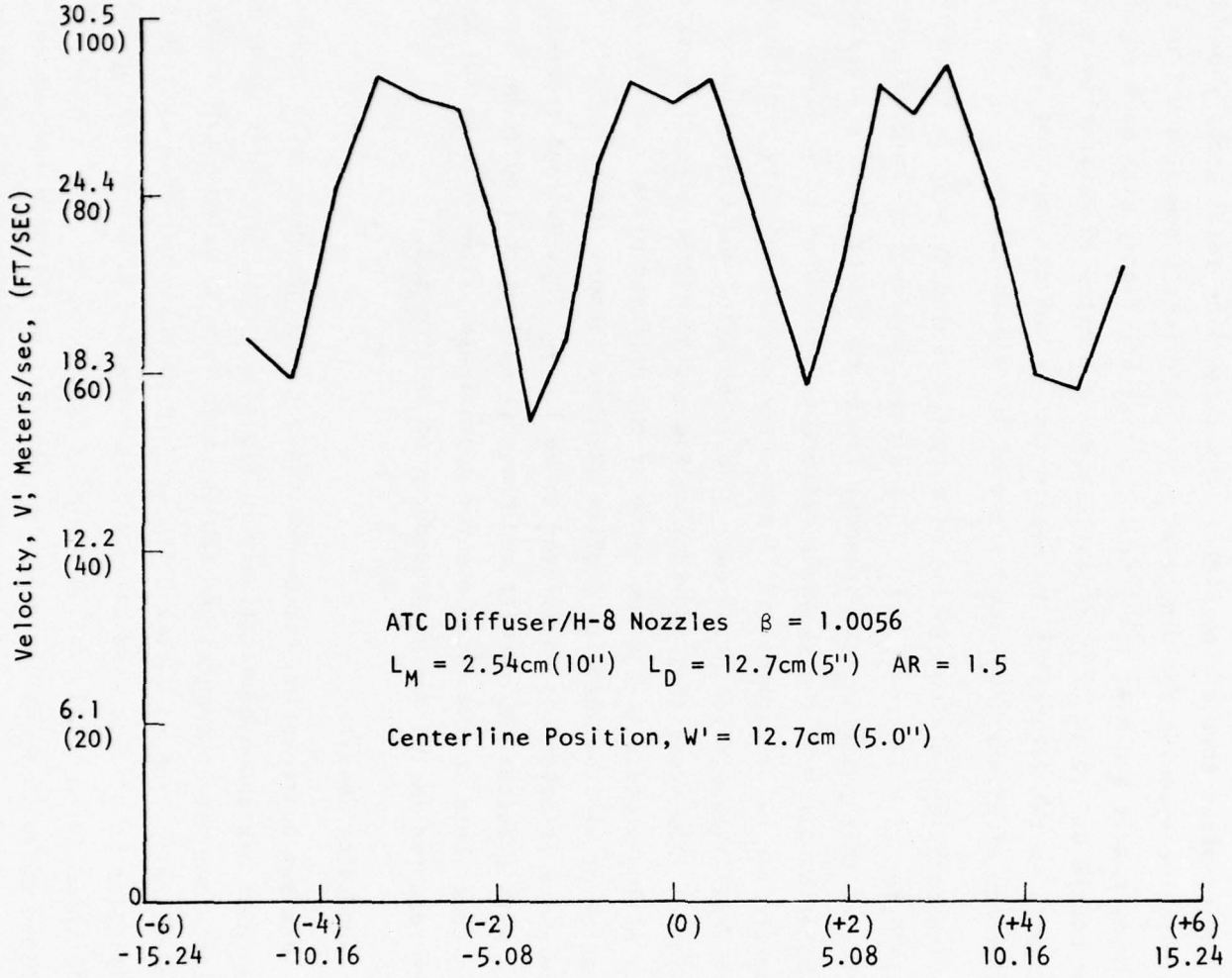

FIGURE 5.1-15. TYPICAL VELOCITY SKEWNESS CHARACTERISTICS

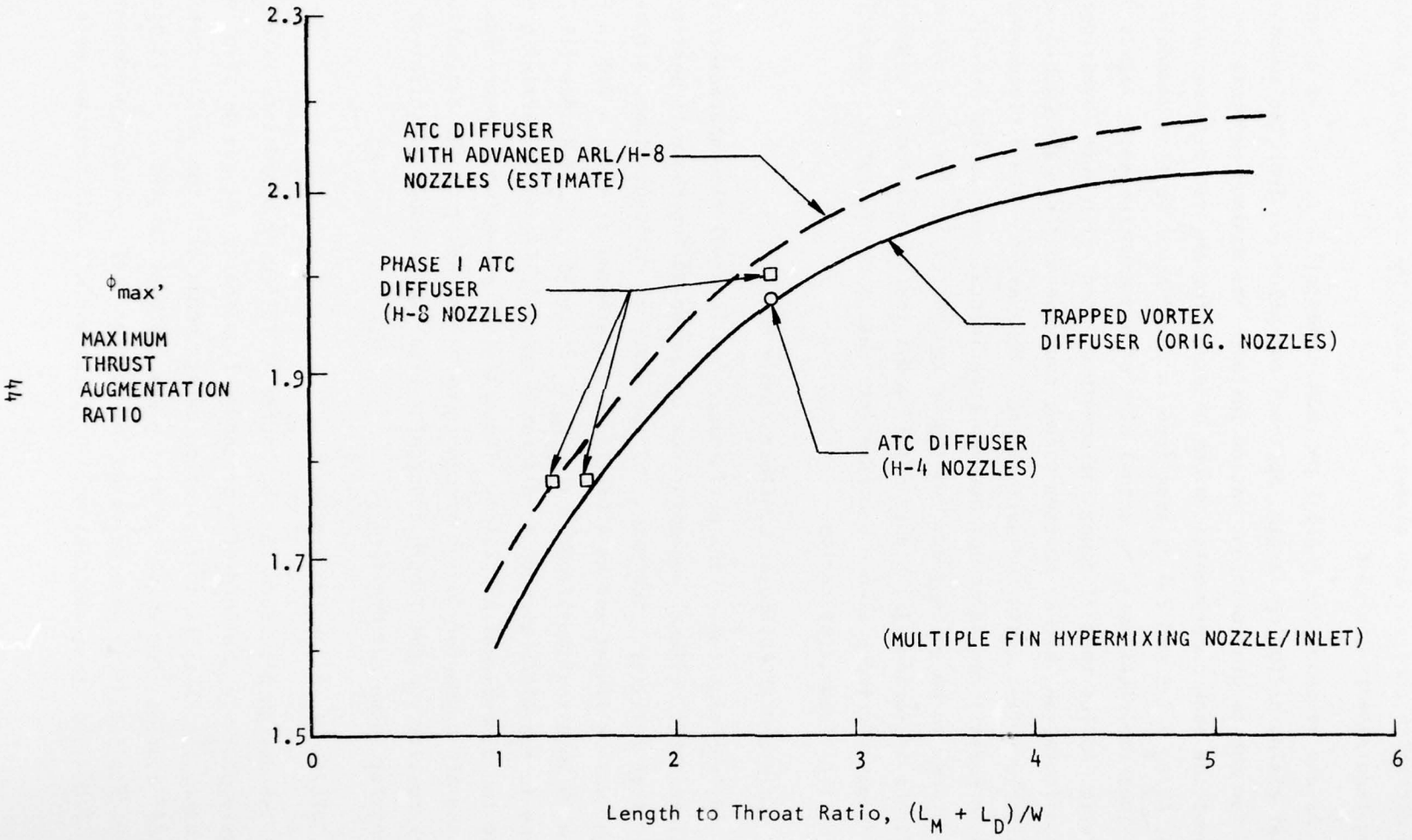

FIGURE 5.1-16. CORRELATION OF PEAK AUGMENTATION RATIO FOR ATC DIFFUSERS

active diffusion control, are always calculated with the auxiliary primary blowing requirements included.

As can be seen, the Phase I maximum augmentation ratios, as a function of total mixing diffusion length, approach the predicted improved augmentation ratios for the length to throat ratios tested. The maximum augmentation ratios represent the peak experimental values obtained for the two diffuser area ratios tested, A_3/A_2 = 1.5 and 2.0 as specified in the Phase I testing schedule. Based on previous empirical data, an actual plot of augmentation ratio versus diffuser area ratio implies that if finer increments of area ratio were investigated for each configuration, higher maximum values could be obtained that would correspond more closely to the estimated performance. However, for the limited area ratios tested in Phase I the agreement between experimental results and H-8/ATC predictions is seen to be quite good. Analogous to the results for previous non-optimum designs (Reference 3), Figure 5.1-17 shows the degradation in augmentation with increased primary plenum pressure for Phase I configurations operating in their best diffuser area ratios.

5.2 Optimized ATC/Diffuser Configuration - Phase II

An investigation of the performance and internal flow characteristics of an optimized ATC/diffuser augmentor was conducted during Phase II testing in the ejector test facility. Schematics of two Phase II configurations, a conventional straight wall diffuser and an ATC/diffuser, are shown at A_3/A_2 = 2.0 in Figure 3.5-1 with both configurations having L_M = 12.7cm (5"), L_D = 29.8cm (11.75"). As in Phase I, the ATC/augmentor incorporated multiple fin H-8 hypermixing nozzles and the two dimensional ARL inlet. The optimized augmentor geometry was defined using the ATC augmentor design procedure with feedback from the evaluation of Phase I results and the length constraint finalized through consultation with the Contract Technical Monitor.

5.2.1 ATC/Augmentor Design Procedure

The design procedure for configured ATC/diffuser augmentors is explained in Figure 5.2-1 in the form of a procedure flow chart. As may be seen in the flow chart, the Phase II configuration design began with the performance/sizing trade-off studies from which the mixing and diffuser lengths, L_M = 12.7cm (5"), L_D = 29.85cm (11.75"), were selected for the range of predicted augmentation ratio (1.8 - 1.9) that was desired. Diffuser and ATC wall contours were modeled

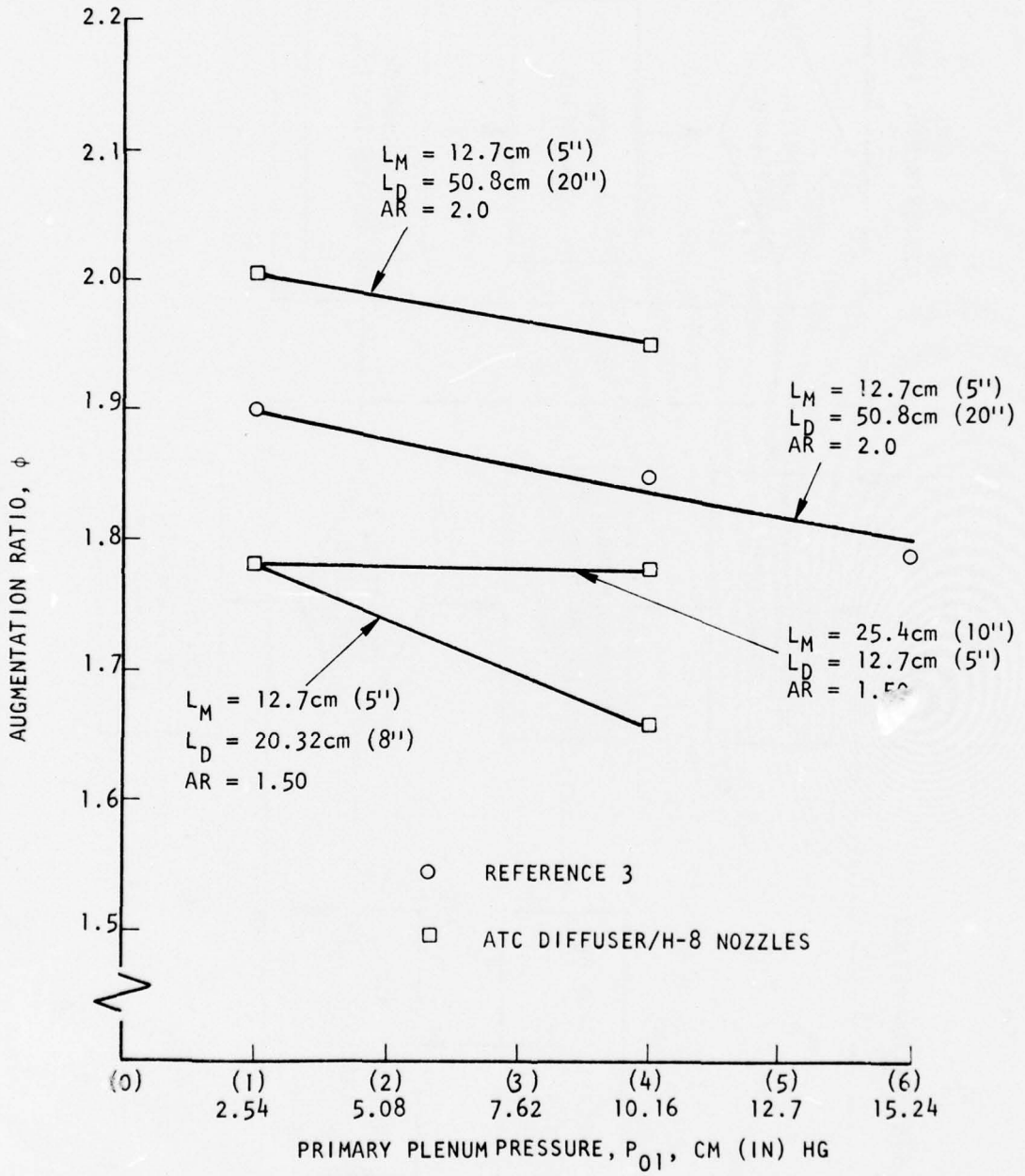

FIGURE 5.1-17. HYPERMIXING PLENUM PRESSURE EFFECTS ON AUGMENTATION RATIOS OF PHASE I CONFIGURATIONS

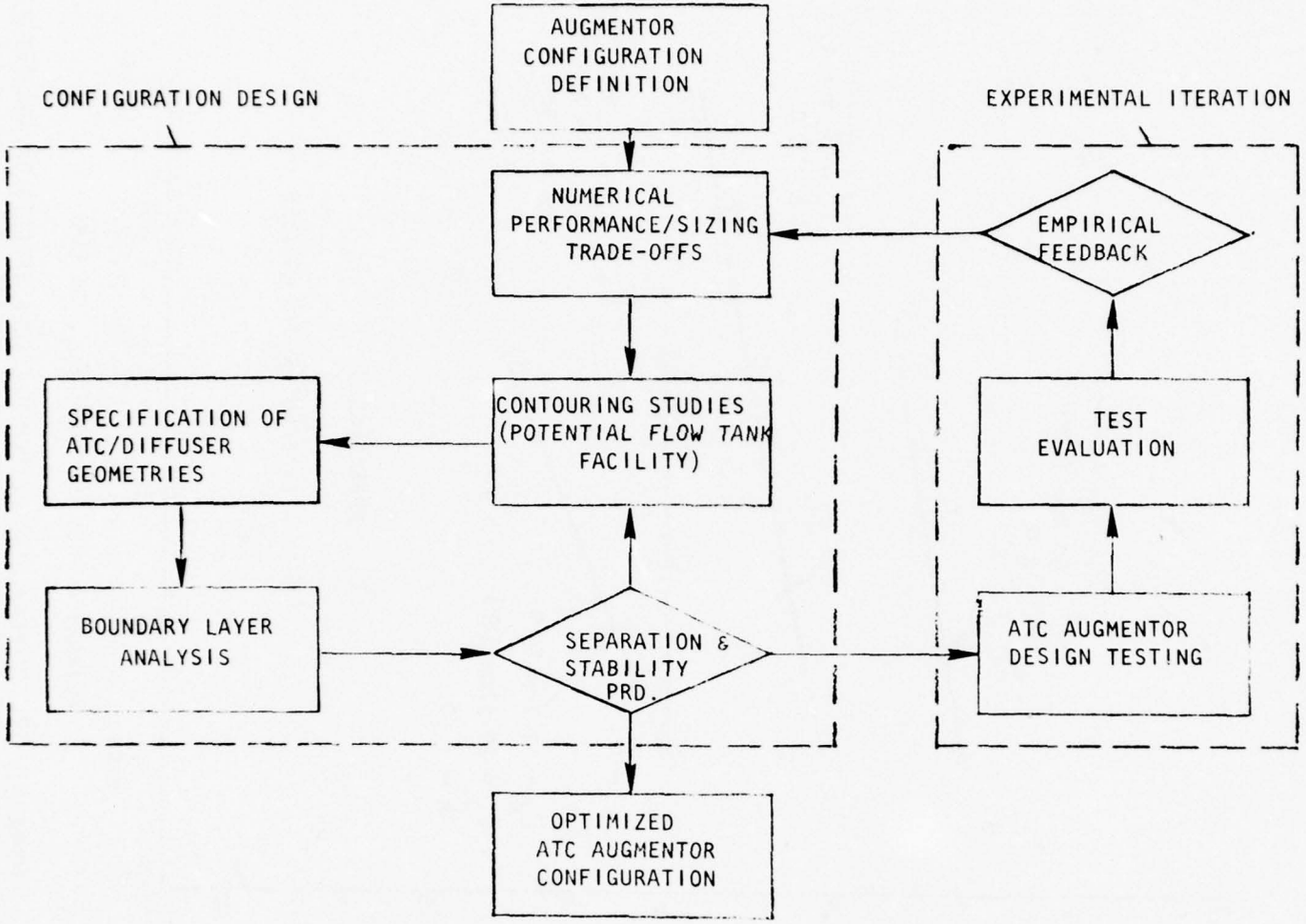

FIGURE 5.2-1. ATC AUGMENTOR DESIGN PROCEDURE

in the rheoelectric analog facility for diffuser ratios up to 2.5, and included the optimum setting, $A_3/A_2 = 2.10$. Turbulent boundary layers were analyzed according to the iteration loop in the flow chart for separation tendencies and stability. Additional information available for the Phase II configuration design were the previous results of Phase I tests which are represented by the experimental iteration segment of the flow chart. The feedback of empirical information such as ATC wall pressure data, lip boundary layers, primary plenum pressure effects, and internal flow velocities aided in designing the optimized ATC/diffuser augmentor to be tested in Phase II.

5.2.2 Wall Pressure Results

The results of the variation in the local pressure coefficient, C_p, along the ATC/diffuser wall for the optimized H-8/ATC ejector/diffuser at an area ratio of 2.0 is compared to the predicted theoretical results from the rheoelectric analog facility in Figure 5.2-2. The local pressure coefficient is again determined as the difference between local and reference static pressure divided by the reference dynamic pressure, $\bar{q}_{ref}$. The reference static pressure, as in Phase I, is calculated to be the average of the constant area mixing wall pressures immediately upstream of the ATC blowing lip location. However, the reference dynamic pressure is now considered to be the difference between the spanwise average free stream total pressure and the reference static pressure, due to the mixing effects of the H-8 ejector nozzles. Internal flow velocity profiles were used to compute the average free stream total pressure for use in the data reduction. Figure 5.2-2 shows the excellent agreement between the ATC/diffuser wall pressure distribution and the predicted theoretical values using the corrected pressure coefficient. The local pressure effect of the blowing slot jet is present in the data near the blowing lip location and the jet, after mixing with the incoming boundary layer, is seen to begin diffusion along the ATC wall at the predicted velocity ratios.

The optimum ATC diffusion contour was designed, in Phase II, by taking into account the nonuniform lip momentum thickness distributions measured in the Phase I boundary layer surveys. With the measured increases in local momentum thickness upwards of 100%, the optimum ATC energization region was sized to accommodate the larger power losses at the blowing lip location. Operating at a primary plenum pressure of $P_{01} = 2.54$cm (1") Hg, the ATC/augmentor wall pressure distributions in Figures 5.2-3 and 5.2-4, show the ATC/diffuser flow to be

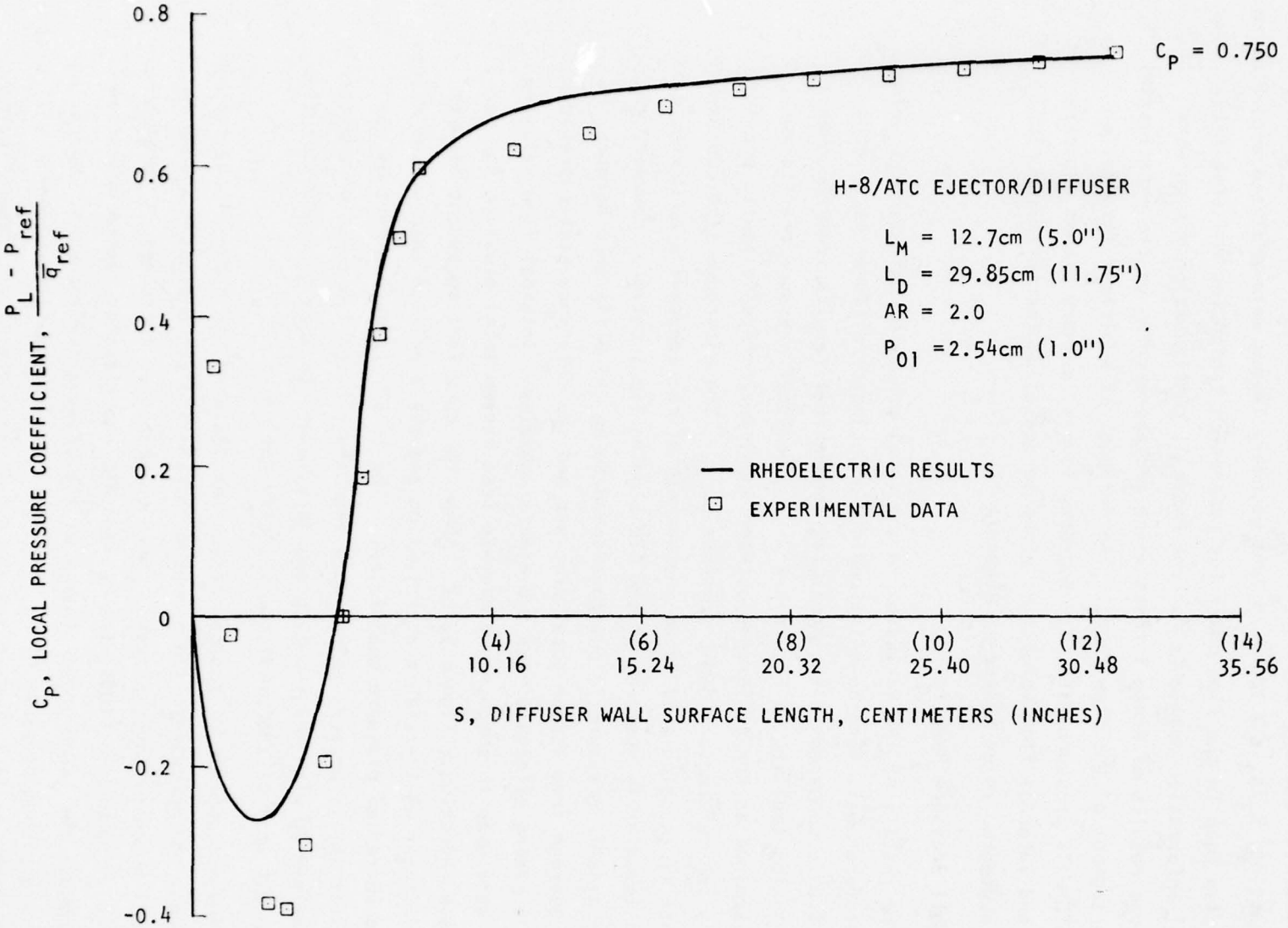

FIGURE 5.2-2. COMPARISON OF PHASE II H-8/ATC DIFFUSER WALL PRESSURE VARIATION WITH RHEOELECTRIC RESULTS FOR P_{01} = 2.54cm (1 INCH)HG.

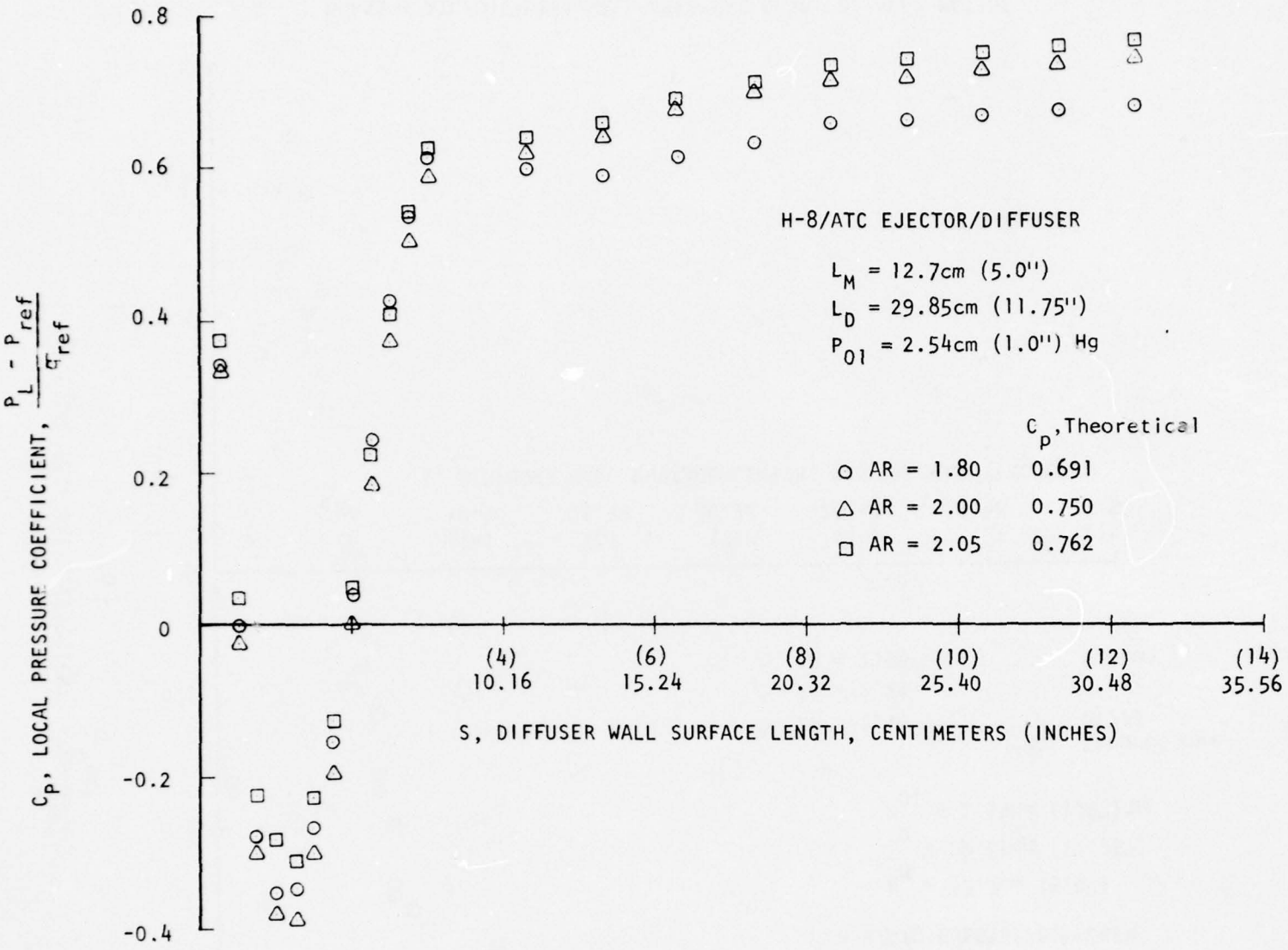

FIGURE 5.2-3. PHASE II ATC/DIFFUSER WALL PRESSURE DATA FOR AREA RATIOS BELOW 2.10 WITH P_{01} = 2.54cm (1 INCH) Hg.

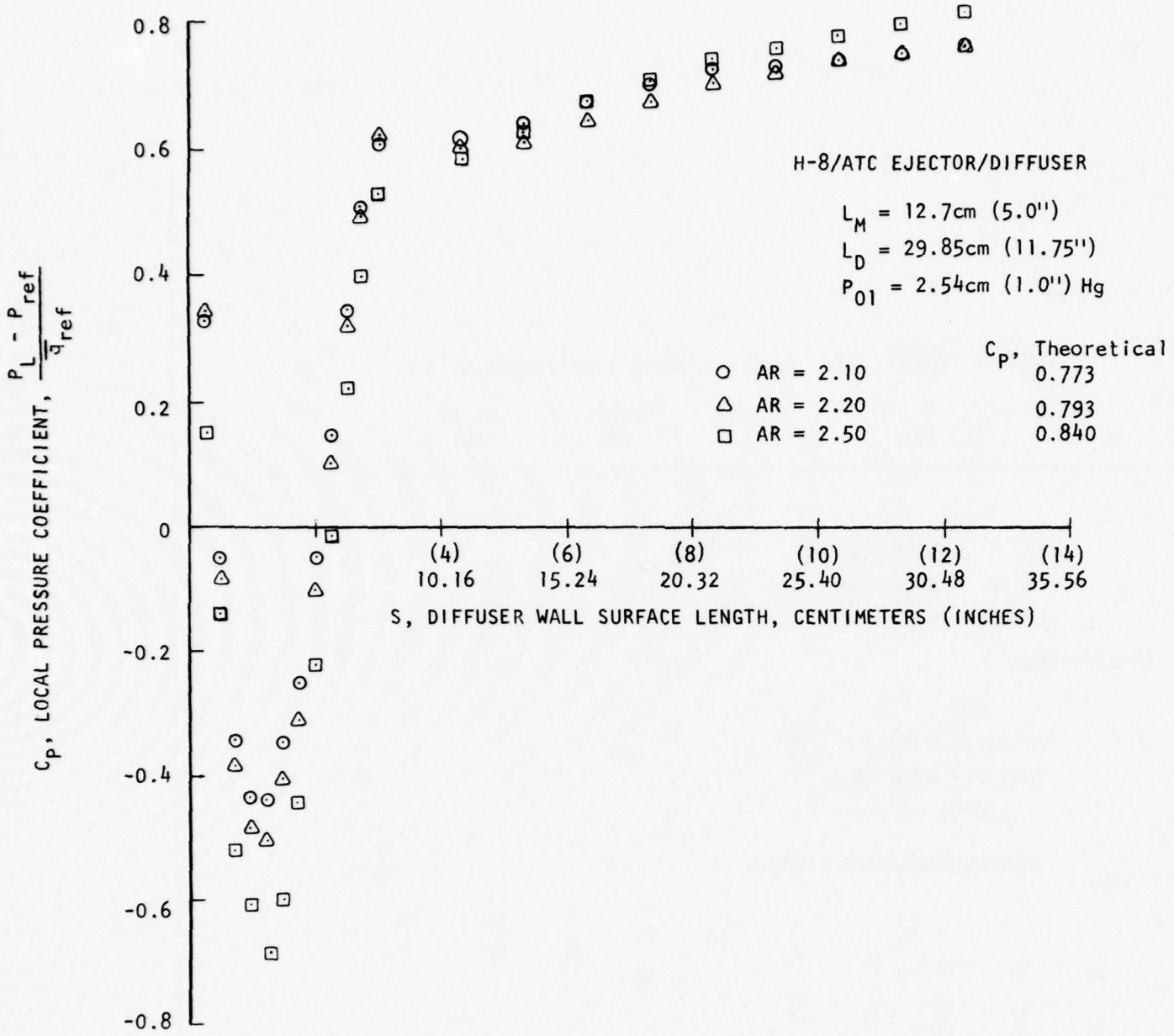

FIGURE 5.2-4. PHASE II ATC/DIFFUSER WALL PRESSURE DATA FOR AREA RATIOS 2.10 AND ABOVE WITH P_{01} = 2.54cm (1 INCH) Hg.

completely attached and diffused for the full range of area ratios tested. The only losses incurred with this optimum ATC/diffuser are those associated with the boundary layer losses along the diffuser wall and any skewness in the exit plane velocity profile. The scan of diffuser area ratios was investigated in order to determine the maximum augmentation ratio for this configuration and in all cases the diffuser exit plane pressure coefficients, Figures 5.2-3 and 5.2-4, achieved or approached the ideal theoretical values of pressure associated with each area ratio. The only noticeable discrepancy in the wall pressure distributions is seen in the region approximately 10.16cm (4 inches) downstream of the ATC blowing slot. At this position the fully energized and diffused incoming boundary layers should essentially start a new turbulent boundary layer and travel the length of the diffuser wall under the influence of a constant or slightly adverse pressure gradient. The discrepancies in pressure coefficient in this region downstream of the ATC are attributed to the mating of the modular ATC and diffuser wall sections.

The influence of primary plenum pressures upon the ATC/diffuser at the optimum AR, $A_3/A_2 = 2.10$, is illustrated in Figure 5.2-5. For each primary plenum pressure, the augmentor has undergone the testing procedure of Section 4.0 in order that the augmentation ratio is maximized with the ATC and endwall mass flows optimized. The results of Figure 5.2-5 show that with BLC blowing balanced, consistent levels of local pressure coefficients are experienced and the ideal exit plane pressure coefficient maintained. In this subsonic diffuser the optimized ATC/diffuser performance appears nearly independent of primary plenum pressures.

5.2.3 Internal Flow Measurements

An extensive survey of the optimized ATC/augmentor internal flow velocity profiles, at $A_3/A_2 = 2.10$, was obtained and analyzed, with the ejector operating at $P_{01} = 2.54$cm (1") Hg and using the internal flow rake descirbed in Section 3.3. Spanwise velocity profiles, parallel to the constant area mixing walls, were taken at 2.54cm (1") increments for ATC blowing lip and diffuser exit plane flow traversing locations. The center span position was utilized for these surveys since the velocity profiles here show the least influence of the three dimensional effects produced by the interacting endwall blowing nozzle jets.

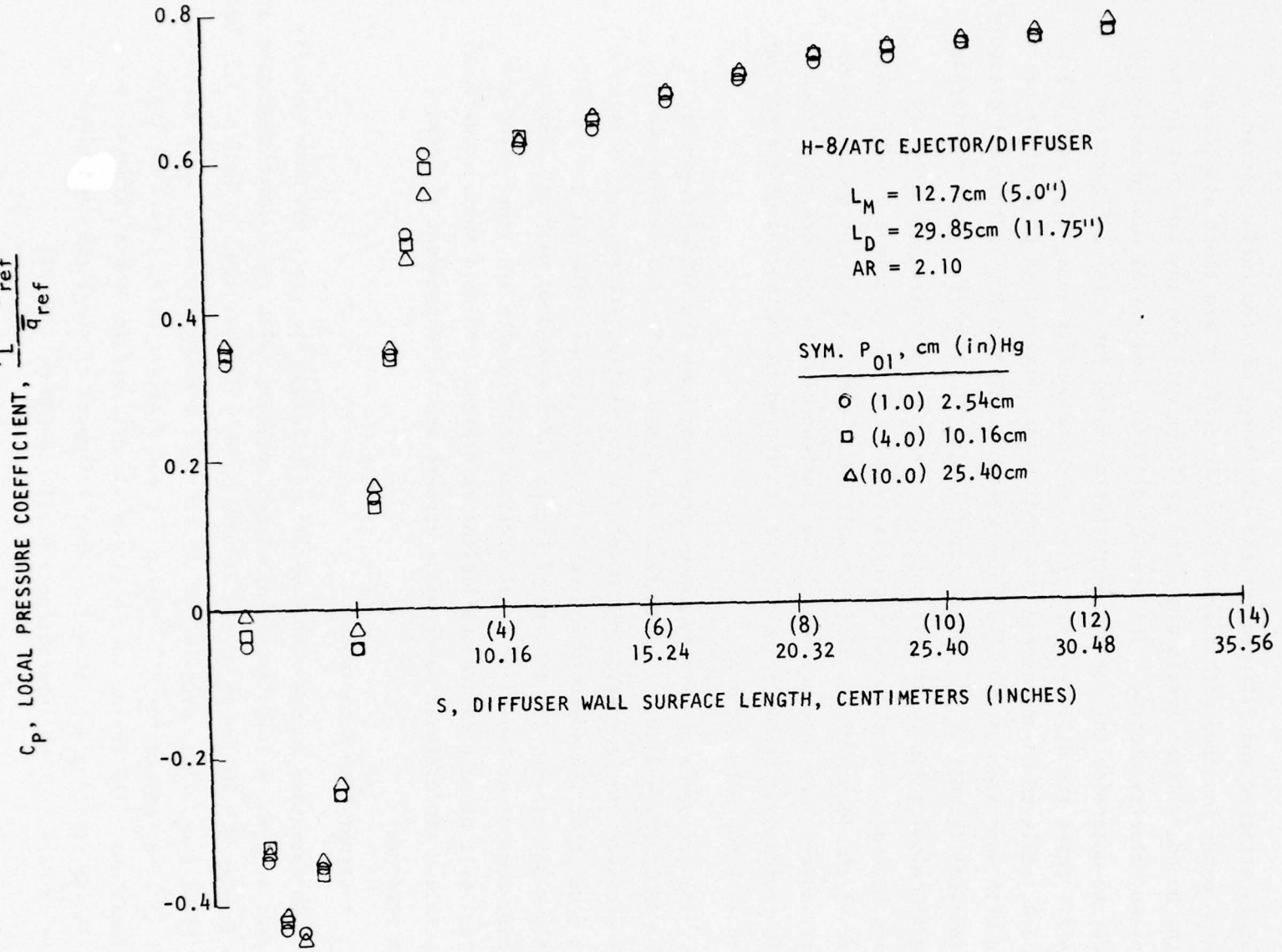

FIGURE 5.2-5. PRIMARY PLENUM PRESSURE EFFECTS ON OPTIMUM ATC/DIFFUSER WALL PRESSURE DISTRIBUTION.

Representative of the characteristics of the transverse internal flow profiles are the velocity profiles of Figures 5.2-7, 8, 9, and 10 taken along the centerline and diffuser wall of the ATC/augmentor. Figure 5.2-6 shows a schematic of the centerspan plane and the relative location of the four internal flow velocity profiles presented in the figures. In all four figures the hypermixing ejector nozzles, spaced at 7.62cm (3") intervals, are 68.6 (27"), 76.2cm (30") and 83.8cm (33") centimeters from the floor, respectively, as indicated in figures.

The general characteristics of the internal flow scans located along the centerline, Figures 5.2-7 and 8, show the jet effects of the upstream hypermixing nozzles. Figures 5.2-9 and 10 for internal flow near the diffuser wall, include the energization effects of the inlet root nozzles. Because of the proximity of the blowing lip plane to the hypermixing nozzles, rapid turbulent mixing of the primary and induced flow is proceeding as is apparent from the highly skewed profiles of Figures 5.2-7 and 9. At the diffuser exit plane the flow profiles of Figures 5.2-8 and 10 show more complete mixing with flow diffusion to lower velocity values.

For analysis, the velocity profile at each particular station is evaluated for its arithmetical mean velocity. The individual velocities are derived from the calculated dynamic pressures of each total probe and the average local static pressures. The ratio of average velocities between positions A and B (Figure 5.2-5) is 2.06 which approaches the ideal diffuser ratio of 2.10. However, because of the energy addition of the ATC blowing slot, the average velocity ratio between C and D is only 1.79. The combination of ATC blowing along the downstream diffuser wall and boundary layer/mixing ahead of the ATC apparently contributes to the slight reduction of the diffusion ratio. An accurate measure of the primary/secondary mixing effect is the calculated skewness factor, β. The profiles in the blowing lip plane which are influenced by the primary jet give large skewness values of 1.048 and 1.042 for positons A and C respectively. After continued mixing through the diffusion region analogous exit plane skewness factors are measured to be 1.029 and 1.020 for positons B and D. Further reduction of the skewness factor towards the ideal value of 1.00 is, of course, desirable since velocity skewness severely degrades augmentation performance. The uniform distribution of skewness in the

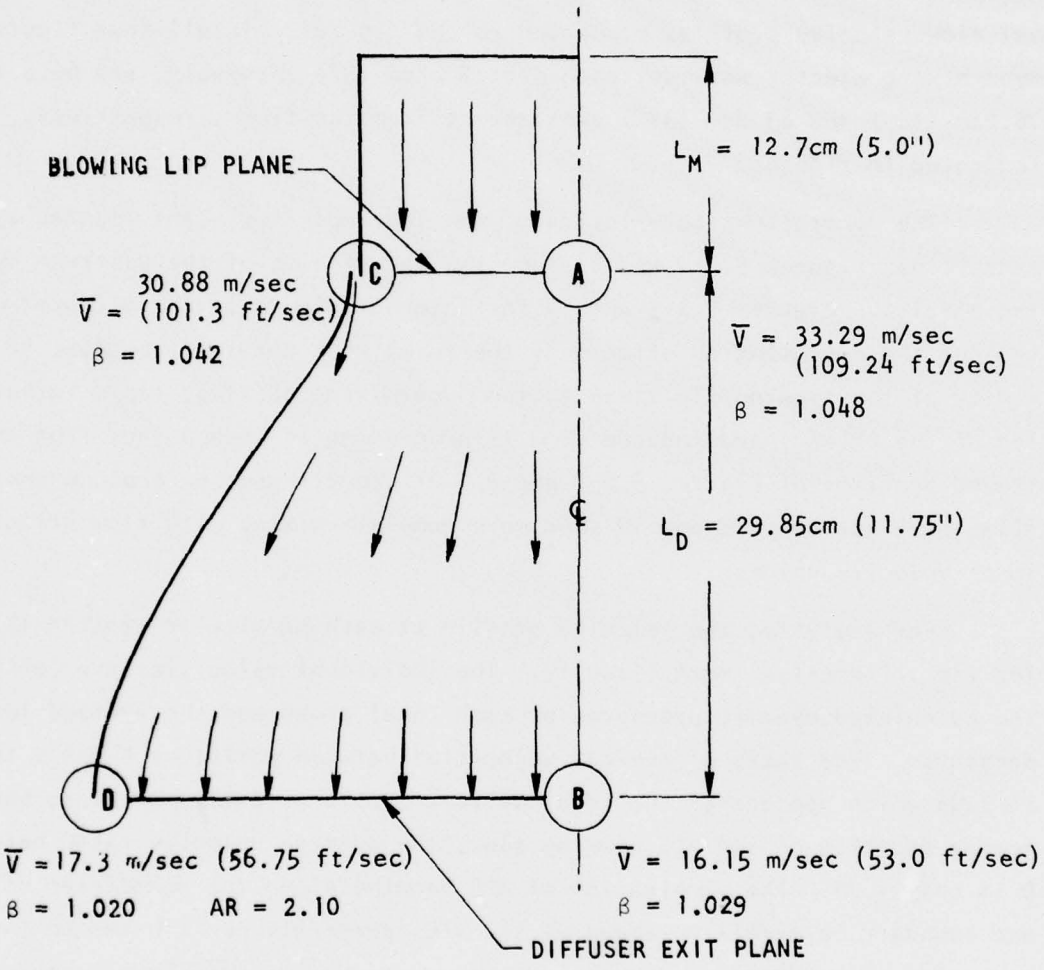

FIGURE 5.2-6. RELATIVE POSITION OF REPRESENTATIVE PHASE II INTERNAL FLOW PROFILES

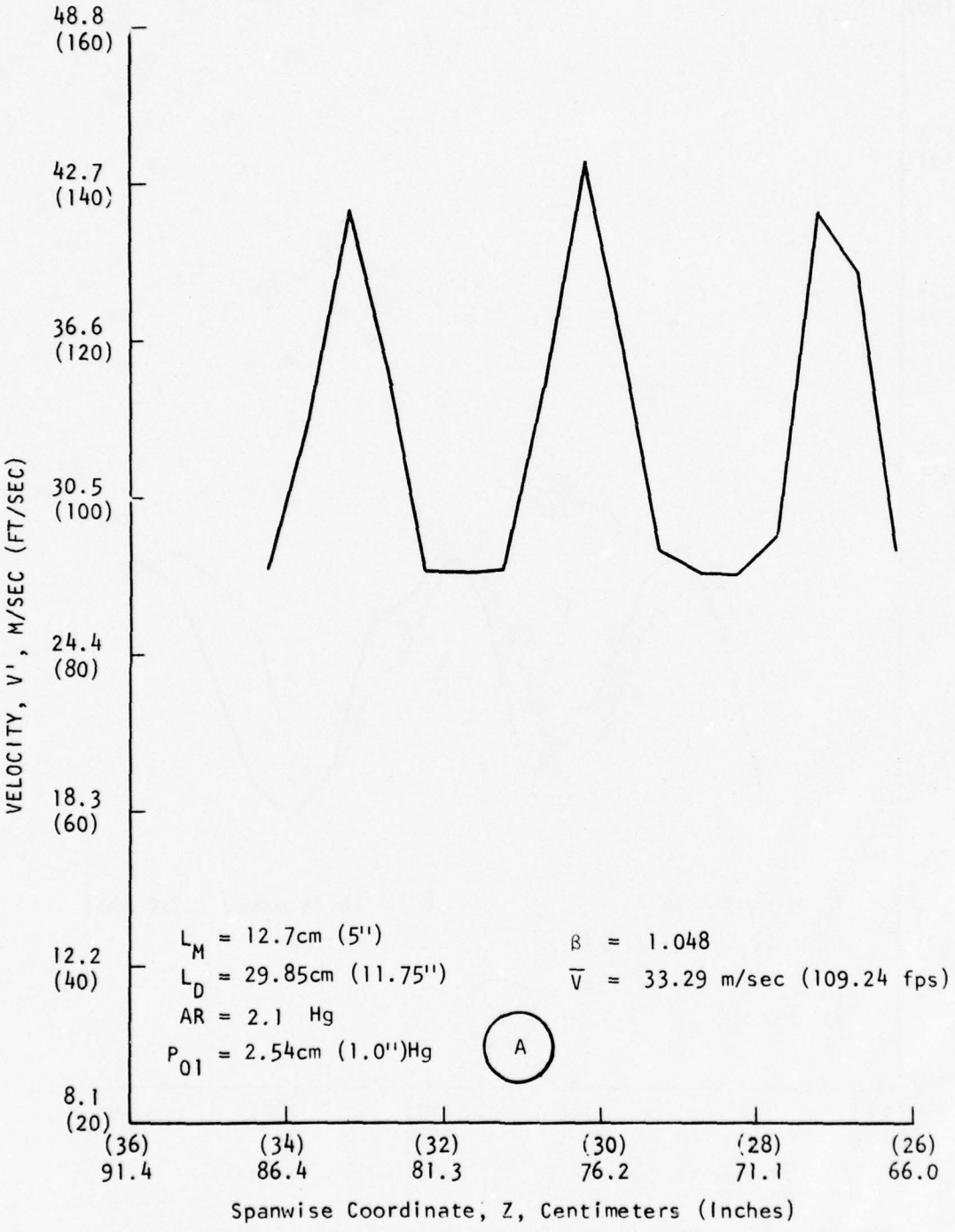

FIGURE 5.2-7. INTERNAL FLOW VELOCITY PROFILE AT THE CENTER SPAN LIP POSITION 12.7CM (5") FROM MIXING WALL

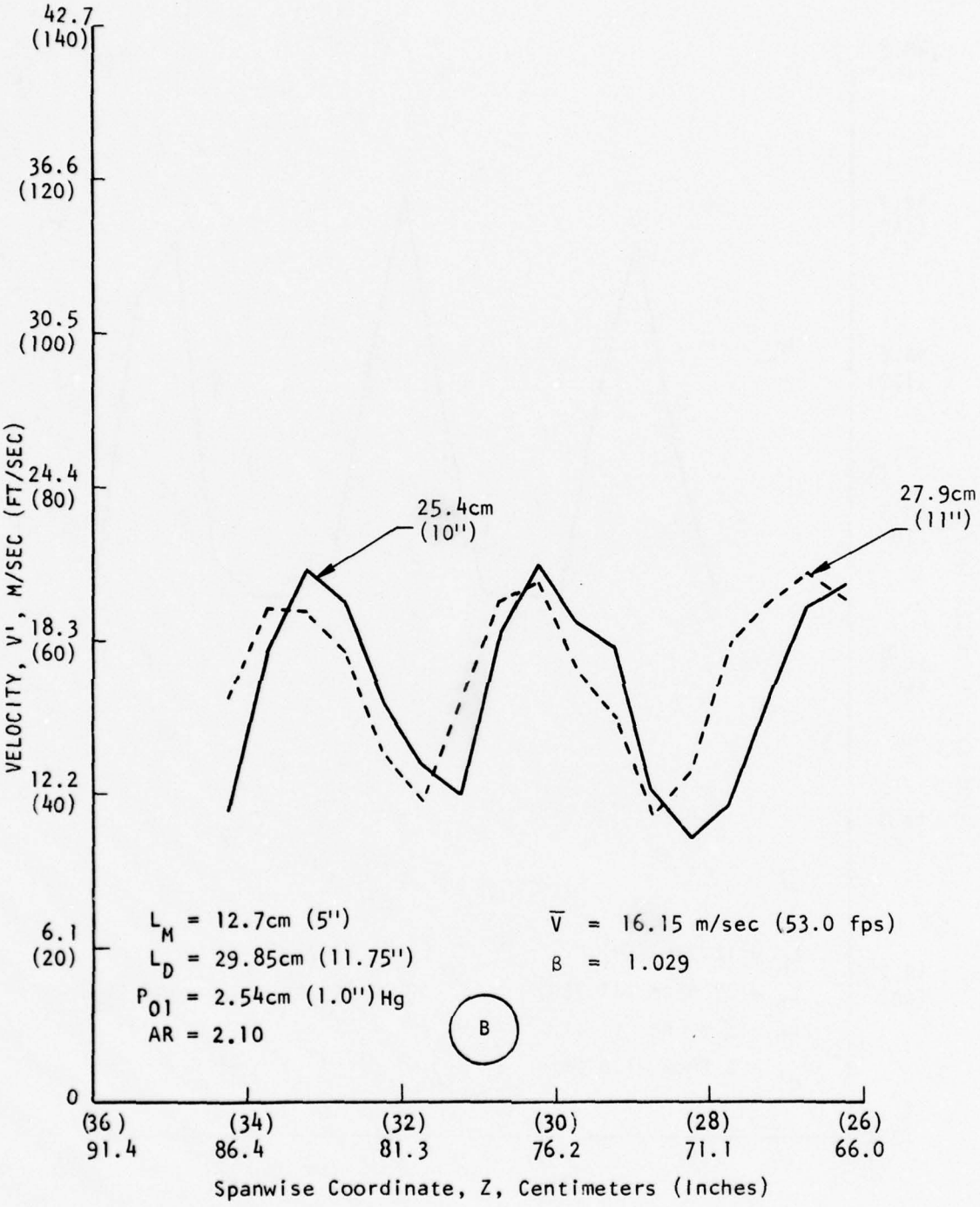

FIGURE 5.2-8. INTERNAL FLOW VELOCITY PROFILES AT THE CENTER SPAN EXIT POSITION 25.4CM (10") and 27.9CM (11") FROM THE DIFFUSER

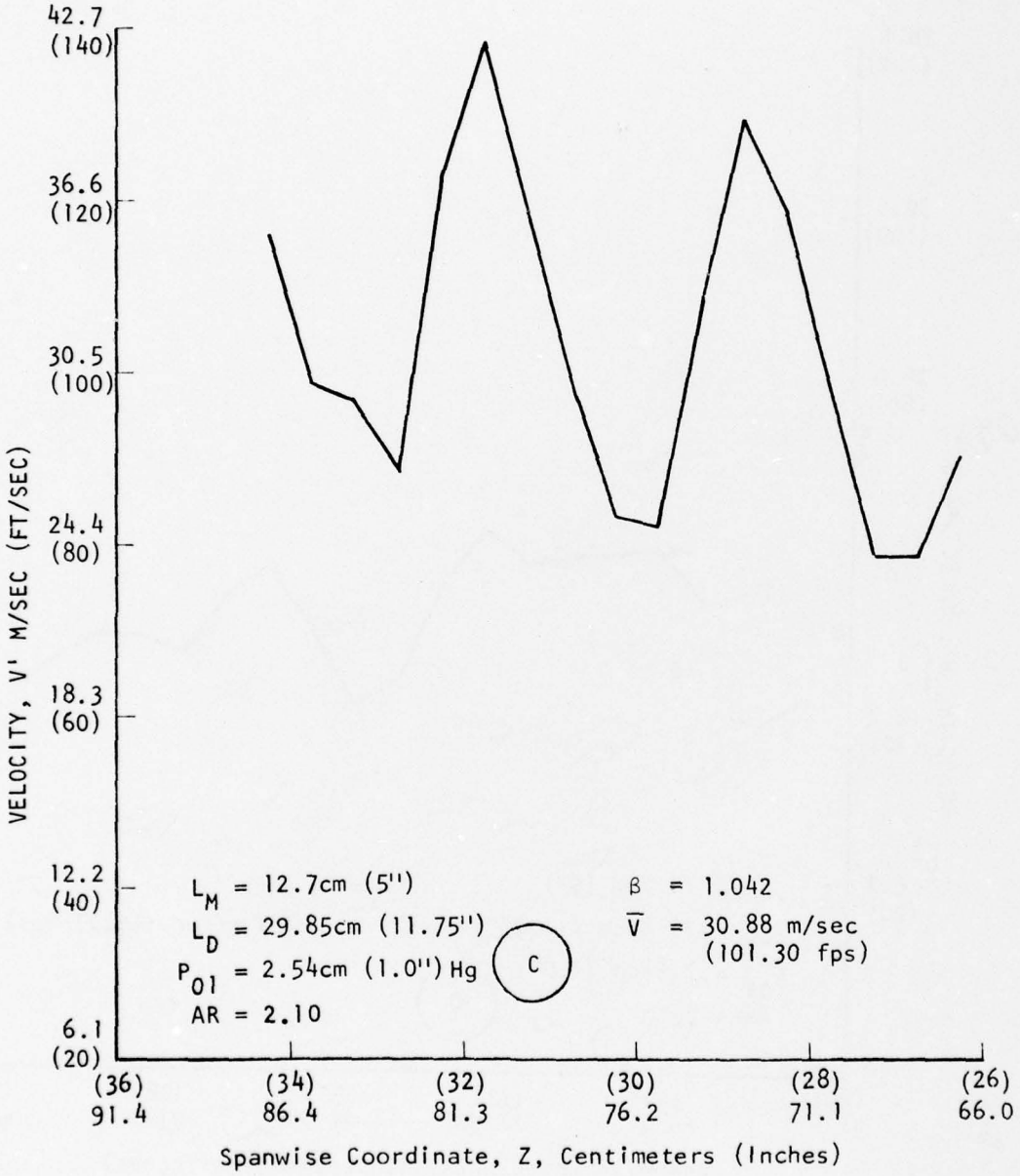

FIGURE 5.2-9. INTERNAL FLOW VELOCITY PROFILE AT THE CENTER SPAN LIP POSITION 0 CM FROM MIXING WALL

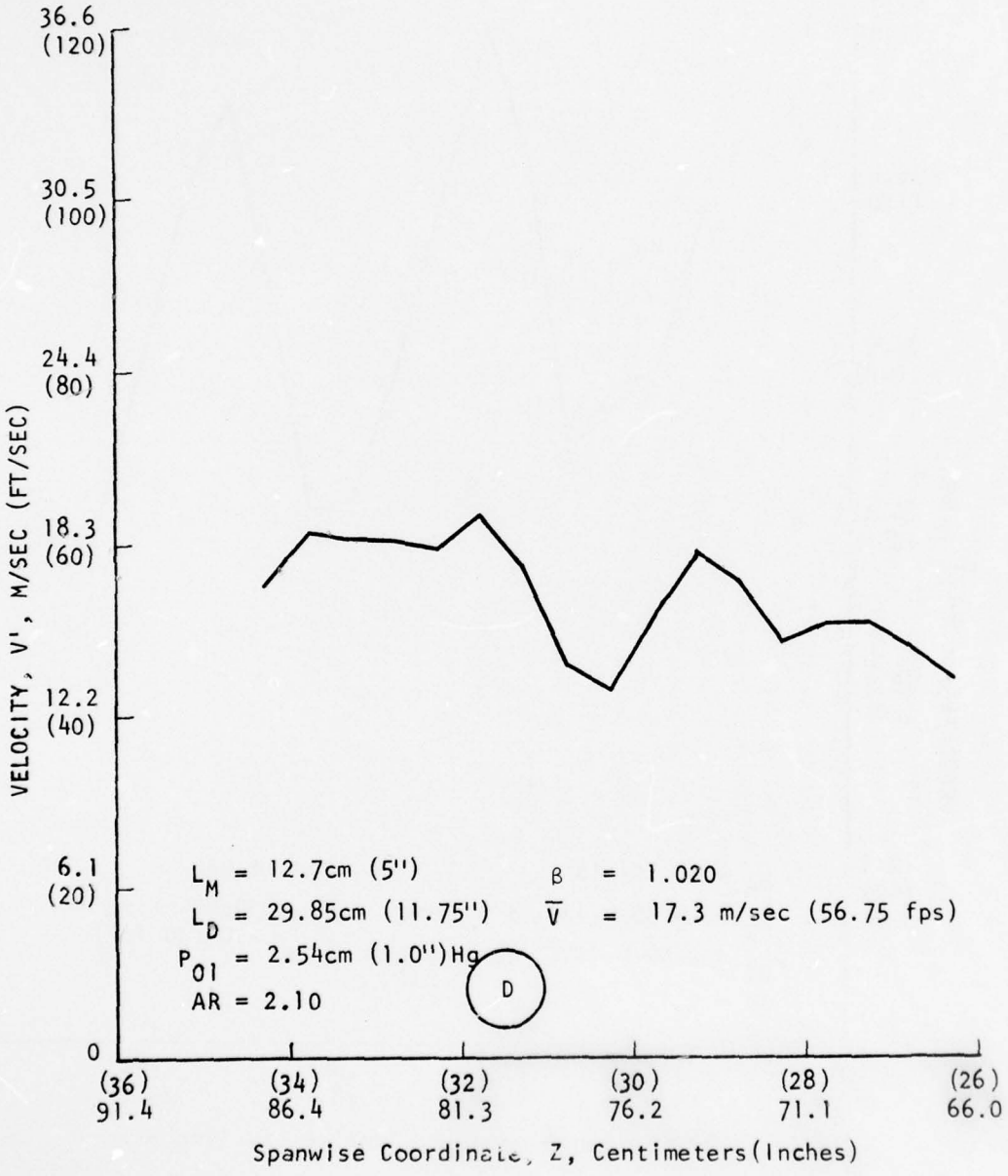

FIGURE 5.2-10. INTERNAL FLOW VELOCITY PROFILE AT THE CENTER SPAN EXIT POSITION 0 CM FROM DIFFUSER WALL

diffuser exit planes does, however, show the diffuser transverse flow control provided by the ATC/diffuser.

5.2.4 Augmentation Performance

A measure of the overall performance of the ATC/augmentor is the thrust augmentation ratio of the ejector/augmentor configuration. Phase II testing results with the optimized ATC ejector/diffuser configuration for a range of diffuser area ratio is shown in Figure 5.2-11. The testing procedure of Section 4.0 was employed in obtaining the maximum augmentation ratio for each area ratio while operating the ejector/diffuser at P_{01} = 2.54cm (1") Hg. The figure shows the maximum augmentation ratio, ϕ_{max}, averaged over numerous runs to be equal to 1.85. As for all ATC/augmentor configurations the high augmentation ratio is obtained with the inclusion of the auxiliary primary blowing in the calculation of ϕ. The curve of Figure 5.2-11 shows that for an optimized ATC/augmentor, augmentation ratios $\geq$ 1.80 are maintained over a wide range of area ratio, $1.925 \leq A_3/A_2 \leq 2.25$, for this compact, $L_M + L_D$ = 42.55 cm (16.75"), ejector/augmentor. The ϕ_{max} value of 1.85, for P_{01} = 2.54cm (1") Hg, is in close agreement with the predicted level of performance for an optimized H-8/ATC ejector/diffuser as may be seen in Figure 5.2-15.

For a baseline comparison with an equivalent length conventional diffuser, with no advanced BLC methods, a straight wall diffuser with L_D = 29.85cm (11.75") was also tested in the ejector test bed facility. With endwall nozzle blowing optimized, the maximum augmentation ratio results for this diffuser are shown in Figure 5.2-12 for P_{01} = 2.54cm (1") Hg. The maximum augmentation ratio measured was 1.69 and occurred at a low area ratio of 1.50. Area ratios below and above the optimum of 1.50 were tested, with diffuser area ratios above 2.0 exhibiting flow separation in the augmentor diffuser section. Figure 5.2-13 gives a comparison between straight wall diffuser baseline augmentation ratios and the optimized ATC/augmentor performance by combining Figures 5.2-11 and 12. An increase of approximately 10% ($\Delta\phi$ = 0.16) in maximum augmentation ratio is seen for the optimized ATC/augmentor with the primary plenum pressure equal to 2.54cm (1") of Hg. This performance improvement is accredited to the rapid controlled diffusion of the optimized ATC/diffuser, since all other ejector parameters have remained fixed.

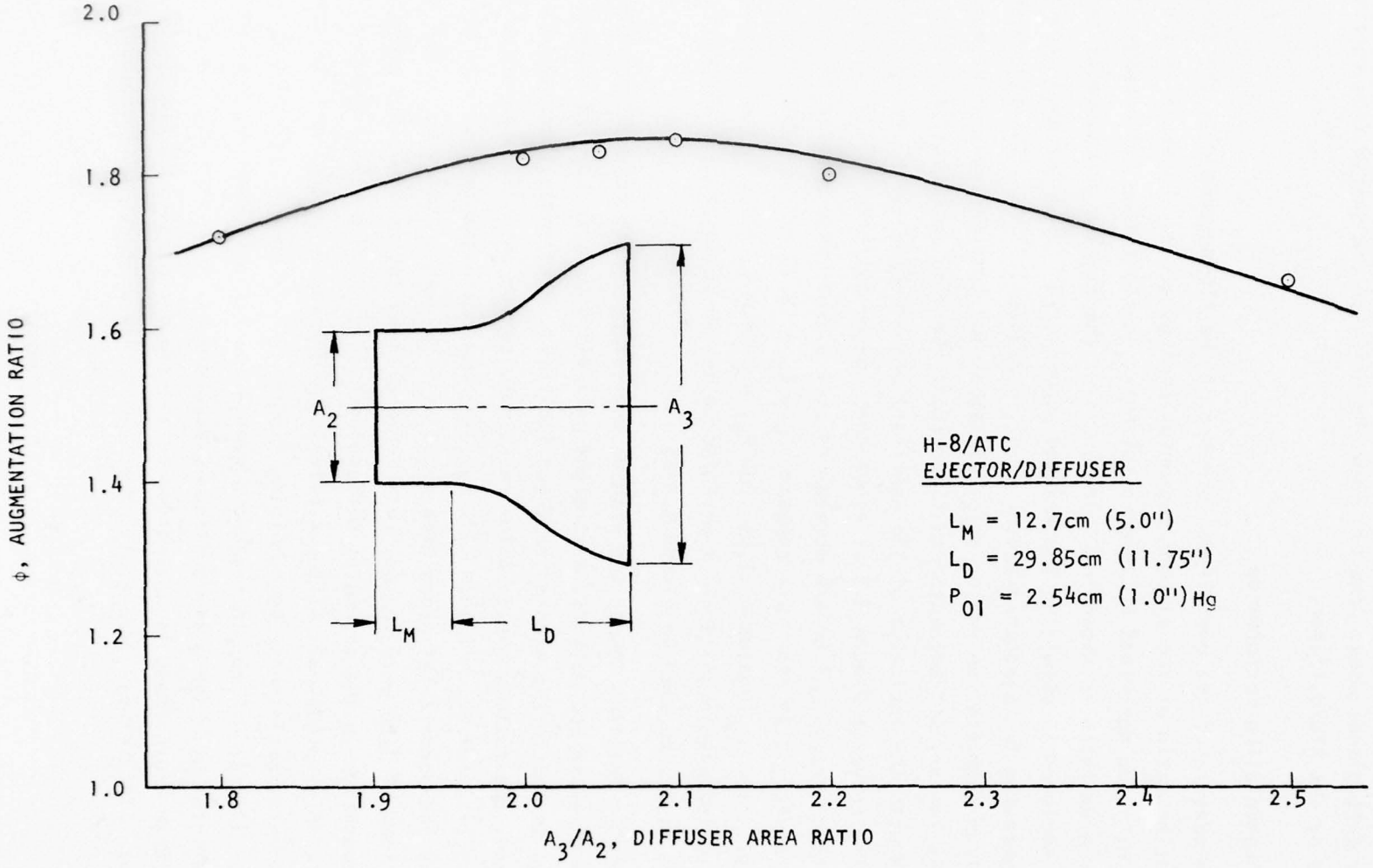

FIGURE 5.2-11. PHASE II H-8/ATC EJECTOR/DIFFUSER AUGMENTATION PERFORMANCE.

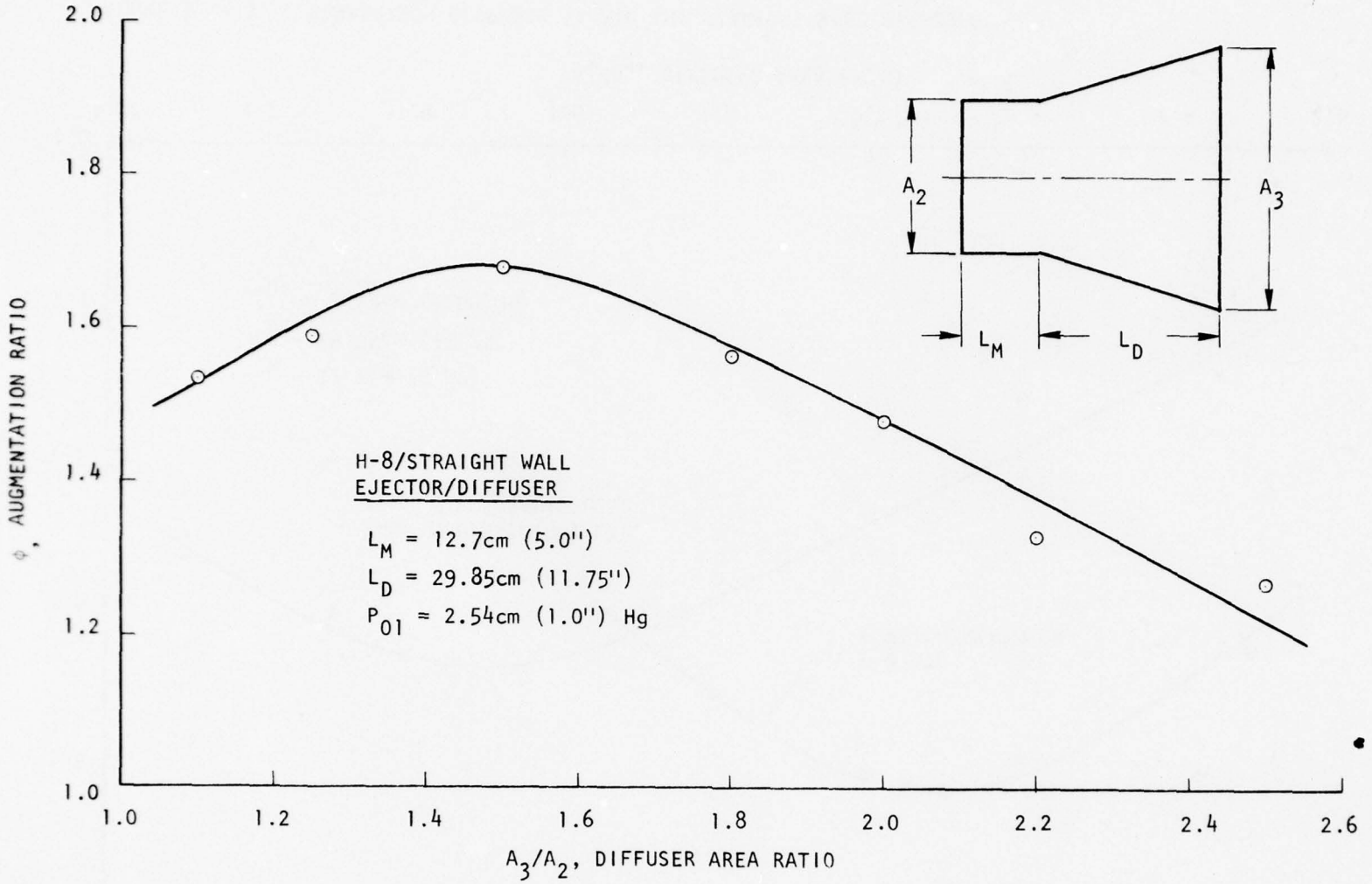

FIGURE 5.2-12. H-8/STRAIGHT WALL DIFFUSER AUGMENTATION PERFORMANCE.

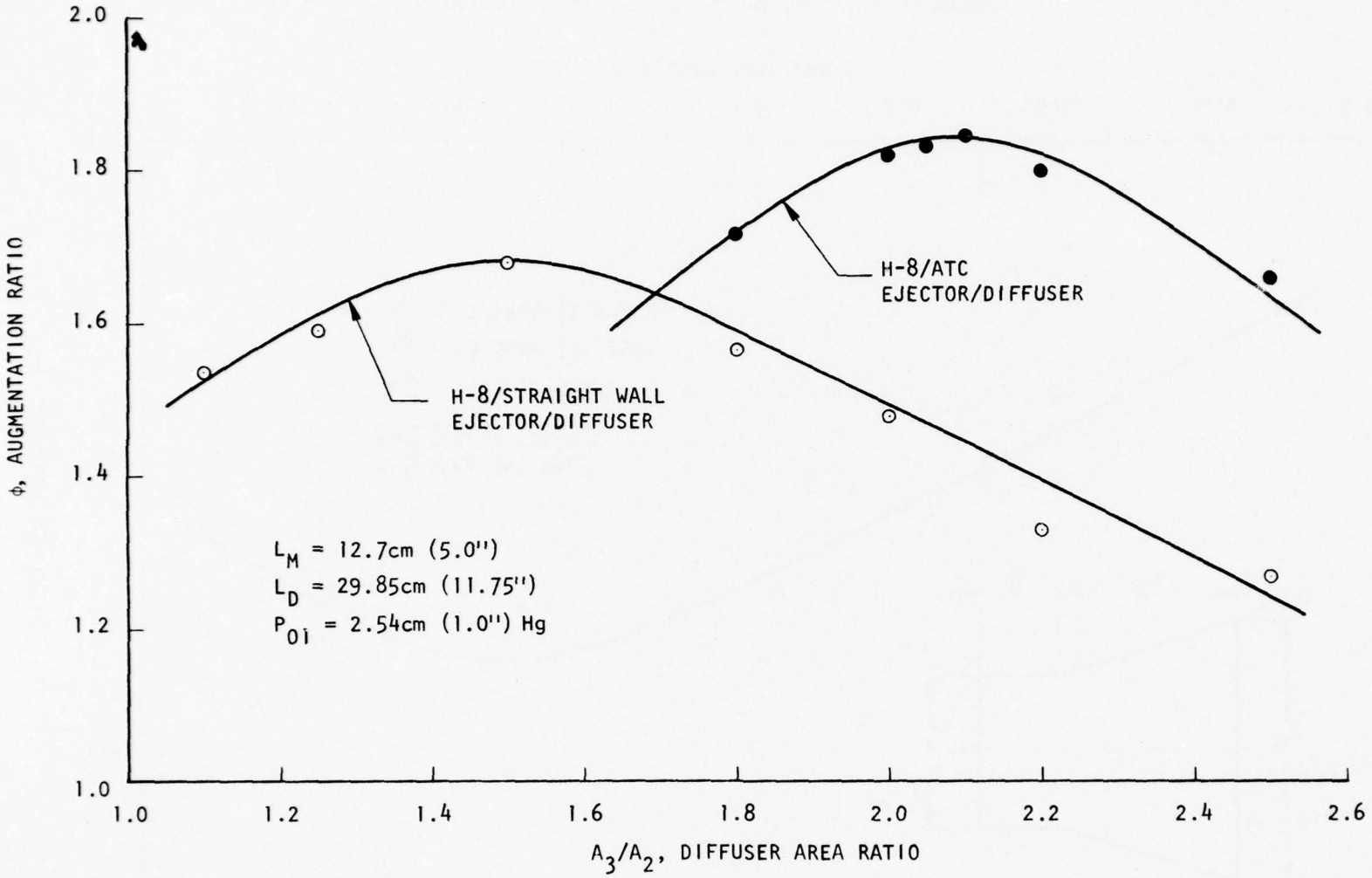

FIGURE 5.2-13. COMPARISON OF PHASE II ATC AND STRAIGHT WALL DIFFUSER AUGMENTATION PERFORMANCE.

At higher primary plenum pressures of P_{01} = 10.16 cm (4") and 25.4cm (10") Hg, the optimized augmentation ratios for the baseline and ATC/augmentor are compared to P_{01} = (1") Hg results at several diffuser area ratios, Figure 5.2-14. In both ejector/diffuser configurations where the diffuser flow was attached, the moderate increase in plenum pressure to 10.16cm (4") Hg improved the augmentation ratio. The improvement in performance was then maintained or slightly degraded with a further increase in plenum pressure to 25.4cm (10") Hg. As may be expected, in the baseline straight wall diffuser configuration at A_3/A_2 = 2.50, which exhibits separated diffuser flow, slight decreases in performance are seen with increased plenum pressures. The baseline results follow the pressure trends of previous data, but the lack of pressure degradation for the ATC/diffuser differs significantly from the Reference 3 and Phase I results (Figure 5.1-17) and is attributable to the optimized ATC contour design.

Augmentation performance of the Phase II optimized ATC/augmentor and conventional straight wall baseline diffusers is related to current ejector/augmentor performance capabilities in Figure 5.2-15. Current configuration results presented represent a pressure averaged ϕ_{max} attained for the length to throat ratio corresponding to the total available mixing/diffusion length, $L_M + L_D$. Development research at ARL using H-4 hypermixing ejector nozzles and lengthy diffusers is shown as the shaded data block, along with reference configuration 'F'. Previous trapped vortex diffuser results with H-4 nozzles are given to illustrate the present advances in BLC augmentor diffuser design.

The previous ejector/augmentor data provides a base for comparison with current contract efforts which employ the advanced H-8 hypermixing ejector nozzles. The use of H-8 nozzles and optimized end wall blowing allowed the performance of recent ARL straight wall diffusers to approach the previous trapped vortex results at length ratios near 2.5 but drastic fall-offs in performance were indicated at other length ratios. With optimized ATC/diffusers, augmentation performance shown by the dashed curve was predicted and substantiated to excede the trapped vortex results at all diffuser lengths.

The final augmentation results of Phases I and II are shown in the above figure for comparison and evaluation. Phase I ATC/diffuser data for length to throat ratios fo 1.3, 1.5, and 2.5 show augmentation ratios approaching the predicted values, even though area ratio was not actually investigated for optimization of ϕ_{max} during Phase I studies. For Phase II H-8/ATC augmentation with a

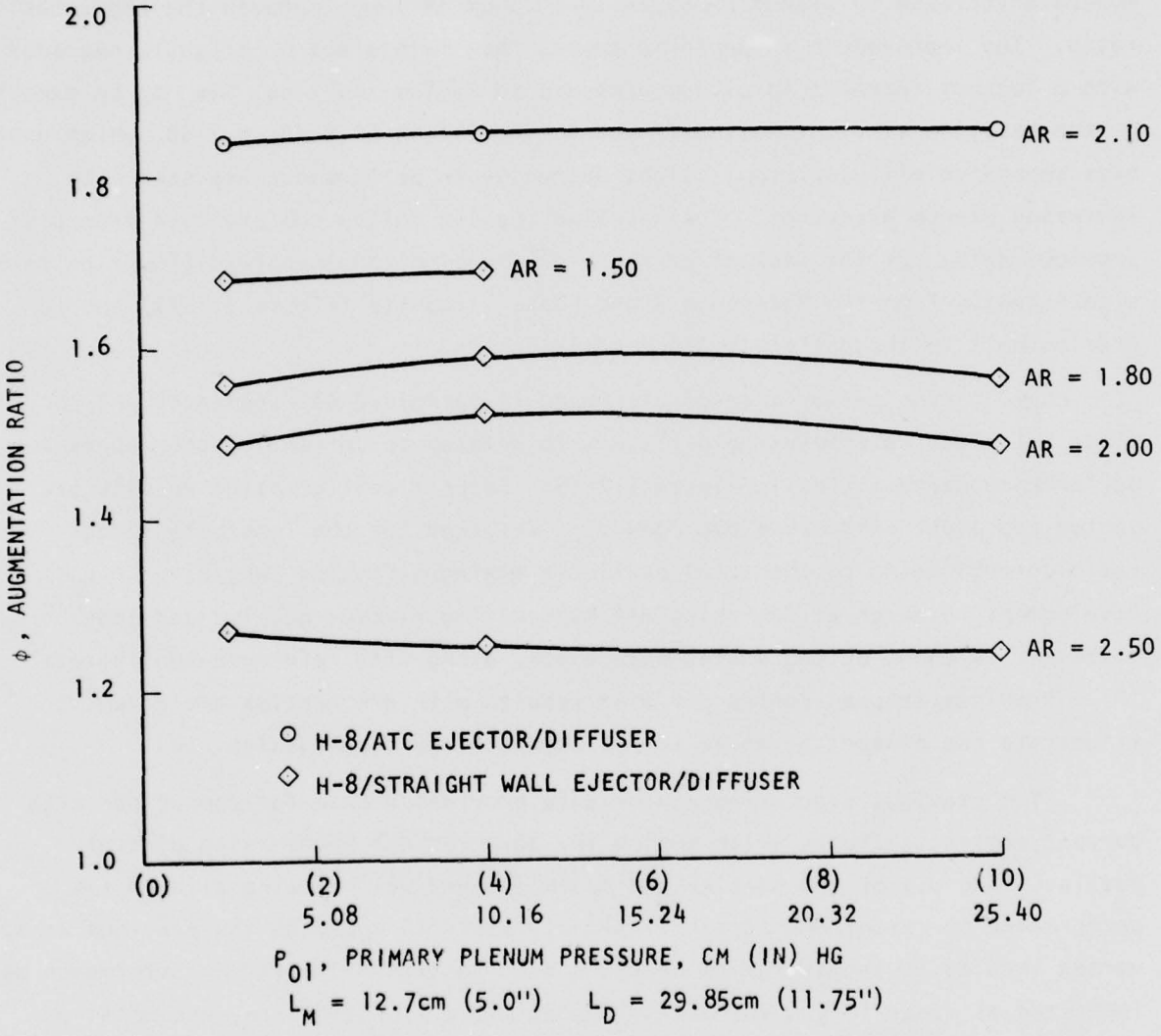

FIGURE 5.2-14. PRIMARY PLENUM PRESSURE EFFECTS ON AUGMENTATION PERFORMANCE OF PHASE II CONFIGURATIONS

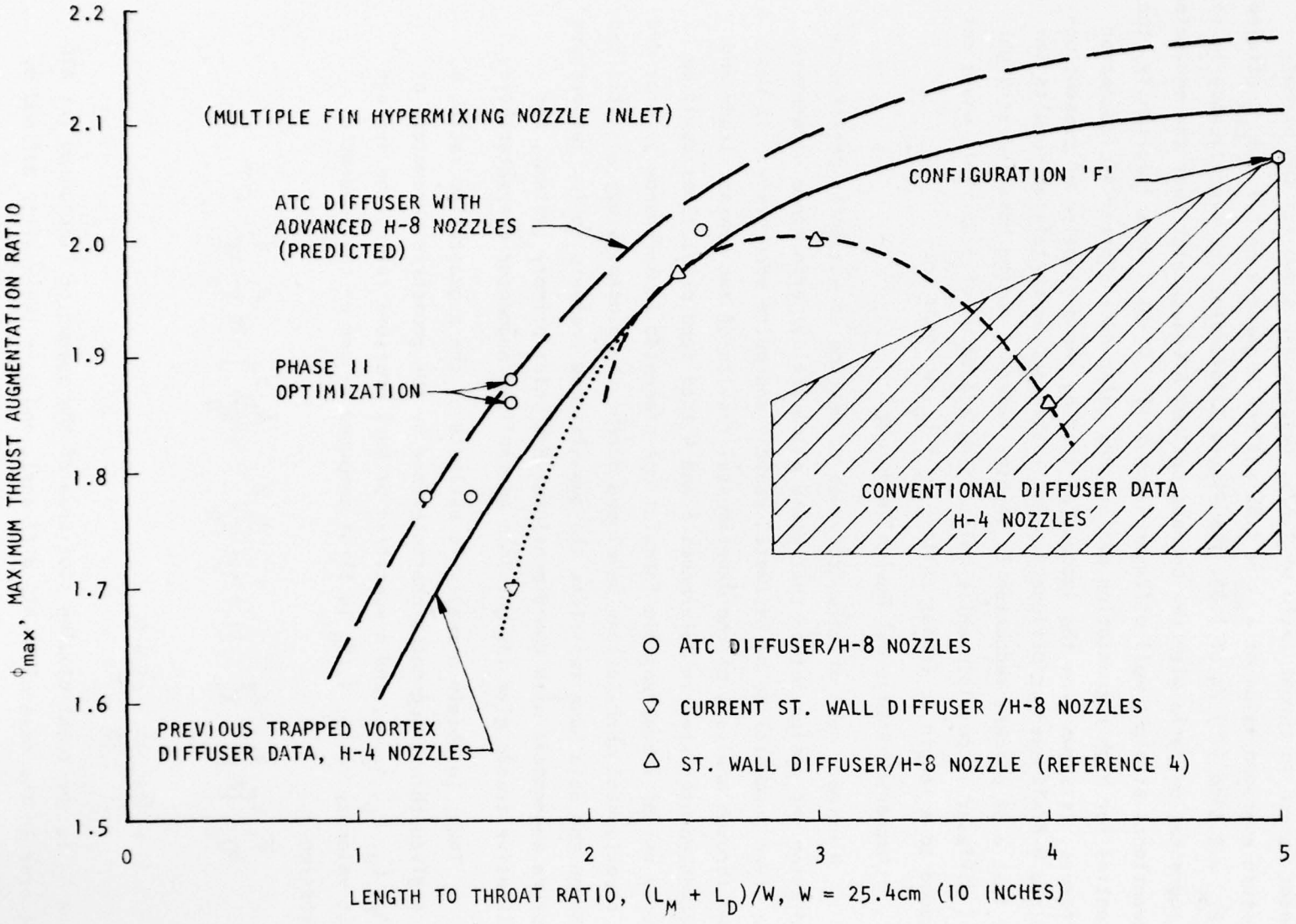

FIGURE 5.2 -15. COMPARISON OF MAXIMUM AUGMENTATION RATIOS FOR ATC AND CONVENTIONAL DIFFUSERS.

compact length to throat ratio of 1.675, results are shown for the primary pressure averaged value of ϕ_{max} = 1.86 and the highest single run ϕ_{max} attained at P_{01} = 2.54cm (1") Hg of 1.88. The figure illustrates the significance in the gain of augmentation ratio with the compact optimum ATC/augmentor over the equivalent conventional straight wall diffuser ($\Delta\phi$ = 0.17 - 0.19). More importantly, the potential for high augmentation performance using even shorter ATC/augmentor diffusers, is shown from the successful testing and evaluation of present optimized H-8/ATC ejector/diffusers. For instance, the correlated results imply that a 36 percent reduction in length, relative to the baseline straight wall diffuser is possible while maintaining a ϕ value of 1.7. This would correspond to a length to throat ratio, $(L_M + L_D)/W$, near one.

5.3 Augmentor Analytical Design Technique

A primary goal of this study was to develop an augmentor performance prediction and design method that would allow sizing/performance parameters of a given augmentor to be estimated rapidly and quite accurately. It was found through analysis of the experimental results of the present study and information presented in References 1 and 4 that such predictions could be made by use of incompressible formulations presented in Reference 2, provided the experimental correlations developed during the present study are utilized. Although the data base restricts the quantitative analysis to low temperature/pressure augmentors with two-dimensional H-8 inlet/primary systems, the qualitative trends give insight into generalized augmentor characteristics.

Thus, to obtain a realistic estimate of the augmentation ratio, ϕ, for a given thrust augmentor characterized by the geometric parameters of A_1/A_0, L_M, L_D, A_3/A_2, and a specified primary pressure ratio, the average inlet velocity ratio, $\overline{V}_1/V_0$ is first computed by use of the quadratic expression

$$\left(\frac{\overline{V}_1}{V_0}\right)^2 \left[2\,\frac{A_1}{A_0}\cdot\frac{A_2}{A_0} - (1+\xi_1)\left(\frac{A_2}{A_0}\right)^2 - q\left(\frac{A_1}{A_0}\right)^2\right] - 2q\,\frac{A_1}{A_0}\left(\frac{\overline{V}_1}{V_0}\right) +$$

$$+ \left[2\beta_0\,\frac{A_2}{A_0} - q\right] = 0$$

where A_0 is the total blowing slot area of the augmentor (including the ATC slot area in the case of an ATC diffuser), and q is the quality defined by the relation,

$$q = \beta_2[2\ \xi_f + 2 - \bar{C}_p]$$

Substitution of the resulting ratio for $\bar{V}_1/V_0$ into the expression

$$\phi = \beta_3 \frac{A_0}{A_3}\left(1 + \frac{A_1}{A_0}\cdot\frac{\bar{V}_1}{V_0}\right)^2\left[\frac{1}{\eta_N^2} - (1+\xi_1)\left(\frac{\bar{V}_1}{V_0}\right)^2\right]^{-1/2}$$

then yields the desired approximate value of the augmentation ratio. In the above equations, losses at the various stations are represented by β's, η's, and ξ's which correspond to flow skewness factors, component efficiencies, and loss parameters, respectively. In particular, the value of the hypermixing nozzle efficiency, η_N, is given as 0.96 in Reference 2. Pressure recovery in the diffuser is denoted by $\bar{C}_p$. Parameter correlations and methods for estimating the other loss factors are detailed in Appendix A.

The above procedure was used to estimate the augmentation ratio of the optimized compact ATC/diffuser experimentally investigated during Phase II of the present study. The estimated value of 1.89 was in good agreement with the measured value of 1.86 averaged over all pressures. Similar computations were performed for the long ARL configuration 'F' straight wall diffuser. Comparison of the predicted performance with that measured during the present program is shown in Figure 5.3-1. As may be noted from the comparison, the agreement is again within about ±0.03.

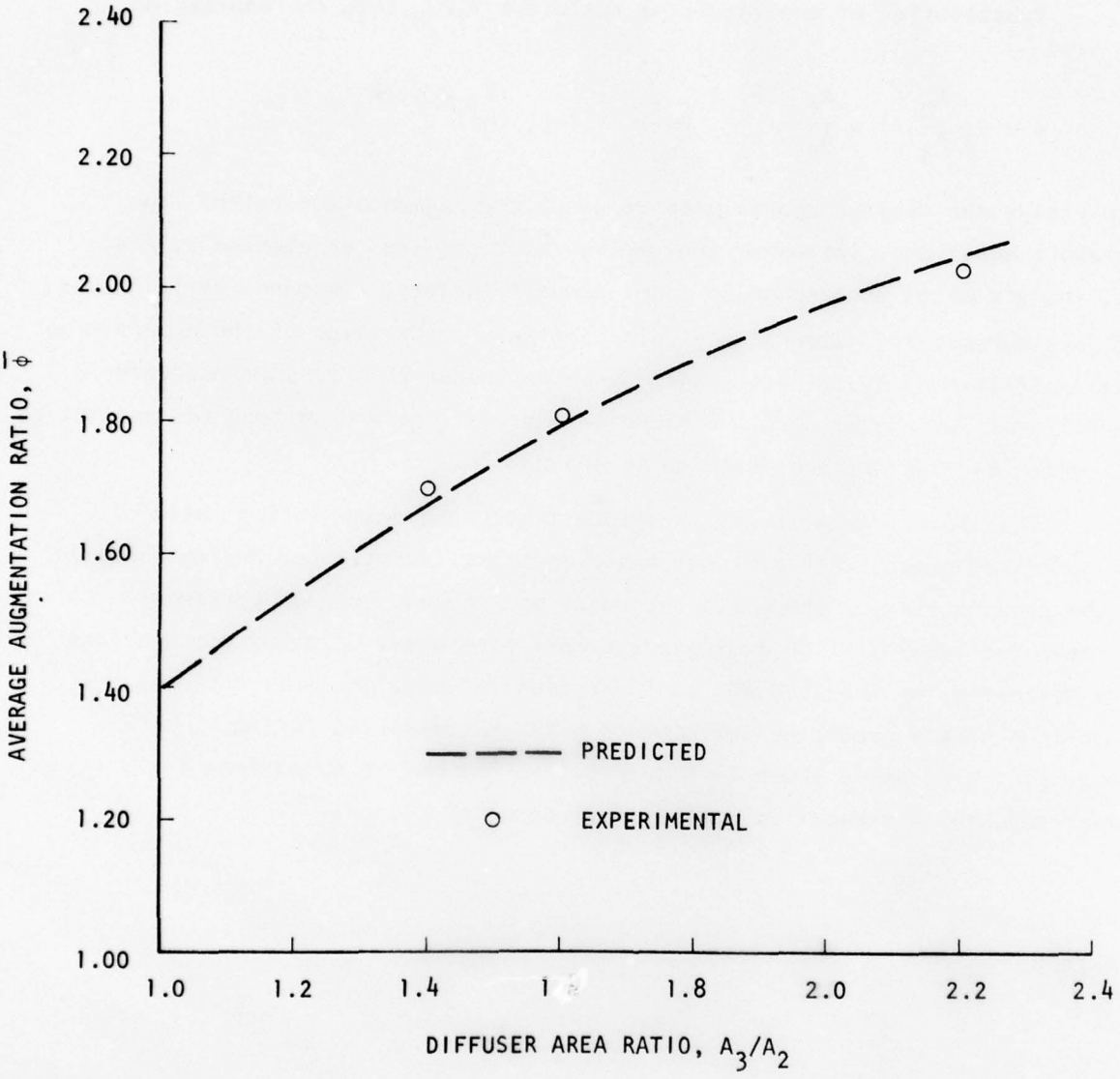

FIGURE 5.3-1. COMPARISON OF PREDICTED AUGMENTATION FOR ARL CONFIGURATION 'F' DIFFUSER WITH THAT OBTAINED EXPERIMENTALLY IN THE LARGE SCALE AUGMENTOR TEST RIG

6.0 CONCLUSIONS

1. The technique of adapting and optimizing compact ATC/diffusers for operation in high performance thrust augmentors has been established for low pressure/temperature operation. The primary factors which influence the performance appear to be the overall length constraints of the augmentor, the diffuser area ratio, the maximum boundary layer momentum thickness at the ATC blowing lip, and attaining proper endwall BLC.

2. Thrust augmentation obtained with the short ATC/diffusers and ARL/H-8 hypermixing nozzles was increased about 3% over the levels obtained when the ARL/H-4 nozzles were used. The experimental augmentation values were in good agreement with the predicted levels.

3. By utilizing knowledge gained from detailed internal flow and boundary layer measurements, the present optimized ATC/augmentor design eliminates the degradations in augmentation ratio with increasing primary plenum pressure observed in previous testing of active diffusion control ejectors.

4. The thrust augmentation ratio obtained for the optimized short ATC/diffuser is 0.16 - 0.19 (~10%) larger than that obtained with a conventional straight wall diffuser of the same length. Without addressing system weight tradeoffs, this improvement approximates a corresponding 10% increase in takeoff gross weight for augmentor VTOL aircraft with a given engine installation.

5. Correlations of the present ATC/augmentor data indicate that a 36 percent length reduction in the mixing/diffuser section, relative to the straight wall baseline case, is attainable while maintaining an augmentation ratio of 1.7. High performance compactness improvements of this magnitude permit augmentor length to throat ratios on the order of one to be used in VTOL installations, thus greatly enhancing VTOL aircraft design flexibility.

6. Measured values of internal flow skewness for various diffuser configurations were found to correlate well with published results through use of a correlation parameter that is based on geometric parameters of the augmentor. Mixing between the primary and induced flow is enhanced and the skewness factor correspondingly lowered with increased diffusion.

7. A design formulation using correlated experimental coefficients in conjunction with an incompressible augmentor analysis allows augmentation values for the class of augmentors discussed to be estimated within about ± 0.03.

7.0 RECOMMENDATIONS

The technique of adapting short ATC/diffusers to a high performance thrust augmentor has been established. Limited theoretical studies by Vought Advanced Technology Center, however, indicate even larger increases in thrust augmentation if the diffuser can be made capable of further area expansion without boundary layer separation. It is recommended, therefore, that an investigation be initiated to determine the effect on the performance of compact thrust augmentors when use is made of advanced single or multiple staged diffusion devices. Analytical studies would precede two-dimensional testing in the Large Scale Augmentor Test Rig.

A second recommendation is that fundamental studies be performed to determine the effects of basic three-dimensional augmentor installation characteristics such as bay aspect ratio and required endwall BLC. The studies should be oriented particularly toward the ultra-compact configurations and should seek to minimize adverse three-dimensionality while maximizing potential performance enhancement factors.

REFERENCES

1. Quinn, Brian, "Experiments with Hypermixing Nozzles in an Area Ratio 23 Ejector," Aerospace Research Laboratories Report No. 72-0084, June 1972, AD 752-207.

2. Quinn, Brian, "Recent Developments in Large Area Ratio Thrust Augmentors," AIAA Paper No. 72-1174, AIAA/SAE 8th Joint Propulsion Specialist Conference, November-December, 1972.

3. Haight, Charles H. and O'Donnell, Robert M., "Experimental Mating of Trapped Vortex Diffusers With Large Area Ratio Thrust Augmentors," ARL TR 74-0115, September, 1974.

4. Bevilaqua, Paul M., "An Analytical Description of Hypermixing and Tests of an Improved Nozzle," AIAA Paper No. 74-1190, AIAA/SAE 10th Propulsion Conference, San Diego, Calif., October, 1974.

5. Haight, C. H., and Spangler, J. G., "Test Verification of a Transonic Airfoil Design Employing Active Diffusion Control," Final Report, NADC Contract No. N62269-74-C-0517, June, 1975.

6. Malavard, L. C., "The Use of Rheoelectric Analogies in Aerodynamics," NATO Agardograph 18, August, 1956.

7. Viets, Hermann, "Directional Effects in 3-D Diffusers," Energy Conversion Research Laboratory/ARL, ARL TR 74-0012, February 1974.

APPENDIX

AUGMENTOR LOSS FACTORS AND CORRELATIONS

The primary constraint under which the prediction method of Section 5.3 operates is that the selected augmentor must have a two-dimensional inlet system composed of ARL/H-8 hypermixing nozzles. This is necessary to maintain correspondence with the data generating the empiricisms since important internal flow parameters such as skewness and blowing lip momentum thickness depend strongly on the inlet/nozzle configuration. The performance of an augmentor utilizing an inlet system identical to the above but with ARL/H-4 nozzles could not be expected to be estimated accurately by the developed method because of the significantly different mixing characteristics of the H-8 and H-4 nozzles (Reference 4). A further constraint in the prediction technique is the assumption that the endwall boundary layer is sufficiently energized to prevent separation.

Friction loss coefficient, skewness factor, and hypermixing nozzle efficiency as related specifically to the ARL/H-8 inlet system is evaluated directly from Reference 4. Skewness coefficients at downstream stations are empiricized both from present measurements and those presented by Bevilaqua in Reference 4. The remaining loss factors are based on the present data.

As noted in Section 5.3, only the incompressible expressions involving $\overline{V}_1/V_0$ and the augmentation ratio, ϕ, require evaluation to estimate the performance of a low pressure/temperature augmentor. In the expression for the average inlet velocity ratio, $\overline{V}_1/V_0$, the coefficient ξ_1 represents the inlet loss coefficient while β_0 is the skewness coefficient at the primary nozzle station. From Reference 2 it is found that $\xi_1 = 0.025$ while $\beta_0 = 1.00$.

Based on the internal flow measurements of the present study and those presented in Reference 4, the skewness coefficient, β, downstream of the H-8 nozzles is strongly dependent on the distribution of the geometric parameters of the augmentor. A qualitative indication of the importance of the various parameters may be seen by comparing exponents in the derived correlation factor $\gamma = (L_M/W)^3 (L_D/W) (A_3/A_2)^{1.25} (L'/W)^{1/2}$, where L' refers to the specific location in the diffuser at which the skewness factor is desired. Since the skewness factor decreases with increasing γ, it may be noted, that mixing is enhanced and the skewness factor lowered as the diffuser area ratio is increased.

This particular effect is in qualitative agreement with the theoretical prediction of Viets (Reference 7). A plot of available experimental skewness factors as they vary with the correlation factor, γ, is given in Figure A-1. The faired curve through the data is within the probable experimental accuracy of the data (0.002).

In the expression for $\overline{V}_1/V_0$,the weighted skin friction coefficient, ξ_f, is determined from the expression

$$\xi_f = \frac{C_f}{2} \left(\frac{A_w}{A_2} \right)$$

where A_w is the wetted area of the constant area mixing section. For augmentors possessing the general mixing area configuration and BLC blowing schemes of the present augmentor, the skin friction coefficient C_f may be estimated from the relation

$$C_f = \frac{2\Theta_L}{L_M}$$

where Θ_L is the momentum thickness of the boundary layer at the entrance to the diffuser. The above momentum thickness Θ_L may be determined from a correlation of the present boundary layer measurements (Figure A-2). It was found that for augmentors of the present type, the skin friction coefficient, ξ_f, was quite small. However, as pointed out in Reference 2, this coefficient can become larger if the main primaries inject along the walls.

The remaining coefficient that must be estimated is the diffuser pressure coefficient, $\overline{C}_p$. It was found that even with attached flow in the diffuser, the performance of the augmentor was strongly dependent on the diffuser pressure coefficient. This coefficient may be estimated from the relation

$$\overline{C}_p = \eta_D C_p'$$

where η_D is the diffuser efficiency and C_p' is the ideal incompressible pressure coefficient which is evaluated by use of the relation

$$C_p' = 1 - \left(\frac{A_2}{A_3}\right)^2$$

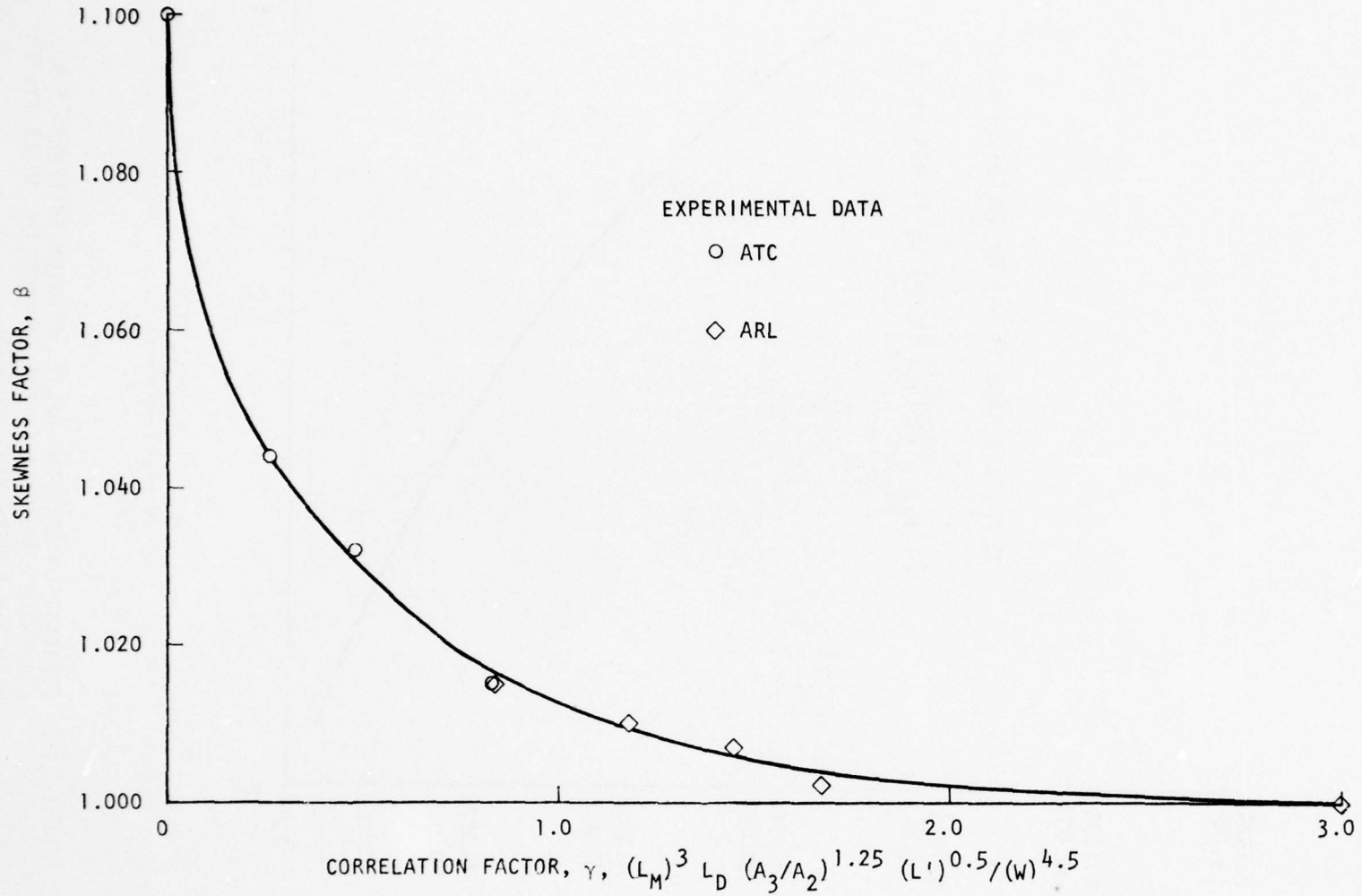

FIGURE A-1. CORRELATION OF FLOW SKEWNESS FACTOR FOR AUGMENTORS HAVING THE ARL HIGH PERFORMANCE INLET WITH H-8 HYPERMIXING NOZZLES

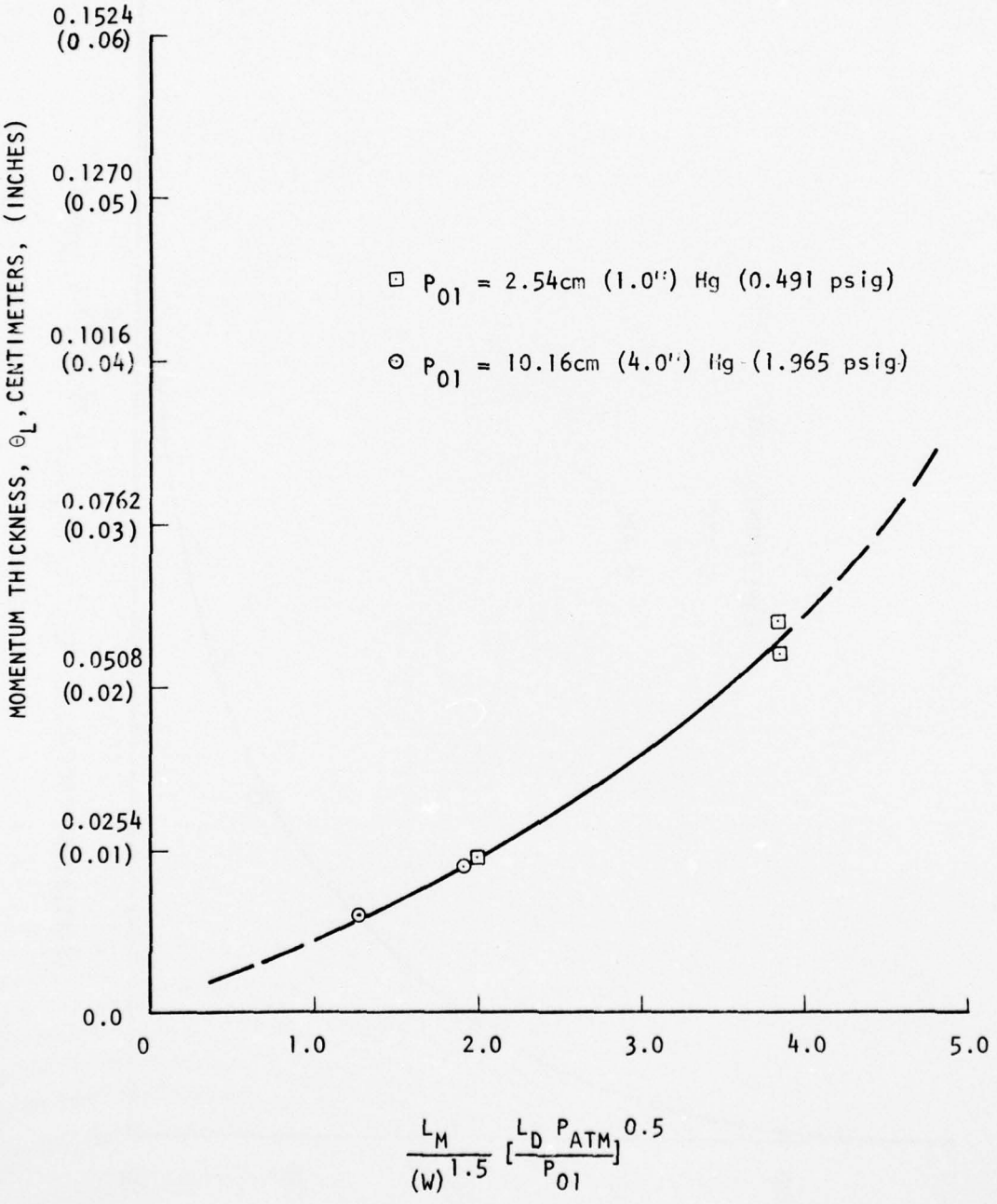

FIGURE A-2. CORRELATION OF BLOWING LIP MOMENTUM THICKNESS FOR AUGMENTORS HAVING HIGH PERFORMANCE ARL INLET SYSTEM WITH H-8 HYPERMIXING NOZZLES

The diffuser efficiency term is more complex and requires a series of computations for its final evaluation, thus

$$\eta_D = 1.00 - (\Delta P_0/q_2)\left(1 - \left(\frac{A_2}{A_3}\right)^2\right)$$

In the above expression, $\Delta P_0/q_2$ represents the total pressure loss across the diffuser due to the viscous boundary layer. It was found that this loss can be estimated quite well by means of the expression

$$\frac{\Delta P_0}{q_2} = C_{f_{EFF}} (1.05)\pi \, L_D \, \bar{D}/A_3$$

where $C_{f_{EFF}}$ is an effective diffuser skin friction coefficient and $\bar{D}$ is the mean hydraulic diameter of the diffuser, or

$$\bar{D} = (D_2 + L_D \, \mathrm{Tan} \, \varepsilon)$$

In the above expression $\varepsilon = \mathrm{Tan}^{-1} \left(\frac{D_3 - D_2}{2L_D}\right)$ where D_2 and D_3 are the hydraulic diameters at stations 2 and 3 respectively. The constant 1.05 was empirically determined from available experimental results. Finally, the effective diffuser skin friction coefficient, $C_{f_{EFF}}$, may be estimated by use of the relation

$$C_{f_{EFF}} = C_{f_{F.P.}} \left[1.0 + 2K/(1+A_3/A_2)^2 \cdot (1-(A_2/A_3)^2)\right]$$

where K is a coefficient accounting for the effect of the diffuser pressure gradient (correlated in Figure A-3) and $C_{f_{F.P.}}$ is the turbulent flat plate skin friction coefficient computed from

$$C_{f_{F.P.}} = 0.074/R_e^{1/5}$$

and the usual Reynolds number $R_e = \rho \bar{u} \, L_D/\mu$. Here $\bar{u}$ is the average velocity through the diffuser and is obtained approximately from

$$\frac{\bar{u}}{u_0} = \frac{1}{2} \cdot \frac{u_3}{u_0} \left(1 + \frac{A_3}{A_2}\right)$$

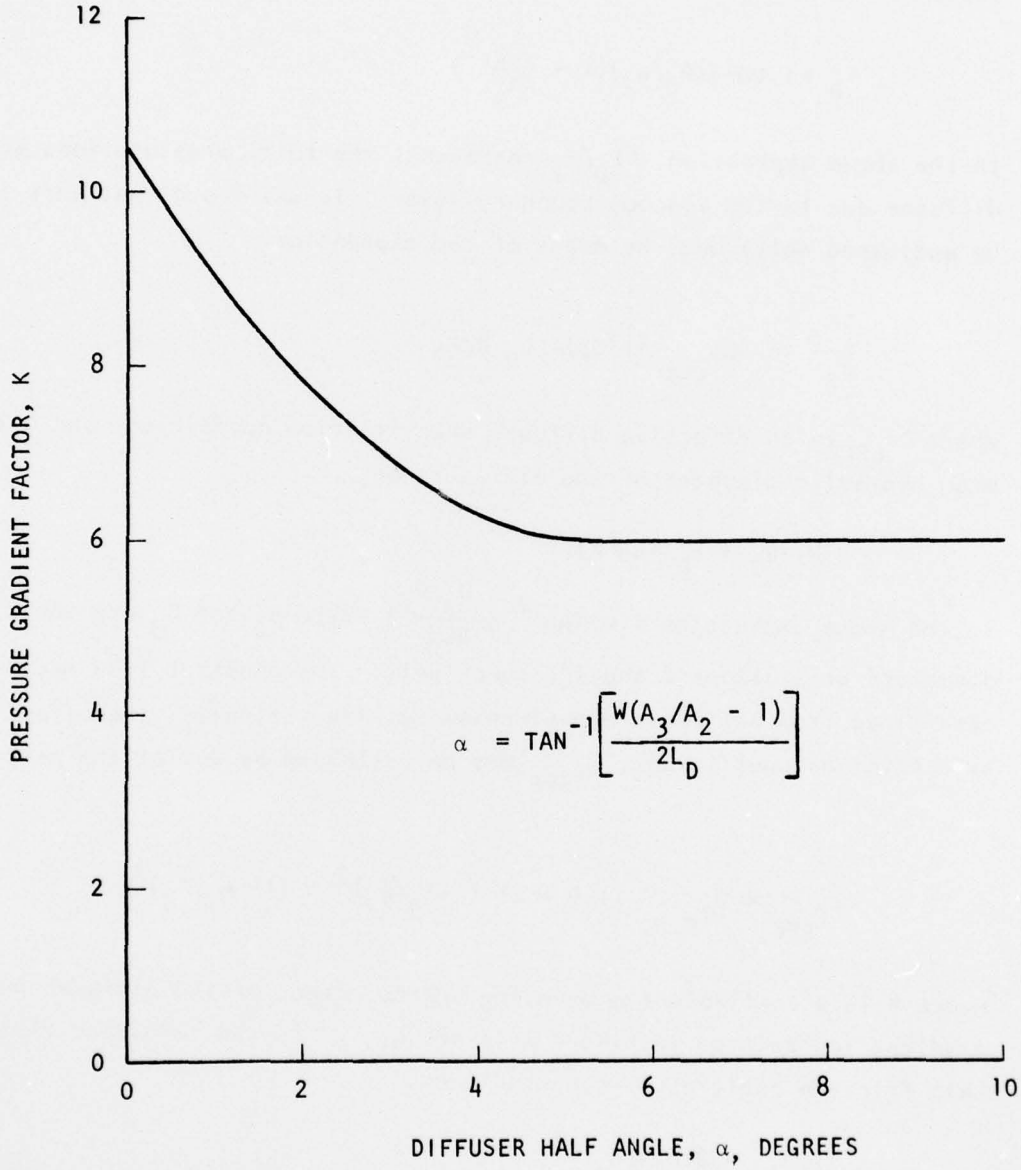

FIGURE A-3. VARIATION OF PRESSURE GRADIENT FACTOR WITH DIFFUSER HALF ANGLE FOR AUGMENTORS HAVING ARL HIGH PERFORMANCE INLET WITH H-8 HYPERMIXING NOZZLES

where

$$\frac{u_3}{u_0} = \left(\frac{A_0}{A_3} \phi_{ideal}\right)^{1/2}$$

The ideal primary jet velocity u_0 is calculated by first computing the ideal velocity ratio u_1/u_0 from the expression,

$$\frac{u_1}{u_0} = \frac{A_0}{A_1} \left(\frac{A_3}{A} \cdot \frac{u_3}{u_0} - 1\right)$$

It then follows for the incompressible case that

$$u_0 = \left[\frac{2}{\rho_{ATM}} (P_0 - P_1)\right]^{1/2}$$

where

$$P_1 = \frac{P_{ATM} - P_0 (u_1/u_0)^2}{1 - \left(\frac{u_1}{u_0}\right)^2}$$

It was found that low pressure, low temperature performance parameters for an augmentor may be estimated quite accurately by use of the above procedure if the various coefficients are calculated for an average primary pressure (P_{01}) of 10.16cm (4.0") Hg. The above equations, along with the empirical correlations of Figures A-1, A-2, and A-3 were used in obtaining the results of Section 5.3.